Emerging Market Business Cycles with Heterogeneous Agents*

Seungki Hong†

January 16, 2023

Abstract

This paper explains emerging market business cycles by estimating a heterogeneous-agent small open economy model where the marginal propensity to consume (MPC) is as high as the estimates from emerging market micro data. A conventional mechanism through which a representative-agent model explains the business cycles does not operate in the heterogeneous-agent model because precautionary saving interrupts it. Instead, emerging market business cycles are explained by a new mechanism in which high MPC and correspondingly strong precautionary saving play essential roles. When MPC is lowered to the U.S. level via recalibration, excess consumption volatility disappears in most of the posterior distribution.

***JEL classification*:** E21, E32, F41, D31

***Keywords*:** emerging economy, business cycle, heterogeneous agents, MPC, precautionary saving

*This paper is a revised version of Chapter 3 of my Ph.D. dissertation at Columbia University. I am highly indebted to Martin Uribe, Stephanie Schmitt-Grohe, and Andres Drenik for their constant guidance, support, and suggestions. I am also grateful to Hassan Afrouzi, Mario Crucini, Nils Gornemann, Emilien Gouin-Bonenfant, Ryan Kim, Christian Moser, Tommaso Porzio, Jesse Schreger, Shang-Jin Wei, Stephen Zeldes, and seminar participants at the Bank of Korea, the Central Bank of Chile, Columbia University, the Federal Reserve Bank of Chicago, the Hong Kong University of Science and Technology, KDI, KIET, KIEP, KIF, KIPF, Purdue University, Seoul National University, the University of British Columbia, and the University of Hong Kong for their helpful comments and discussions. All errors are my own.

†Department of Economics, Krannert School of Management, Purdue University. E-mail: hong397@purdue.edu

1 Introduction

One of the most salient patterns of emerging market business cycles is the phenomenon of 'excess consumption volatility': consumption is more volatile than output in emerging economies, while it is not in developed economies. Extensive literature is devoted to explaining excess consumption volatility, and the dominant modeling framework is representative-agent small open economy (RASOE) models. At the heart of these models, representative households optimize according to the permanent income hypothesis (PIH). Importantly, widely accepted mechanisms for excess consumption volatility in the literature, such as the permanent income effect of a trend shock (Aguiar and Gopinath, 2007) and the intertemporal substitution effect of interest rate fluctuations (Neumeyer and Perri, 2005), crucially depend on the household PIH behavior.

However, micro data suggest that household consumption behavior deviates significantly from the PIH in emerging economies, and the deviation is greater than that in developed economies. Under the PIH, the marginal propensity to consume (MPC) out of a transitory income shock is essentially zero. However, when Hong (2022) estimates the MPC by applying a standard method (developed by Blundell, Pistaferri, and Preston (2008)) to a Peruvian household survey, he finds that Peruvian MPCs are substantially higher than U.S. MPCs, which are already greater than zero.

Motivated by this observation, this paper revisits emerging market business cycles through the lens of a heterogeneous-agent small open economy (HASOE) model in which household MPCs are as high as the empirical estimates. To this end, I incorporate Kaplan, Moll, and Violante (2018)'s two-asset household heterogeneity over liquid and illiquid assets into a standard RASOE model. The financial friction in illiquid asset trading is calibrated (jointly with the time discount factor) such that both household MPC and wealth are empirically realistic.[1] Then, I take the HASOE model to Peruvian macro data through Bayesian estimation to explain emerging market business cycles. For comparison, I also estimate the corresponding RASOE model.

I report three main findings. First, the RASOE model explains Peruvian macro data through the conventional Aguiar and Gopinath (2007) mechanism, while this mechanism does not operate in the HASOE model. In the RASOE model, the Aguiar and Gopinath (2007) mechanism operates as follows: when a trend shock hits the economy, earnings mildly jump on impact but grow strongly in the future; the permanent income effect of the future earnings growth drives a strong consumption response, generating excess consumption volatility. In the HASOE model, the future aggregate earnings growth also means that households must face a greater idiosyncratic income risk in the future and thus enhance their precautionary saving. The enhanced precautionary saving effect offsets the permanent income effect, and the consumption response to a trend shock is muted.

[1] The two-asset structure allows me to capture both realistically high MPCs and the correct amount of aggregate wealth. In a one-asset model, on the other hand, households must hold a small amount of assets to yield high MPCs. This leads to an insufficient amount of aggregate capital, which is problematic for a business cycle analysis.

Second, the HASOE model, once augmented with a financial friction shock, can successfully explain emerging market business cycles through a new mechanism in which households' high MPC and correspondingly strong precautionary saving motive play essential roles. Specifically, large consumption fluctuations are mainly driven by two channels: (i) in the face of heightened financial friction, households substantially reduce their consumption either because of an aggravated consumption smoothing failure or because of enhanced precautionary saving[2]; (ii) when a stationary productivity shock hits the economy, households' individual income fluctuates, and the income fluctuations are strongly translated into consumption fluctuations due to their high MPC.

Third, to evaluate the quantitative importance of the high MPC and strong precautionary saving, I conduct a counterfactual experiment in which household MPCs are adjusted to the U.S. level, which is substantially lower than the Peruvian level, via recalibration. In the counterfactual experiment, I find that excess consumption volatility disappears in most of the posterior distribution, including the posterior mean, median, and mode.

My paper is related to multiple strands of literature. First, there is rapidly growing literature examining how microlevel household behavior and its heterogeneity affect macroeconomic outcomes. Well-known works in this literature include Kaplan et al. (2018), Auclert (2019), Krueger, Mitman, and Perri (2016), McKay, Nakamura, and Steinsson (2016), Auclert, Rognlie, and Straub (2018), Bayer, Luetticke, Pham-Dao, and Tjaden (2019), and Oh and Reis (2012), among many others. Many studies in this literature focus on the fact that even in advanced economies such as the U.S., a sizable fraction of households exhibit significantly higher MPC than what the PIH predicts. This paper contributes to this literature by exploiting a different margin: MPC is substantially higher in emerging economies than in developed economies. It finds that the difference in microlevel consumption behavior matters for aggregate dynamics to the extent that it can explain one of the most salient patterns of emerging market business cycles, excess consumption volatility.

Second, there have been recent efforts to expand the first literature to open and emerging economies, such as Auclert, Rognlie, Souchier, and Straub (2021), De Ferra, Mitman, and Romei (2020), Zhou (2021), Ferrante and Gornemann (2022), Guntin, Ottonello, and Perez (2022), Guo, Ottonello, and Perez (2022), Oskolkov (2022), Villalvazo (2021), and Sunel (2018). My paper contributes to this literature by studying emerging market business cycles through a HASOE model disciplined by micro moments. Among the abovementioned papers, my paper is most closely related to Guntin et al. (2022). These two papers share the view that micro data, when interpreted through a heterogeneous-agent model, provide important information about what drives

[2]Those facing a bad idiosyncratic income shock need to cash out their assets to smooth consumption. When financial friction is heightened, however, it becomes more costly to cash out assets, and they fail to smooth consumption more significantly. Those who do not face an immediate need to cash out their assets at the moment of heightened financial friction recognize that it will be more expensive to cash out their assets for a while. Therefore, they prepare themselves by accumulating more buffer stocks and reducing consumption.

large consumption fluctuations. However, they come to different conclusions: Guntin et al. (2022) find that the permanent income effect of a trend shock drives large consumption swings, while I find that a financial friction shock and a stationary productivity shock mainly drive consumption fluctuations. In this sense, a long-standing debate on what drives consumption fluctuations in emerging economies, particularly between a trend shift and financial frictions[3], continues in the heterogeneous-agent open economy landscape.[4]

Third, there is rich literature devoted to explaining emerging market business cycles, in which representative-agent models are dominantly used. Important examples include Neumeyer and Perri (2005), Aguiar and Gopinath (2007), Uribe and Yue (2006), Garcia-Cicco et al. (2010), Chang and Fernández (2013), Chen and Crucini (2016), and Fernández-Villaverde, Guerrón-Quintana, Rubio-Ramirez, and Uribe (2011), among many others. My paper contributes to this literature by bringing new intuitions and tools from the first literature regarding how household heterogeneity and microlevel behavior affect aggregate dynamics, applying them in the context of emerging market business cycles, and deriving new explanations.

Fourth, in terms of methodology, this paper has a commonality with Bayer, Born, and Luetticke (2022) and Auclert, Rognlie, and Straub (2020) in that Bayesian methods are applied to estimate a heterogeneous-agent model. Bayesian estimation requires a model to be solved many times. It only recently became possible to solve heterogeneous-agent models fast enough to conduct Bayesian estimation due to the development of new computational methods. The main contributors to this recent computational development include Auclert, Bardóczy, Rognlie, and Straub (2021), Boppart, Krusell, and Mitman (2018), Ahn, Kaplan, Moll, Winberry, and Wolf (2018), Bayer and Luetticke (2020), Winberry (2018), and Reiter (2009). Among the new methods, I use the one developed by Auclert et al. (2021).

The remainder of this paper is organized as follows. Section 2 specifies models. Section 3 takes the models to data through a two-step procedure composed of calibration and Bayesian estimation. Section 4 augments the HASOE model with a financial friction shock. Section 5 conducts a counterfactual experiment in which Peruvian households are replaced with those exhibiting U.S. MPCs. Section 6 concludes.

2 Model

One of the goals of this paper is to compare the ways in which the RASOE and HASOE models explain emerging market business cycles. In this section, I introduce a standard RASOE model that

[3]For a trend shift, see Aguiar and Gopinath (2007). For financial frictions, see Neumeyer and Perri (2005), Garcia-Cicco, Pancrazi, and Uribe (2010), Chang and Fernández (2013), Mendoza (2010), and Bianchi (2011).

[4]For interested readers, I discuss key differences between the two papers (in both micro moments and macro models) and how they come to different conclusions in Online Appendix J.

is widely used in the literature (Neumeyer and Perri (2005), Aguiar and Gopinath (2007), Garcia-Cicco et al. (2010), and Chang and Fernández (2013)) and a HASOE model that I construct by incorporating household heterogeneity into the RASOE model.

2.1 Representative-Agent Small Open Economy (RASOE) Model

In this subsection, I present a decentralized version of a standard RASOE model.[5] Consider an economy composed of representative households, firms, and banks.

Households. Households trade assets A_t, which are the shares of firms, and supply labor L_t. They optimize Greenwood, Hercowitz, and Huffman (1988)'s preference (GHH preference hereafter) subject to budget constraints and the no-Ponzi-game constraint as follows.

$$\max_{\{C_t,A_t,L_t\}_{t=0}^{\infty}} E_0 \sum_{t=0}^{\infty} (\beta_R)^t \frac{(C_t - \kappa_R X_{t-1} L_t^{1+\omega})^{1-\gamma}}{1-\gamma}$$
$$s.t. \quad C_t + A_t = w_t L_t + (1+r_t^a)A_{t-1},\ t \geq 0, \text{ and}$$
$$\lim_{j\to\infty} E_t \left[A_{t+j} \Big/ \left(\prod_{s=1}^{j} (1+r_{t+s}^a) \right) \right] \geq 0,$$

where C_t is consumption, w_t is wage, $(1+r_t^a)$ is the gross return on A_{t-1}, and X_{t-1} is the stochastic trend of the economy. As a result of imposing the GHH preference, the wealth effect is removed in the labor supply decision, as L_t is determined by $w_t = (1+\omega)\kappa_R X_{t-1} L_t^{\omega}$.[6]

Firms. Competitive firms produce output Y_t using capital K_{t-1} and labor L_t, make investment I_t, and borrow funds F_t from domestic banks. They solve the following optimization problem.

$$\max_{\{K_t,F_t,L_t,Y_t,I_t,\Pi_t\}_{t=0}^{\infty}} E_0 \sum_{t=0}^{\infty} Q_{0,t}\Pi_t \tag{1}$$
$$s.t. \quad \Pi_t = Y_t - w_t L_t - I_t - \Phi(K_t, K_{t-1}) + F_t - (1+r_{t-1})F_{t-1},$$
$$Y_t = z_t K_{t-1}^{\alpha} (X_t L_t)^{1-\alpha},$$
$$I_t = K_t - (1-\delta)K_{t-1},$$
$$\Phi(K_t, K_{t-1}) = \frac{\phi}{2}\left(\frac{K_t}{K_{t-1}} - g^* \right)^2 K_{t-1},$$

[5] In Online Appendix A.4, I present an equivalent, centralized version of the RASOE model, which appears far more frequently in related studies. Here, I intentionally present a decentralized version because I will construct a HASOE model by incorporating household heterogeneity into this version.

[6] The wealth effect removal is an important reason why the GHH preference is common in emerging market business cycle models; if it is not removed, the wealth effect can create a countercyclical labor supply, which is inconsistent with data, particularly when a model is fitted to an emerging economy with large consumption fluctuations.

$$Q_{0,t} = \begin{cases} 1 & \text{if} \quad t = 0, \\ 1/(\prod_{s=1}^{t}(1+r_s^a)) & \text{if} \quad t \geq 1, \end{cases} \quad \text{and}$$

$$\lim_{j\to\infty} E_t\left[F_{t+j}\Big/(\prod_{s=1}^{j}(1+r_{t+s}^a))\right] \leq 0,$$

where Π_t is the per-period profit, $\Phi(K_t, K_{t-1})$ is an adjustment cost for capital accumulation, z_t is the stationary component of firms' productivity, and X_t is the nonstationary component (or stochastic trend) of firms' productivity. Firms discount profit flows using return rates on their shares. As we shall see below, the firms' objective function is the total value of the firms.

Asset Return and Price. Let s_t be the shares of firms that each representative household holds when the total shares are normalized to 1. Let q_t be the price of the shares after the current profits are distributed as dividends. Since total shares are normalized to 1, q_t also represents the total value of the firms after distributing current profits. By construction, we have the following equations.

$$\begin{aligned} & A_t = s_t q_t, \quad (1+r_t^a)A_{t-1} = s_{t-1}(\Pi_t/s_{t-1} + q_t), \quad \text{and} \quad s_t = 1, \quad \forall t \\ \Rightarrow \quad & A_t = q_t, \quad t \geq 0, \quad \text{and} \qquad (2) \\ & 1 + r_t^a = (\Pi_t + q_t)/q_{t-1}, \quad t \geq 0. \qquad (3) \end{aligned}$$

By iterating equation (3) forward to solve q_0 and taking an expectation, we can verify that the firms' objective function $E_0 \sum_{t=0}^{\infty} Q_{0,t}\Pi_t$ is equal to $\Pi_0 + q_0$. In other words, firms maximize their total value before distributing current profits. This explains why firms discount profit flows with asset returns in their optimization.

It is worth noting how $\{r_t^a\}_{t=0}^{\infty}$ are determined in equilibrium. From period 1 onward, $\{r_t^a\}_{t=1}^{\infty}$ are subject to the following optimality condition for firms.

$$E_t\left[(1+r_t)/(1+r_{t+1}^a)\right] = 1, \quad t \geq 0. \qquad (4)$$

When we consider impulse responses to an MIT shock (*i.e.*, without aggregate uncertainty), this equation becomes $r_{t+1}^a = r_t$, $t \geq 0$. On the other hand, the return in period 0, r_0^a, is not determined by equation (4). Instead, r_0^a is solely determined by Π_0, q_0, and q_{-1} through equation (3).

Banks. Banks in this economy play a passive role. They lend funds F_t to firms by issuing debt D_t in the international financial market. Since they are competitive, they charge an interest rate on F_t that is equal to the financing cost, which is the interest rate in the international financial market, r_t. Moreover, F_t and D_t should be balanced in each period or, equivalently,

$$F_t = D_t, \quad t \geq 0. \qquad (5)$$

International Financial Market. The interest rate r_t in the international financial market is specified as follows.

$$r_t = r^* + \psi\left\{\exp\left(\frac{\bar{D}_t/X_t - \tilde{D}^*}{\tilde{Y}^*}\right) - 1\right\} - \theta_z(z_t - 1) - \theta_g\left(\frac{g_t}{g^*} - 1\right) + \mu_t - 1, \quad t \geq 0, \tag{6}$$

where $\psi > 0$, $\theta_z > 0$, and $\theta_g > 0$. $\bar{D}_t$ is the cross-sectional average of banks' international debt. Individual banks and firms regard $\bar{D}_t$ as exogenous, but at equilibrium, individual banks' international debt D_t is equal to $\bar{D}_t$. $\tilde{D}^*$, $\tilde{Y}^*$, g^*, and r^* are the long-run averages of $\bar{D}_t/X_t$, Y_t/X_{t-1}, $g_t := X_t/X_{t-1}$, and r_t, respectively, and μ_t is an exogenous disturbance to interest rates.[7]

Aggregate Shocks. Three aggregate shocks hit the economy: a stationary productivity shock z_t, a trend shock g_t, and an interest rate shock μ_t. I assume that each shock follows an AR(1) process:

$$\begin{aligned} \log z_t &= \rho_z \log z_{t-1} + \varepsilon_t^z, \quad \varepsilon_t^z \sim N(0, \sigma_z^2), \\ \log(g_t/g^*) &= \rho_g \log(g_{t-1}/g^*) + \varepsilon_t^g, \quad \varepsilon_t^g \sim N(0, \sigma_g^2), \quad \text{and} \\ \log \mu_t &= \rho_\mu \log \mu_{t-1} + \varepsilon_t^\mu, \quad \varepsilon_t^\mu \sim N(0, \sigma_\mu^2). \end{aligned} \tag{7}$$

Trade Balance. The trade balance of the economy, TB_t, is determined as follows.

$$TB_t = -D_t + (1 + r_{t-1})D_{t-1}, \quad t \geq 0. \tag{8}$$

In Online Appendix A.1, I present the complete set of equilibrium conditions.

2.2 Heterogeneous-Agent Small Open Economy (HASOE) Model

I construct a HASOE model by incorporating Kaplan et al. (2018)'s two-asset household heterogeneity over liquid and illiquid assets into the RASOE model presented in section 2.1.[8] I adopt two-asset heterogeneity (instead of one-asset heterogeneity) because it allows my model to capture both realistically high MPC and the correct amount of aggregate capital.[9] Consider an economy composed of heterogeneous households and representative firms and banks.

Working Households. Almost all households (with fraction p) work and earn labor income (work-

[7] A reduced-form specification of the interest rate in the international financial market, such as equation (6), is widely used in emerging market business cycle studies, particularly when models are intended to be first-order approximated with respect to aggregate shocks. (See, for instance, Neumeyer and Perri (2005), Garcia-Cicco et al. (2010), and Chang and Fernández (2013).) In equation (6), interest rates are higher when the international debt $\bar{D}_t$ is larger and the productivities z_t and g_t are lower. In this aspect, equation (6) reflects the theoretical implication of sovereign default models such as Arellano (2008) and Mendoza and Yue (2012) in a reduced-form manner.

[8] However, I do not incorporate the nominal rigidity in Kaplan et al. (2018)'s model because my model is intended to be as close as possible to the conventional real models of emerging economies except for household heterogeneity.

[9] See footnote 1. Additionally, see Kaplan and Violante (2018) for a more detailed discussion.

ers hereafter). Workers face idiosyncratic earnings risk and trade liquid and illiquid assets. Liquid assets are bank deposits, and illiquid assets are the shares of firms. Compared to liquid assets, illiquid assets yield higher returns but are more expensive to trade. Workers exhibit idiosyncratic labor productivity, which can be decomposed into a component predictable with their observable characteristics (Γ) and an unpredictable component bearing earnings risk (e). Workers cannot take short positions in both liquid and illiquid assets. Each worker i solves the following problem.[10]

$$\max_{\{c_{i,t},b_{i,t},a_{i,t},v_{i,t}\}_{t=0}^{\infty}} E_0 \sum_{t=0}^{\infty} \beta^t \frac{c_{i,t}^{1-\gamma}}{1-\gamma} \tag{9}$$

$$\begin{aligned} s.t. \quad & c_{i,t} + b_{i,t} + v_{i,t} + \chi_t(v_{i,t}, a_{i,t-1}; \Gamma_i) = w_t \Gamma_i e_{i,t} \bar{l}_t + (1-\xi)(1+r_t^b) b_{i,t-1}, \qquad (10) \\ & v_{i,t} = a_{i,t} - (1+r_t^a) a_{i,t-1}, \quad \text{and} \\ & b_{i,t} \geq 0, \quad a_{i,t} \geq 0. \end{aligned}$$

In the budget constraint (10), $b_{i,t}$ and $a_{i,t}$ are liquid and illiquid asset holdings, respectively, and $(1-\xi)(1+r_t^b)$ and $(1+r_t^a)$ are their gross return rates. Since $r^a = r^b$ on the balanced growth path and $\xi > 0$, illiquid assets yield higher returns than liquid assets.[11] To trade illiquid assets, workers must pay adjustment cost $\chi_t(v_{i,t}, a_{i,t-1}; \Gamma_i)$.

For the functional form of the illiquid asset adjustment cost, I closely follow Auclert et al. (2021)'s discrete-time version of Kaplan et al. (2018)'s model as follows.

$$\chi_t(v_{i,t}, a_{i,t-1}; \Gamma_i) = \chi_1 \left| \frac{v_{i,t}}{(1+r_t^a) a_{i,t-1} + \chi_0 \Upsilon(\Gamma_i) X_{t-1}} \right|^{\chi_2} \left((1+r_t^a) a_{i,t-1} + \chi_0 \Upsilon(\Gamma_i) X_{t-1} \right),$$

where $\chi_0 > 0, \chi_1 > 0$, and $\chi_2 > 1$. X_{t-1} is the stochastic trend of the economy, and $\Upsilon(\Gamma_i)$ is the predictable component of earnings in a detrended steady state, $E\left[w_t \Gamma_i e_{i,t} \bar{l}_t / X_{t-1} \,\middle|\, \Gamma_i \right]$.

Parameter χ_1 is the scaling factor for the adjustment cost and determines the overall importance

[10] Unlike in the RASOE model in subsection 2.1, I do not let households choose labor supply under the GHH preference. Instead, I delegate the labor supply decision to a labor union and write its optimization problem such that the labor supply equation coincides with that of the RASOE model. The reason is as follows: when individual households facing idiosyncratic earnings risk choose labor supply under the GHH preference, they exhibit abnormally high MPC compared to data. Under the GHH preference, households try to smooth $(c - h(l))$ rather than c, where $h(l)$ is labor disutility. As a result, consumption comoves too strongly with earnings, yielding excessively high MPC.

Alternatively, one might consider imposing separable labor disutility instead of the GHH preference on individual households. Then, the issue discussed in footnote 6 returns; the wealth effect can create a countercyclical labor supply pattern when the model is fitted to emerging economies' large consumption swings.

In the heterogeneous-agent New Keynesian (HANK) literature, researchers also find that imposing the GHH preference creates problems, although in different dimensions. Some researchers prefer to circumvent these problems by introducing a labor union to which the labor supply decision is delegated. (See Auclert, Bardóczy, and Rognlie (2021) for a detailed discussion.) In the same spirit, I introduce a labor union to circumvent the problem caused by individual labor supply decisions under the GHH preference.

[11] As we shall see later, the liquid assets are bank deposits, and $\xi(1+r_t^b)$ is a deposit service fee that banks charge.

of the adjustment cost in workers' optimization. When χ_1 increases, workers i) save more and ii) exhibit higher MPC for two reasons. First, workers exhibit stronger precautionary saving behavior because they fear the realization of a low-earnings path more intensely, as illiquid assets become more expensive to cash out. Second, workers who are currently facing a bad earnings shock fail to smooth consumption more significantly; thus, they save more (as they cash out their assets less), and their consumption responds more strongly to a transitory income shock.

Parameter χ_2 captures how less costly it is for wealthier households to adjust illiquid asset positions. When $\chi_2 = 1$, the adjustment cost becomes proportional to the absolute amount of illiquid asset position adjustment, $v_{i,t}$. As χ_2 increases above one, the adjustment cost becomes less costly for wealthier households, who have higher values of $(1+r_t^a)a_{i,t-1}$. For this reason, parameter χ_2 is useful to make wealthy and poor households face different degrees of financial frictions and thus exhibit different MPCs. Later, I calibrate χ_1 and χ_2 (jointly with β) by targeting ten MPC moments over earnings deciles and workers' aggregate wealth.[12]

In the budget constraint (10), workers' earnings are $w_t\Gamma_i e_{i,t}\bar{l}_t$, where w_t is a wage rate per efficiency unit of labor, Γ_i and $e_{i,t}$ are the predictable and unpredictable components of idiosyncratic labor productivity, respectively, and $\bar{l}_t$ is a common labor supply determined by a labor union. The labor union makes a labor supply decision by linearly weighting the aggregate labor income $w_t L_t$ and labor disutility $X_{t-1}\frac{1}{1+\omega}\bar{l}_t^{1+\omega}$ as follows.

$$\begin{aligned} &\max_{\bar{l}_t, L_t} \; w_t L_t - \kappa\left(X_{t-1}\frac{1}{1+\omega}\bar{l}_t^{1+\omega}\right) \\ &s.t. \quad L_t = p\bar{\Gamma}\bar{e}\bar{l}_t, \end{aligned} \tag{11}$$

where $\kappa > 0$, L_t is aggregate labor supply (in efficiency units), and $\bar{\Gamma}$ $(:= E[\Gamma_i])$ and $\bar{e}$ $(:= E[e_{i,t}])$ are the cross-sectional average of the predictable and unpredictable components of workers' idiosyncratic productivity, respectively. As a result of the optimization, the labor supply is determined as follows.

$$w_t(p\bar{\Gamma}\bar{e})^{1+\omega} = \kappa X_{t-1}L_t^{\omega}, \quad t \geq 0. \tag{12}$$

This labor supply equation is identical to that in the RASOE model under $(1+\omega)\kappa_R = \frac{\kappa}{(p\bar{\Gamma}\bar{e})^{1+\omega}}$. In other words, the HASOE model does not deviate from the RASOE model in the dimension of the aggregate labor supply.

The predictable component of idiosyncratic labor productivity, Γ_i, follows a lognormal distribution: $\log\Gamma_i \sim N(0, \sigma_\Gamma)$. The unpredictable component of idiosyncratic labor productivity, $e_{i,t}$, is

[12] What about χ_0? The term $\chi_0\Upsilon(\Gamma_i)X_{t-1}$ appears in the functional form of $\chi_t(v_{i,t}, a_{i,t-1}; \Gamma_i)$ only to ensure that the denominator of $[v_{i,t} \;/\; \{(1+r_t^a)a_{i,t-1} + \chi_0\Upsilon(\Gamma_i)X_{t-1}\}]$ is nonzero. (Reflecting its purpose, in calibration, I assign an arbitrary small number, 0.01, to χ_0.) In this term, χ_0 is augmented with $\Upsilon(\Gamma_i)X_{t-1}$ to make workers' problem i) stationary after detrending and ii) identical across different Γ_i's after normalization. See Online Appendix B.3.

composed of a persistent component ($e_{1,i,t}$) and a transitory component ($e_{2,i,t}$) as follows.[13]

$$\begin{aligned}\log e_{i,t} &= \log e_{1,i,t} + \log e_{2,i,t},\\ \log e_{1,i,t} &= \rho_{e_1} \log e_{1,i,t-1} + \varepsilon_{1,i,t}, \quad \varepsilon_{1,i,t} \sim N(0, \sigma^2_{\varepsilon_1}), \quad \text{and}\\ \log e_{2,i,t} &= \varepsilon_{2,i,t}, \quad \varepsilon_{2,i,t} \sim N(0, \sigma^2_{\varepsilon_2}).\end{aligned}$$

Let $G(\Gamma)$ denote the cumulative distribution function (CDF) of Γ, and $\Psi_t(e_1, e_2, b_-, a_-|\Gamma)$ denote the CDF of (e_1, e_2, b_-, a_-) conditional on Γ in period t among workers. Moreover, let $c_t(e_1, e_2, b_-, a_-; \Gamma)$, $b_t(e_1, e_2, b_-, a_-; \Gamma)$, and $a_t(e_1, e_2, b_-, a_-; \Gamma)$ denote the policy functions of workers with Γ in period t.[14] The law of motion for $\Psi_t(e_1, e_2, b_-, a_-|\Gamma)$ is determined as follows.

$$\begin{aligned}\Psi_{t+1}(e_1', e_2', b, a|\Gamma) = \int_{e_1, e_2, b_-, a_-} &\Big[P(e_{1,t+1} \le e_1'|e_{1,t} = e_1)\, P(e_{2,t+1} \le e_2')\\ &I_{\{b_t(e_1,e_2,b_-,a_-;\Gamma) \le b,\ a_t(e_1,e_2,b_-,a_-;\Gamma) \le a\}}(e_1, e_2, b_-, a_-)\Big]\, d\Psi_t(e_1, e_2, b_-, a_-|\Gamma),\end{aligned} \tag{13}$$

where $I_{\{X\}}(x)$ is an indicator function (*i.e.*, $I_{\{X\}}(x) = 1$ if $x \in X$, 0 otherwise).

Entrepreneurial Households A tiny fraction $(1-p)$ of households do not work and earn income only from the returns on firm share holdings and pure rents from banks (entrepreneurs hereafter). Unlike workers, entrepreneurs do not face idiosyncratic earnings risk and do not pay adjustment cost when trading firm shares. Entrepreneurs solve the following optimization problem.

$$\begin{aligned}&\max_{\{C_t^E, A_t^E\}_{t=0}^{\infty}} E_0 \sum_{t=0}^{\infty} (\beta_E)^t \frac{(C_t^E)^{1-\gamma}}{1-\gamma}\\ s.t. \quad &C_t^E + A_t^E = R_t^E + (1 + r_t^a) A_{t-1}^E, \quad \text{and}\\ &\lim_{j \to \infty} E_t \left[A_{t+j}^E \Big/ \left(\prod_{s=1}^{j} (1 + r_{t+s}^a) \right) \right] \ge 0,\end{aligned} \tag{14}$$

where C_t^E, A_t^E, and R_t^E are entrepreneurs' consumption, shareholdings, and pure rents, respectively.

I introduce entrepreneurs in my model for three reasons. First, as Bayer et al. (2019) note, the presence of entrepreneurs allows the model to have a more realistic wealth distribution, in which a tiny fraction of the richest households hold a significant fraction of wealth. Second, the top wealth share is unlikely to be accumulated by a precautionary saving motive. By introducing entrepreneurs, the aggregate precautionary savings can exclude the top wealth share in the model

[13] The labor productivity process specification in the model is consistent with the income process specification imposed in the MPC estimation. See Online Appendix F.1.

[14] I attach the time subscript to the policy functions because they depend on the state vector $\mathbf{S}_t$, which includes conditional distribution $\Psi_t(e_1, e_2, b_-, a_-|\Gamma)$, stochastic trend X_{t-1}, and other predetermined and exogenous variables in the economy. See footnote 16 for details on the state vector $\mathbf{S}_t$.

(as it is held by entrepreneurs) and be calibrated by matching a relevant empirical target.[15] Third, as also noted by Bayer et al. (2019), the pure rents of the economy can be allocated back to households without distorting factor returns or introducing a new asset.

Banks. As in the RASOE model, banks lend funds F_t to firms and finance part of the funds by issuing debt D_t in the international financial market. In addition, banks in the HASOE model play two more roles. First, they also finance funds by intermediating household deposits, B_t. Thus, equation (5) in the RASOE model is replaced with the following equation in the HASOE model:

$$F_t = D_t + B_t, \quad t \geq 0. \tag{15}$$

The gross rate of banks' financing cost for the intermediation of household deposit B_{t-1} is $(1+r_t^b)$. This financing cost consists of a gross return on household deposits $(1-\xi)(1+r_t^b)$ and a service charge $\xi(1+r_t^b)$. Banks can frictionlessly adjust the sources of financing, and thus, the financing cost is equalized between the two sources, household deposits and international debt, as follows.

$$1+r_t^b = 1+r_{t-1}, \quad t \geq 0. \tag{16}$$

Second, banks facilitate trades in firm shares among workers and earn facilitation fees χ_t^{agg}. Through these two new roles, banks now create pure rents, $\xi(1+r_t^b)B_{t-1}$ and χ_t^{agg}. As discussed above, entrepreneurs hold the right to claim these pure rents:

$$(1-p)R_t^E = \xi(1+r_t^b)B_{t-1} + \chi_t^{agg}. \tag{17}$$

Other Parts. Other parts of the economy are identical to the corresponding parts in the RASOE model. Specifically, firms solve the problem (1). Asset return r_t^a and price q_t satisfy

$$\begin{aligned} &a_{i,t} = s_{i,t} q_t, \quad (1+r_t^a) a_{i,t-1} = s_{i,t-1}(\Pi_t / s_{t-1} + q_t), \\ &A_t^E = s_t^E q_t, \quad \text{and} \quad (1+r_t^a) A_{t-1}^E = s_{t-1}^E (\Pi_t / s_{t-1} + q_t), \quad \forall t, \end{aligned}$$

where $s_{i,t}$, s_t^E, and s_t are worker i's shares of firms, an entrepreneur's shares of firms, and the total shares of firms, respectively. Under the normalization that $s_t = 1$, asset return r_t^a and price q_t again satisfy equations (2) and (3). The interest rate r_t in the international financial market is determined by equation (6). Three aggregate shocks, z_t, g_t, and μ_t, hit the economy and are assumed to follow an AR(1) process, as specified in equation (7). Trade balance is determined by equation (8).

Aggregation. Let C_t, A_t, B_t, and χ_t^{agg} denote the aggregate consumption, firm value, deposit, and

[15] As we shall see later, the power of precautionary saving plays several important roles in the main results of this paper. Without having entrepreneurs in the model, the power of precautionary saving can be significantly overrated.

illiquid asset adjustment cost, respectively, and C_t^W, A_t^W, B_t^W, and χ_t^W denote the cross-sectional average of workers' consumption, illiquid asset holdings, liquid asset holdings, and illiquid asset adjustment cost, respectively. The aggregate quantities are constructed as follows.

$$C_t = pC_t^W + (1-p)C_t^E, \quad C_t^W = \int_\Gamma \int_{e_1,e_2,b_-,a_-} c_t(e_1,e_2,b_-,a_-;\Gamma)\, d\Psi_t dG. \tag{18}$$

$$A_t = pA_t^W + (1-p)A_t^E, \quad A_t^W = \int_\Gamma \int_{e_1,e_2,b_-,a_-} a_t(e_1,e_2,b_-,a_-;\Gamma)\, d\Psi_t dG. \tag{19}$$

$$B_t = pB_t^W, \quad B_t^W = \int_\Gamma \int_{e_1,e_2,b_-,a_-} b_t(e_1,e_2,b_-,a_-;\Gamma)\, d\Psi_t dG. \tag{20}$$

$$\chi_t^{agg} = p\chi_t^W, \quad \chi_t^W = \int_\Gamma \int_{e_1,e_2,b_-,a_-} \chi_t\big(a_t(e_1,e_2,b_-,a_-;\Gamma) - (1+r_t^a)a_-, a_-;\Gamma\big)\, d\Psi_t dG. \tag{21}$$

Equilibrium. Given the initial conditions on $\Psi_0(e_1,e_2,b_-,a_-|\Gamma)$, X_{-1}, A_{-1}, A_{-1}^E, K_{-1}, D_{-1}, B_{-1}, F_{-1}, and r_{-1},[16] *(i)* individual workers' policy functions $\{c_t(e_1,e_2,b_-,a_-;\Gamma), b_t(e_1,e_2,b_-,a_-;\Gamma), a_t(e_1,e_2,b_-,a_-;\Gamma)\}_{t=0}^\infty$ that solve workers' problem (9), *(ii)* conditional cumulative distributions $\{\Psi_t(e_1,e_2,b_-,a_-|\Gamma)\}_{t=1}^\infty$ that evolve over time according to equation (13), *(iii)* prices and aggregate variables $\{r_t^b, r_t^a, r_t, w_t, q_t, \bar{l}_t, L_t, \Pi_t, Y_t, I_t, K_t, F_t, D_t, TB_t, C_t, C_t^E, A_t, A_t^E, R_t^E, B_t, \chi_t^{agg}\}_{t=0}^\infty$ satisfying the optimality conditions for entrepreneurs' problem (14), the optimality conditions for firms' problem (1), aggregation equations (18)-(21), and other equilibrium conditions (2), (3), (6), (8), (11), (12), (15), (16), and (17), and *(iv)* aggregate shocks $\{z_t, g_t, \mu_t\}_{t=0}^\infty$ that follow the stochastic processes specified in equation (7) constitute the equilibrium of the economy.

2.3 Solving the Models

To study business cycles using Bayesian estimation, a model needs to be solved fast enough. There is well-established literature on the Bayesian estimation of representative-agent models, but for heterogeneous-agent models, it only recently became possible to solve these models fast enough to conduct Bayesian estimation due to the development of new solution methods.[17]

Among the new methods, I adopt Auclert et al. (2021)'s method, which computes linearized aggregate dynamics based on Boppart et al. (2018)'s finding that the MA(∞) representation of a linearized model regarding aggregate uncertainty can be fully recovered from impulse responses to an MIT shock due to certainty equivalence. Since this method exploits impulse responses to an MIT shock, in Online Appendices A.1 and B.1, I characterize the equilibrium of the RASOE and HASOE models, respectively, when the economy is subject to deterministic paths of aggregate

[16] The initial conditions given here specify the predetermined objects in state vector $\mathbf{S}_0$. Referring back to footnote 14, state vector $\mathbf{S}_t$ is composed of predetermined objects $\Psi_t(e_1,e_2,b_-,a_-|\Gamma)$, X_{t-1}, A_{t-1}, A_{t-1}^E, K_{t-1}, D_{t-1}, B_{t-1}, F_{t-1}, and r_{t-1} and aggregate exogenous variables z_t, g_t, and μ_t.

[17] The main contributors to this recent development include Auclert et al. (2021), Boppart et al. (2018), Ahn et al. (2018), Bayer and Luetticke (2020), Winberry (2018), and Reiter (2009).

exogenous variables $\{z_t, g_t, \mu_t\}_{t=0}^{\infty}$.

Both my RASOE and HASOE models exhibit a stochastic trend, and thus, the equilibrium needs to be detrended to become stationary. In Online Appendices A.2 and B.2, I present a detrended stationary equilibrium of the RASOE and HASOE models, respectively. I solve the detrended equilibrium using Auclert et al. (2021)'s method. Online Appendix C discusses how this method is applied to the detrended equilibrium. Then, in Online Appendix D, I discuss how to recover the original equilibrium from the detrended equilibrium.

3 Taking Models to Data

Both the RASOE and HASOE models are fitted to the Peruvian economy. Specifically, I take the models to Peruvian data through two steps. First, I calibrate parameters determining key moments on the balanced growth path. Second, I estimate parameters governing aggregate dynamics around the balanced growth path using Bayesian methods. This two-step procedure is possible because the parameters estimated in the second step do not affect the balanced growth path.

3.1 Calibration

In both the RASOE and HASOE models, the time unit is a quarter. Table 1 reports the calibrated parameter values and target moments or information sources used for the calibration. For parameters $g^*, r^*, \alpha, \delta, \tilde{D}^*, \gamma$, and ω, I assign the same parameter values to the RASOE and HASOE models. Parameters g^* and r^* are calibrated to the long-run average output growth rate and real lending interest rate in data, respectively. Parameters α, δ, and $\tilde{D}^*$ are calibrated by matching the long-run average capital-output ratio (10.91), investment-output ratio (0.191), and trade-balance-to-output ratio (0.043) from data in the related equilibrium conditions.[18,19] Parameters γ and ω are

[18]The output growth, investment-output ratio, and trade-balance-to-output ratio are computed using Banco Central de Reserva del Perú (BCRP)'s national account data from 1980–2018. (Specifically, real quarterly national account data are obtained, seasonally adjusted, and transformed to a per capita term.) The capital-output ratio is computed using Feenstra, Inklaar, and Timmer (2015)'s Penn World Table (version 9.1) capital and output data from 1980–2017. The real lending interest rates are computed by deflating BCRP's data on lending rates in foreign currency (TAMEX) from 1992–2018 with the expected inflation on U.S. CPIs. The expected inflation is constructed by taking an average inflation rate over the current and past three quarters, following Neumeyer and Perri (2005) and Uribe and Yue (2006). (Atkeson and Ohanian (2001) empirically support this approximation of expected inflation.)

[19]In the literature, interest rates are often constructed by adding J.P. Morgan's EMBIG sovereign bond spreads with U.S. interest rates. ('EMBIG interest rates' hereafter). Instead, I construct interest rates based on BCRP data series ('BCRP interest rates' hereafter). I find that these two interest rates are highly correlated (correlation 0.863), but their means are substantially different; the average nonannualized quarterly EMBIG interest rate is 0.007, while that of the BCRP interest rate is 0.021. Given that the long-run average value of TB_t/Y_t is calibrated to its data counterpart, there is a one-to-one relationship between r^* and D_t/Y_t on the balanced growth path through an equilibrium condition $r^* = \frac{TB_t/Y_t}{D_t/Y_t} g^* + (g^* - 1)$. Using this equation, I recover the value of r^* that corresponds to the long-run average value of D_t/Y_t in Milesi-Ferretti and Lane (2017)'s dataset. The value of such r^* is 0.025, which is far closer to the average BCRP rate than the average EMBIG rate. Based on this observation, I use BCRP interest rates rather than EMBIG

Table 1: Calibration for the Peruvian Economy

	Description	Value	Target / Source
Common in RASOE and HASOE			
g^*	long-run average gross growth rate	1.004	$E[Y_t/Y_{t-1}]$
r^*	long-run average lending rate	0.021	BCRP, U.S. CPI
α	capital income share	0.378	$(K/Y)(r^*+\delta)/g^*$
δ	depreciation rate	0.014	$g^*(I/Y)/(K/Y)-(g^*-1)$
$\tilde{D}^*$	international debt	10.57	$(TB/Y)\,\tilde{Y}^*/(1+r^*-g^*)$
γ	inverse of IES	2.000	Garcia-Cicco et al. (2010)
ω	inverse of labor supply elasticity	0.600	Garcia-Cicco et al. (2010)
RASOE only			
β_R	representative households' discount factor	0.987	$(g^*)^\gamma/(1+r^*)$
κ_R	scale parameter for labor disutility	1.660	$L=1$ on the b.g.p
HASOE only - earnings process			
σ_Γ	S.D. of the predictable component	0.656	ENAHO
ρ_{e_1}	persistence of the unpredictable, AR(1) component	0.968	ENAHO
σ_{ε_1}	S.D. of shocks to the unpredictable, AR(1) component	0.134	ENAHO
σ_{ε_2}	S.D. of shocks to the unpredictable, *i.i.d.* component	0.464	ENAHO
HASOE only - targeting MPCs & Workers' Aggregate Wealth			
β	workers' discount factor	0.948	MPC estimates & earnings-income ratio in ENAHO
χ_1	scale parameter for illiquid asset adjustment cost	6.694	MPC estimates & earnings-income ratio in ENAHO
χ_2	convexity parameter for illiquid asset adjustment cost	1.724	MPC estimates & earnings-income ratio in ENAHO
χ_0	non-zero denominator in illiquid asset adjustment cost	0.010	
HASOE only - other parameters			
κ	scale parameter for labor disutility	5.449	$L=1$ on the b.g.p
ξ	long-run average spread	0.020	BCRP, U.S. CPI
β_E	entrepreneurs' discount factor	0.987	$(g^*)^\gamma/(1+r^*)$
p	share of workers ($=1-$ share of entrepreneurs)	0.987	WID

Notes: The time unit is a quarter. 'b.g.p' in the 'Target/Source' column represents the balanced growth path.

assigned the values used in Garcia-Cicco et al. (2010), which are common in the related literature.

Parameters β_R and κ_R appear only in the RASOE model. Parameter β_R is calibrated such that representative households' Euler equation holds on the balanced growth path. Parameter κ_R is calibrated such that the aggregate labor supply is normalized to 1 on the balanced growth path.

Parameters σ_Γ, ρ_{e_1}, σ_{ε_1}, σ_{ε_2}, β, χ_1, χ_2, χ_0, κ, ξ, β_E, and p appear only in the HASOE model. Parameters σ_Γ, ρ_{e_1}, σ_{ε_1}, and σ_{ε_2} govern workers' earnings process. I calibrate them using earnings data from the 2011–2018 waves of a nationally representative Peruvian household survey, Encuesta

interest rates so that the model generates D_t/Y_t close to Milesi-Ferretti and Lane (2017)'s debt data.

Nacional de Hogares (ENAHO). I first remove predictable components from household earnings using observable characteristics. Then, I calibrate σ_Γ using the predictable components and ρ_{e_1}, σ_{ε_1}, and σ_{ε_2} by applying Floden and Lindé (2001)'s method to the residual components.[20]

Parameters β, χ_1, and χ_2 are calibrated by targeting MPC moments and workers' aggregate wealth.[21] For the target MPC moments, I estimate the Peruvian quarterly MPC at each residual earnings ($e_{i,t}$) decile by applying Blundell et al. (2008)'s method to the ENAHO data, as in Hong (2022).[22,23] To target the correct amount of workers' aggregate wealth, I match the earnings-income ratio (or, equivalently, (labor income) / (labor income + capital income)) on the balanced growth path of the model with the ratio in the ENAHO data, 0.817.[24] I implement this joint calibration by minimizing the following objective function J:

$$J = \varpi \left\{ \frac{w_t \bar{\Gamma} \bar{e} \bar{l}_t}{w_t \bar{\Gamma} \bar{e} \bar{l}_t + [r_t^a A_{t-1}^W + \{(1-\xi)(1+r_t^b)-1\} B_{t-1}^W]} \text{ on the balanced growth path} - 0.817 \right\}^2$$
$$+ (1-\varpi) \left\{ (MPC_{model} - MPC_{data}) \cdot V_{mpc} \cdot (MPC_{model} - MPC_{data})' \right\},$$

where ϖ denotes a weight on the first target (workers' earnings-income ratio), MPC_{model} and MPC_{data} denote a 10-by-1 vector of the model-predicted MPC on the balanced growth path and the estimated MPC at each earnings decile, respectively, and V_{mpc} is a weight matrix, which I choose to be a diagonal matrix whose diagonal elements equal the earnings share of each decile.

The joint calibration matches targets well, even though only three parameters are used to target eleven moments. First, workers' earnings-income ratio is 0.832 in the model, and its data counterpart is 0.817. Second, Figure 1 plots the model-predicted MPC (labeled 'Model') and the estimated MPC (labeled 'Data') at each earnings decile and shows that the former tracks the latter closely. Importantly, the data strongly suggest that households significantly deviate from the PIH, as the mean quarterly MPC estimate across deciles (0.209) is substantially greater than zero, and

[20] See Online Appendix F.1 for details.

[21] For χ_0, I assign an arbitrary small number, 0.01, as discussed in footnote 12.

[22] In estimating and targeting MPCs, observations are grouped by residual earnings $e_{i,t}$ (or, equivalently, unpredictable component of earnings) instead of total earnings ($w_t \Gamma_i e_{i,t} \bar{l}_t$) because $e_{i,t}$ bears risk and thus induces precautionary saving and MPC heterogeneity, while Γ_i does not.

[23] Compared to Hong (2022), the consumption measure is changed from nondurable consumption to total consumption (including durable consumption) to be consistent with the aggregate consumption measure. The sample period is also changed to 2011–2018. Some of the early waves (2004–2010) used in Hong (2022) are not used here because quarterly expenses of some key durable goods are unavailable in these waves. Online Appendix F provides further details of the MPC estimation and data processing procedures.

[24] In ENAHO, labor and capital incomes are not distinguishable within self-employment income. As in Diaz-Gimenez, Quadrini, and Rios-Rull (1997), Krueger and Perri (2006), and Hong (2022), I split self-employment income into labor and capital income parts using the ratio between unambiguous labor and capital incomes. In ENAHO, the ratio of (unambiguous labor income) / (unambiguous labor income + unambiguous capital income) is 0.817, and it becomes the earnings-income ratio once self-employment income is split according to this ratio. This ratio is close to the ratio that Diaz-Gimenez et al. (1997) and Krueger and Perri (2006) use for their U.S. sample, 0.864.

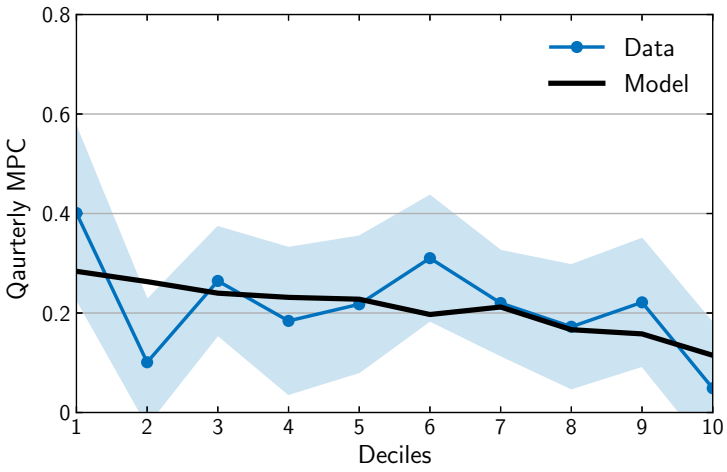

Figure 1: Quarterly MPCs in Peru: Data vs. Model

Notes: This figure plots the model-predicted MPC (labeled 'Model') and the estimated MPC (labeled 'Data') at each earnings decile. Integer 1 on the x-axis denotes the bottom decile. Shaded areas represent 95% confidence intervals.

the model successfully captures such deviation by matching the MPC moments.

The rest of the HASOE-specific parameters (κ, ξ, β_E, and p) are calibrated as follows. Parameter κ is calibrated such that the aggregate labor supply is normalized to 1 on the balanced growth path. Parameter ξ is calibrated to a spread between long-run average lending and deposit interest rates in data.[25] Parameter β_E is calibrated such that entrepreneurs' Euler equation holds on the balanced growth path. Parameter p is calibrated such that the entrepreneurs' wealth share matches the top $100(1-p)\%$ share of wealth in data.[26]

Among the calibration targets used for the HASOE model, only three are distributional moments: the top 1.3% $(= 100(1-p)\%)$ share of wealth and the standard deviations of predictable and unpredictable earnings components. The model, however, predicts many more distributional moments than the three targets. Table 2 compares some key moments for wealth, earnings, and consumption distributions between the model and data. All the moments compared in the table are untargeted except for the top 1.3% wealth share. Table 2 suggests that the HASOE model overall captures Peruvian wealth, earnings, and consumption distributions reasonably well, even though

[25]The real deposit interest rates are computed by deflating BCRP's data on deposit rates in foreign currency (TIPMEX) during 1992–2018 with the expected inflation on U.S. CPIs, which are constructed as in footnote 18.

[26]For this purpose, I use wealth inequality data from the World Inequality Database (WID). Since Peru does not have micro wealth data, the WID imputes the wealth inequality of Peru based on its income inequality and the wealth inequality of other countries that exhibit a similar degree of income inequality with Peru and have micro wealth data (Bajard, Chancel, Moshrif, and Piketty, 2022). As Alvaredo, Atkinson, et al. (2021) note, the WID's wealth concept is a market value of wealth, which includes financial assets yielding nonproductive pure rents, such as entrepreneurs' claims to rents R_t^E in the model. Thus, I evaluate the market value of the claims assuming that entrepreneurs can trade the claims among themselves and include this value as part of entrepreneurs' wealth. See Online Appendix G for details.

Table 2: Distributional Moments: Model (HASOE) vs. Data

Moment	Model	Data	Note	Data Source
Wealth distribution				
top 1.3% share	0.458	0.458	targeted	WID
top 5% share	0.532	0.644	untargeted	WID
top 10% share	0.594	0.760	untargeted	WID
Gini	0.642	0.874	untargeted	WID
Earnings distribution of workers (residualized)				
top 5% share	0.172	0.172	untargeted	ENAHO
top 10% share	0.279	0.273	untargeted	ENAHO
Gini	0.380	0.362	untargeted	ENAHO
Earnings distribution of workers (unresidualized)				
top 5% share	0.246	0.197	untargeted	ENAHO
top 10% share	0.373	0.311	untargeted	ENAHO
Gini	0.503	0.446	untargeted	ENAHO
Consumption distribution of workers (residualized)				
top 5% share	0.119	0.149	untargeted	ENAHO
top 10% share	0.211	0.238	untargeted	ENAHO
Gini	0.270	0.298	untargeted	ENAHO
Consumption distribution of workers (unresidualized)				
top 5% share	0.203	0.178	untargeted	ENAHO
top 10% share	0.320	0.283	untargeted	ENAHO
Gini	0.436	0.396	untargeted	ENAHO

Notes: 'Residualized' means that predictable components are removed, and 'unresidualized' means they are not.

only a small number of distributional moments are targeted.

Table 3 reports the size of stock variables in the RASOE and HASOE models. The two models exhibit the same values of K/Y (10.91) and D/Y (2.487) as a result of calibration. The value of D/Y (2.487) is close to its data counterpart in Milesi-Ferretti and Lane (2017)'s dataset (1.783), although not directly targeted.[27] As formally shown in Online Appendices A.3 and B.4, on the

Table 3: The Size of Stock Variables

	(K/Y)	(A/Y)	(A^W/Y)	(A^E/Y)	(B/Y)	(B^W/Y)	(D/Y)
RASOE	10.91	8.419	-	-	-	-	2.487
HASOE	10.91	7.785	6.016	142.2	0.633	0.642	2.487

[27] See footnote 19 for a related discussion.

balanced growth path, the stock variables satisfy '$K/Y = A/Y + D/Y$' in the RASOE model and '$K/Y = A/Y + B/Y + D/Y$' in the HASOE model.[28] It is also worth noting that B/Y (0.633) is very small in the HASOE model. This is because workers barely save in liquid assets in the model under the low deposit interest rate observed in data.

3.2 Bayesian Estimation

Parameters $\psi, \phi, \theta_z, \theta_g, \rho_z, \sigma_z, \rho_g, \sigma_g, \rho_\mu$, and σ_μ govern the aggregate dynamics around the balanced growth path in both the RASOE and HASOE models. I estimate these parameters using standard Bayesian methods and macro data. For the macro data, I use output, consumption, investment, and trade-balance-to-output ratio, following the existing studies that conduct Bayesian estimation to examine emerging market business cycles. Specifically, I use the time series of $[\Delta \log Y_t, \Delta \log C_t, \Delta \log I_t, \Delta(TB_t/Y_t)]$, as in Chang and Fernández (2013).[29] I construct these data series using BCRP's national account data from 1980–2018.[30] In the estimation, I allow *i.i.d.* measurement errors on each data series and estimate their standard errors, σ_y^{me}, σ_c^{me}, σ_i^{me}, and σ_{tby}^{me}.

I construct a posterior distribution by sampling 300,000 draws through the Random Walk Metropolis Hastings (RWMH) algorithm described in Herbst and Schorfheide (2015) and burning the initial 50,000 draws. A successful implementation of the algorithm requires i) a variance-covariance matrix of the proposal distribution that is close to the variance-covariance matrix of the posterior distribution after scaling and ii) a scaling factor for the matrix that achieves an acceptance rate in the range 0.2–0.4. To this end, I run multiple preliminary stages of the RWMH algorithm and its variant before the main RWMH algorithm, through which i) the draws of the chain move close to the posterior mode, ii) the variance-covariance matrix of the proposal distribution is updated to become close to the variance-covariance matrix of the posterior distribution after scaling, and iii) the scaling factor is updated to achieve an acceptance rate close to 0.27.[31]

Table 4 presents the prior and posterior distributions. I impose a fairly flat prior distribution, as reported in the 'Prior' panel. Measurement errors are allowed to explain up to 6.25% of the observed variances. Parameters ρ_z, ρ_g, and ρ_μ in the prior distribution follow a beta distribution

[28] In the HASOE model, the wealth-output ratio is 12.13, which is greater than the capital-output ratio because the market value of entrepreneurs' claims to pure rents is included in wealth. See footnote 26 for a related discussion.

[29] Garcia-Cicco et al. (2010) use the same set of statistics except for using TB_t/Y_t instead of $\Delta(TB_t/Y_t)$. Both choices are acceptable from a statistical perspective, as neither inherits a trend in the data and the model. I choose $\Delta(TB_t/Y_t)$ over TB_t/Y_t because the countercyclicality of trade balance, a stylized pattern for both emerging and developed economies, is better captured when $\Delta \log Y_t$ is correlated with $\Delta(TB_t/Y_t)$ rather than with TB_t/Y_t.

[30] As described in footnote 18, I obtain BCRP's real quarterly national account data, seasonally adjust them, and transform them to a per capita term. For the last step (transformation to a per capita term), I construct quarterly population series by linearly interpolating BCRP's annual population data.

[31] As a result, I obtain the acceptance rates of 0.278, 0.264, and 0.297 in the main RWMH algorithm for the estimation of the RASOE model in subsection 2.1, the HASOE model in subsection 2.2, and the HASOE model revised by augmenting a financial friction shock in section 4, respectively.

Table 4: Prior and Posterior Distributions in the Bayesian Estimation

	Prior		Posterior - RASOE (z, g, μ)		Posterior - HASOE (z, g, μ)		Posterior - HASOE (z, g, μ, η)	
	Density	[Meta1,Meta2]	Mode	Mean [0.05 ,0.95]	Mode	Mean [0.05 ,0.95]	Mode	Mean [0.05 ,0.95]
ψ	Uniform	[0.000,4.000]	0.513	2.471 [0.864,3.851]	0.005	0.004 [0.002,0.007]	1.472	3.154 [1.860,3.944]
ϕ	Gamma	[15.00,15.00]	1.661	2.364 [1.095,3.976]	7.126	7.307 [5.823,8.970]	3.094	1.731 [0.288,3.143]
θ_z	Uniform	[0.000,2.000]	0.017	0.245 [0.017,0.672]	0.000	0.001 [0.000,0.004]	0.000	0.090 [0.005,0.279]
θ_g	Uniform	[0.000,2.000]	0.006	0.079 [0.003,0.255]	0.350	0.360 [0.270,0.456]	0.084	0.476 [0.023,1.446]
ρ_z	0.99·Beta	[0.500,0.200]	0.931	0.919 [0.873,0.954]	0.988	0.986 [0.979,0.989]	0.942	0.943 [0.899,0.974]
σ_z	Invgamma	[0.010,0.020]	0.017	0.017 [0.015,0.019]	0.029	0.030 [0.027,0.034]	0.017	0.017 [0.015,0.019]
ρ_g	0.99·Beta	[0.500,0.200]	0.988	0.988 [0.985,0.989]	0.044	0.065 [0.018,0.128]	0.795	0.809 [0.691,0.900]
σ_g	Invgamma	[0.010,0.020]	0.006	0.006 [0.006,0.007]	0.039	0.039 [0.034,0.045]	0.006	0.006 [0.005,0.007]
ρ_μ	0.99·Beta	[0.500,0.200]	0.919	0.878 [0.746,0.961]	0.694	0.749 [0.609,0.868]	0.488	0.522 [0.184,0.835]
σ_μ	Invgamma	[0.010,0.020]	0.011	0.047 [0.018,0.073]	0.003	0.003 [0.002,0.004]	0.004	0.006 [0.002,0.013]
ρ_η	0.99·Beta	[0.500,0.200]	-	-	-	-	0.904	0.555 [0.150,0.927]
σ_η	Invgamma	[0.010,0.020]	-	-	-	-	0.404	0.822 [0.344,1.323]
σ_y^{me}	Uniform	[0.000,0.007]	0.007	0.006 [0.006,0.007]	0.007	0.007 [0.006,0.007]	0.006	0.006 [0.006,0.007]
σ_c^{me}	Uniform	[0.000,0.009]	0.009	0.009 [0.008,0.009]	0.009	0.009 [0.008,0.009]	0.009	0.009 [0.008,0.009]
σ_i^{me}	Uniform	[0.000,0.045]	0.045	0.044 [0.043,0.045]	0.045	0.044 [0.043,0.045]	0.045	0.044 [0.043,0.045]
σ_{tby}^{me}	Uniform	[0.000,0.004]	0.004	0.004 [0.004,0.004]	0.004	0.004 [0.004,0.004]	0.004	0.004 [0.004,0.004]

Notes: Estimation is based on the Peruvian quarterly national account data from 1980–2018. In the prior density column, '0.99 · Beta' means that the corresponding parameter multiplied by (1/0.99) follows a beta distribution. The column labeled '[Meta1,Meta2]' reports the meta parameters of the prior distributions. For the uniform distribution, [Meta1,Meta2] is [lower bound, upper bound]. For the inverse gamma distribution and gamma distribution, [Meta1,Meta2] is [mean, standard deviation]. For '0.99 · Beta', [Meta1,Meta2] is [mean, standard deviation] of the beta distribution part. Posterior statistics are based on 300,000 posterior draws from the RWMH algorithm, of which the initial 50,000 draws are burned.

after being scaled by (1/0.99). This scaling is to ensure that these parameters do not exceed 0.99 under any posterior draw, as the precision of Auclert et al. (2021)'s computation method can be compromised when the economy becomes too persistent.[32] The 'Posterior - RASOE (z, g, μ)' and 'Posterior - HASOE (z, g, μ)' panels report key statistics of the posterior distributions for the RASOE and HASOE models introduced in subsections 2.1 and 2.2, respectively.

3.3 Model Performance

Table 5 compares key business cycle moments between models and data after the Bayesian estimation. Starting from the data, the Peruvian national accounts exhibit the stylized patterns of emerging market business cycles well. First, Peruvian output is substantially more volatile than that of typical developed economies: $\sigma(\Delta \log Y_t)$ is 0.027 in Peru, which far exceeds the average in rich economies, 0.008, as reported in Table 1.6 of Uribe and Schmitt-Grohé (2017). Second, consumption is more volatile than output in Peru (excess consumption volatility): $\sigma(\Delta \log C_t)$ is 0.036, which is substantially greater than $\sigma(\Delta \log Y_t)$, 0.027. Third, trade balance is countercyclical in Peru: $corr(\Delta(TB_t/Y_t), \Delta \log Y_t)$ is -0.346. I highlight one more moment for later discussion, although it has received less attention in the literature; $corr(\Delta \log C_t, \Delta \log I_t)$ is substantially less than one.[33] Moreover, the low correlation is not an abnormal phenomenon of the Peruvian data: the correlation is 0.189 for emerging countries and 0.278 for developed countries, on average.[34]

How successful are the models at explaining these data patterns? Table 5 reports the business cycle moments predicted by the RASOE model described in subsection 2.1 in the rows labeled 'RASOE (z, g, μ) model' and suggests that the RASOE model explains the data patterns reasonably well: consumption is more volatile than output ($\sigma(\Delta \log C_t)/\sigma(\Delta \log Y_t) = 0.046/0.040 = 1.144$), trade balance is countercyclical ($corr(\Delta(TB_t/Y_t), \Delta \log Y_t) = -0.111$), and the correlation between consumption and investment is low ($corr(\Delta \log C_t, \Delta \log I_t) = 0.287$). The RASOE model exhibits a few discrepancies against data, as well: the output and consumption volatilities are noticeably greater than the data counterparts, and the output and consumption autocorrelations with two- and three-quarter lags are as substantial as those with one-quarter lag.

Table 5 also reports the moments predicted by the HASOE model described in subsection 2.2 in

[32] Auclert et al. (2021)'s sequence space approach requires a truncation of sequences, and truncation errors can be nontrivial when the economy is extremely persistent. In this paper, I truncate sequences at $T = 700$ when solving models and drop the last seven periods further when evaluating moments. In Online Appendix E, I verify that at the posterior mode, truncation errors are negligible in the model statistics used in this paper.

[33] It is indeed negative, but as we shall see later, what matters in this paper is that this value is substantially less than one.

[34] In computing the correlation for emerging and developed countries, I use the quarterly macro data series and country categorization used for the business cycle statistics in Chapter 1 of Uribe and Schmitt-Grohé (2017). From the dataset, sample countries are selected if all five data series of output, investment, exports, imports, and consumption are available for at least twenty consecutive years. After the sample selection, 16 emerging countries and 17 rich countries remain in the sample. In averaging the correlation across multiple countries, I use population weights.

Table 5: Business Cycle Moments: Model vs. Data

		$\Delta \log Y_t$	$\Delta \log C_t$	$\Delta \log I_t$	$\Delta(TB_t/Y_t)$
Standard deviation					
	RASOE (z, g, μ) model	0.040	0.046	0.143	0.029
	HASOE (z, g, μ) model	0.066	0.059	0.288	0.036
	HASOE (z, g, μ, η) model	0.029	0.036	0.167	0.018
	Data	0.027	0.036	0.179	0.017
Contemporaneous correlation					
with $\Delta \log Y_t$	RASOE (z, g, μ) model		0.776	0.520	-0.111
	HASOE (z, g, μ) model		0.938	0.913	-0.824
	HASOE (z, g, μ, η) model		0.598	0.509	-0.248
	Data		0.681	0.437	-0.346
with $\Delta(TB_t/Y_t)$	RASOE (z, g, μ) model		-0.461	-0.610	
	HASOE (z, g, μ) model		-0.821	-0.921	
	HASOE (z, g, μ, η) model		-0.180	-0.632	
	Data		-0.318	-0.460	
with $\Delta \log C_t$	RASOE (z, g, μ) model			0.287	
	HASOE (z, g, μ) model			0.788	
	HASOE (z, g, μ, η) model			-0.223	
	Data			-0.158	
Autocorrelation					
with lag 1	RASOE (z, g, μ) model	0.474	0.312	-0.202	-0.229
	HASOE (z, g, μ) model	-0.165	-0.028	-0.280	-0.126
	HASOE (z, g, μ, η) model	0.036	-0.048	-0.080	-0.131
	Data	0.404	0.078	-0.304	0.023
with lag 2	RASOE (z, g, μ) model	0.472	0.312	-0.046	-0.079
	HASOE (z, g, μ) model	0.006	0.008	-0.032	-0.044
	HASOE (z, g, μ, η) model	0.027	-0.039	-0.067	-0.078
	Data	0.009	0.036	-0.094	-0.077
with lag 3	RASOE (z, g, μ) model	0.471	0.312	0.006	-0.028
	HASOE (z, g, μ) model	0.015	0.001	-0.015	-0.041
	HASOE (z, g, μ, η) model	0.022	-0.025	-0.053	-0.058
	Data	-0.090	-0.112	0.026	-0.061

Notes: The model statistics are computed under each posterior draw, and the means across the posterior distribution are reported.

the rows labeled 'HASOE (z, g, μ) model.' The reported numbers suggest that the HASOE model fails to explain the data patterns in several important dimensions: output and consumption are far

greater than the data counterparts, consumption is less volatile than output ($\sigma(\Delta \log C_t)/\sigma(\Delta \log Y_t) = 0.059/0.066 = 0.897$), and the correlation between consumption and investment is close to 1 ($corr(\Delta \log C_t, \Delta \log I_t) = 0.788$).

How does the RASOE model explain the data patterns? Why does the HASOE model fail to do so, on the other hand? The following subsection addresses these questions.

3.4 How RASOE Works and Why HASOE Does Not

I start by examining the driving mechanism of the RASOE model. The 'RASOE (z, g, μ) model' panel in Table 6 presents variance decomposition in the RASOE model and shows that trend shocks are the main driver of output and consumption fluctuations: 50.8% of output fluctuations and 83.6% of consumption fluctuations are driven by trend shocks. This result is consistent with Aguiar and Gopinath (2007)'s finding that trend shocks drive emerging market business cycles.

In Figure 2a, I examine the consumption response to a trend shock in the RASOE model and verify that the permanent income effect of a trend shock drives excess consumption volatility, exactly as Aguiar and Gopinath (2007) argue. The first panel shows that the impact effect of a trend shock on consumption is greater than that on output. The RASOE model imposes the GHH preference, under which households smooth per-period utility $GHH_t := C_t - h_t(L_t)$ subject to budget constraints, where $h_t(L_t) := \kappa_R X_{t-1} L_t^{1+\omega}$ is labor disutility. Since $C_t = GHH_t + h_t(L_t)$, the strong impact effect of a trend shock on consumption can come either from GHH_t or from $h_t(L_t)$. In the second panel, I decompose the consumption response into the responses of GHH_t and $h_t(L_t)$ and find that almost all the impact effect on consumption comes from the impact effect on GHH_t. A trend shock affects GHH_t by affecting w_t and r_t^a in the budget constraints as well as labor disutility function $h_t(\cdot)$ via X_{t-1} . In particular, the effects on w_t and $h_t(\cdot)$ transmit to GHH_t through earnings $w_t L_t$ in the budget constraints, as labor supply L_t is determined by wage w_t and labor disutility $h_t(\cdot)$. In the third panel, I decompose the response of GHH_t into the response driven by w_t and $h_t(\cdot)$ and the response driven by r_t^a and find that it is dominantly driven by the former.[35] The last panel plots the impulse response of earnings $w_t L_t$, which mildly jumps on impact but grows strongly in the future.[36] These panels show that the permanent income effect of the future growth of earnings generates a strong impact effect on GHH_t and thus on C_t.

In the literature, a competing hypothesis exists on the driving mechanism of emerging market business cycles: emerging economies face volatile interest rates, and they cause excess consumption volatility because households respond to them by intertemporally substituting consumption (Neumeyer and Perri, 2005). This mechanism is muted in explaining the Peruvian data largely be-

[35] The consumption response decomposition into driving factors in the RASOE model requires an extra computational step in addition to solving the model (unlike that in the HASOE model). See Online Appendix H for details.

[36] In fact, the impulse response of $w_t L_t$ is the same as that of Y_t because $w_t L_t = (1-\alpha) Y_t$ at equilibrium.

Table 6: Variance Decomposition

	$\Delta \log Y_t$	$\Delta \log C_t$	$\Delta \log I_t$	$\Delta(TB_t/Y_t)$
RASOE (z, g, μ) *model*				
stationary productivity shock (z)	0.492	0.163	0.341	0.020
	(0.048)	(0.026)	(0.053)	(0.015)
trend shock (g)	0.508	0.836	0.056	0.353
	(0.048)	(0.026)	(0.013)	(0.041)
interest rate shock (μ)	0.001	0.001	0.603	0.627
	(0.000)	(0.001)	(0.054)	(0.042)
HASOE (z, g, μ) *model*				
stationary productivity shock (z)	0.547	0.826	0.236	0.370
	(0.043)	(0.030)	(0.033)	(0.045)
trend shock (g)	0.452	0.164	0.708	0.380
	(0.043)	(0.030)	(0.036)	(0.046)
interest rate shock (μ)	0.000	0.010	0.056	0.251
	(0.000)	(0.002)	(0.011)	(0.038)
HASOE (z, g, μ, η) *model*				
stationary productivity shock (z)	0.918	0.318	0.189	0.021
	(0.024)	(0.052)	(0.039)	(0.011)
trend shock (g)	0.078	0.030	0.379	0.929
	(0.023)	(0.013)	(0.048)	(0.044)
interest rate shock (μ)	0.000	0.000	0.009	0.034
	(0.000)	(0.000)	(0.012)	(0.042)
financial friction shock (η)	0.004	0.652	0.423	0.016
	(0.002)	(0.051)	(0.043)	(0.015)

Notes: The decomposed shares are computed under each posterior draw, and their means and standard deviations across the posterior distribution are reported. The numbers in parentheses are the posterior standard deviations.

cause of the low correlation between consumption and investment; when the interest rate increases, both consumption and investment plunge[37]; thus, if interest rates drove the business cycles, consumption and investment would be strongly positively correlated.[38]

Now, I turn to the failure of the HASOE model. The 'HASOE (z, g, μ) model' panel in Table 6 presents variance decomposition in the HASOE model and shows that trend shocks do not play an important role in generating consumption fluctuations. Instead, stationary productivity shocks

[37]Investment decreases because the marginal rate of capital should increase toward the interest rate after reflecting capital adjustment costs. See equation (A.8) in Online Appendix A.

[38]Rather, low $corr(\Delta \log C_t, \Delta \log I_t)$ is achieved in the RASOE model by appointing two different shocks, g and μ shocks, as the main drivers of consumption and investment fluctuations, respsectively.

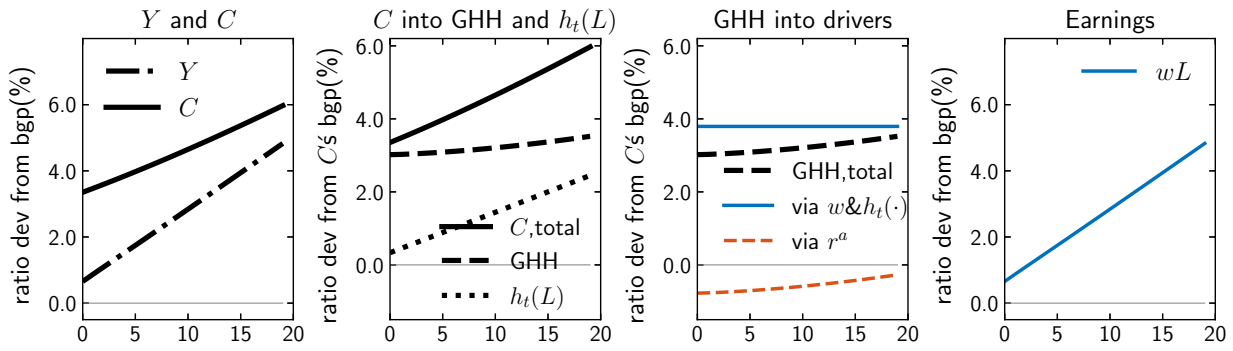

(a) RASOE Model Prediction under the RASOE Posterior

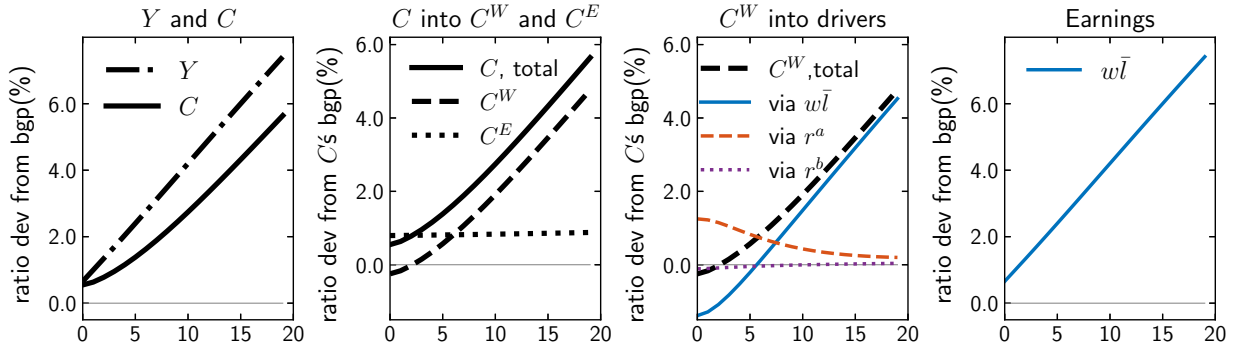

(b) HASOE Model Prediction under the RASOE Posterior

Figure 2: Consumption Response to g Shock: RASOE vs. HASOE under the RASOE Posterior

Notes: Figures 2a and 2b plot the impulse response of consumption and other related variables to a one-standard-deviation trend shock in the RASOE and HASOE models, respectively, evaluated at the same parameter draws from the RASOE model's posterior distribution. The model statistics are computed at each posterior draw, and their means across the posterior distribution are plotted. The unit of the y-axis is either 'ratio dev from bgp(%),' which represents the deviation from the balanced growth path (b.g.p) of the variable of interest divided by its value on the b.g.p, or 'ratio dev from C's bgp(%),' which represents the deviation of the variable of interest divided by the value of C_t on the b.g.p.

(z) generate most consumption fluctuations (82.6%). As we see in Table 5, however, stationary productivity shocks cannot generate excess consumption volatility.

Why can't the Aguiar and Gopinath (2007) mechanism operate in the HASOE model as it does in the RASOE model? To answer this question, I feed the RASOE model's posterior parameter draws into the HASOE model and examine how consumption responds to a trend shock. The first panel in Figure 2b plots the consumption and output responses in this experiment. The impact effect on output is similar between the RASOE and HASOE models, but output grows more strongly in the HASOE model. Despite this stronger future output growth (and a consequent stronger permanent income effect), the impact effect on consumption in the HASOE model is much weaker than that in the RASOE model and is only as much as the impact effect on output. Since

$C_t = pC_t^W + (1-p)C_t^E$ in the HASOE model, the muted initial response of consumption might come from either C_t^W or C_t^E. In the second panel, I decompose the consumption response into the responses of C_t^W and C_t^E and find that the muted impact effect on consumption comes entirely from the muted initial response of C_t^W. A trend shock affects workers' consumption by affecting $w_t\bar{l}_t$, r_t^a, and r_t^b in their budget constraints. In the third panel, I decompose the response of C_t^W into the responses driven by $w_t\bar{l}_t$, r_t^a, and r_t^b and find that the muted initial response of C^W is entirely driven by its response to aggregate earnings, $w\bar{l}$.[39] The last panel plots the impulse response of $w\bar{l}$, which mildly jumps on impact, as in the RASOE model, but grows more rapidly in the following periods than it does in the RASOE model.

At first, it may be surprising that workers do not increase consumption despite a strong future growth of aggregate earnings and a consequent permanent income increase. The economic mechanism behind this result is as follows. Individual workers' earnings are determined by aggregate earnings $w_t\bar{l}_t$ multiplied by idiosyncratic productivity $\Gamma_i e_{i,t}$, where $e_{i,t}$ bears idiosyncratic earnings risk. Thus, the future growth of aggregate earnings due to a trend shift means not only a greater permanent income but also a greater idiosyncratic earnings risk that workers must face in the future. The greater future idiosyncratic risk enhances workers' precautionary saving, and the enhanced precautionary saving effect offsets the permanent income effect. In short, the presence of a strong precautionary saving motive hinders the Aguiar and Gopinath (2007) mechanism in the HASOE model.[40]

4 Reviving the HASOE Model

Thus far, I have shown the following: i) a RASOE model can explain stylized patterns of emerging market business cycles, consistent with conventional wisdom; ii) however, the driving mechanism in the RASOE model crucially hinges on the PIH behavior of representative households, which are inconsistent with the consumption behavior observed in micro data; iii) a HASOE model that successfully captures the microlevel consumption behavior (by incorporating household heterogeneity into the RASOE model) fails to explain the business cycle patterns. In this section, I show that by adding one aggregate shock to the HASOE model, we can revive it such that it accounts for the business cycle patterns well through a new mechanism.

[39] To be precise, aggregate earnings of the economy are $w_t L_t = (p\bar{\Gamma}\bar{e})w_t\bar{l}_t$, and $w_t\bar{l}$ should be named an 'aggregate earnings per efficiency unit.' Given that $w_t L_t$ is a scaled-up version of $w_t\bar{l}_t$ and they exhibit the same impulse responses, I refer to both terms as 'aggregate earnings' for brevity unless a distinction between the two is necessary.

[40] Another way to understand this result is to focus on aggregate savings. For simplicity, assume for a moment that the economy does not grow in the long-run (*i.e.*, $g_{ss} = 1$), there is no aggregate shock, and the economy is in a steady state. Then, a one-time trend shock hits the economy, and after certain periods, the economy reaches a new steady state in which all the quantity variables are 10% greater than the old steady state. The aggregate savings must also be 10% greater in the new steady state, and the greater aggregate savings are achieved by enhanced precautionary saving over the transition periods (and after reaching the new steady state, as well) due to a greater idiosyncratic risk.

I consider a financial friction shock that directly interrupts workers' consumption smoothing.[41] Given that workers barely use liquid assets as a saving vehicle (see Table 3), I impose a shock to the trading cost of illiquid assets. Specifically, workers' budget constraint (10) is revised as follows.

$$c_{i,t} + b_{i,t} + v_{i,t} + \eta_t \chi_t(v_{i,t}, a_{i,t-1}; \Gamma_i) = w_t \Gamma_i e_{i,t} \bar{l}_t + (1-\xi)(1+r_t^b) b_{i,t-1}, \tag{22}$$

where η_t is the financial friction shock. The aggregation equation (21) is revised accordingly:

$$\chi_t^{agg} = p\chi_t^W, \quad \chi_t^W = \int_\Gamma \int_{e_1,e_2,b_-,a_-} \eta_t \chi_t \left(a_t(e_1,e_2,b_-,a_-;\Gamma) - (1+r_t^a)a_-, a_-; \Gamma\right) d\Psi_t dG. \tag{23}$$

The balanced-growth-path value of η_t is 1, and $\log \eta_t$ follows an AR(1) process:

$$\log \eta_t = \rho_\eta \log \eta_{t-1} + \varepsilon_t^\eta, \quad \varepsilon_t^\eta \sim N(0, \sigma_\eta^2). \tag{24}$$

For the Bayesian estimation of the revised HASOE model, I impose the same prior distribution as before on all the parameters to be estimated except two newly added parameters, ρ_η and σ_η. For ρ_η and σ_η, I impose the same prior distribution as the one imposed on the other exogenous shock processes. See the 'Prior' panel in Table 4 for details. The 'Posterior - HASOE (z, g, μ, η)' panel in Table 4 reports key statistics of the posterior distribution for the revised HASOE model.

Table 5 reports the business cycle moments predicted by the revised HASOE model in the rows labeled 'HASOE (z, g, μ, η) model' and suggests that the revised HASOE model explains the stylized patterns of emerging market business cycles quite well: consumption is more volatile than output ($\sigma(\Delta \log C_t)/\sigma(\Delta \log Y_t) = 0.036/0.029 = 1.215$), trade balance is countercyclical ($corr(\Delta(TB_t/Y_t), \Delta \log Y_t) = -0.248$), and the correlation between consumption and investment is low ($corr(\Delta \log C_t, \Delta \log I_t) = -0.223$). Moreover, even better than the RASOE model, the revised HASOE model predicts output and consumption volatilities that are close to their data counterparts ($\sigma(\Delta \log Y_t) = 0.029$ in the model, 0.027 in data; $\sigma(\Delta \log C_t) = 0.036$ in the model, 0.036 in data). The revised HASOE model also closely matches other business cycle moments reported in Table 5 except the autocorrelation of $\Delta \log Y_t$ with a one-quarter lag (0.036 in the model, 0.404 in data).[42]

[41] Consideration of such a shock is partly motivated by studies emphasizing the role of financial frictions in the international financial market, such as ψ, θ_z, and θ_g in equation (6) (see Neumeyer and Perri (2005), Garcia-Cicco et al. (2010), and Chang and Fernández (2013), for instance). These frictions translate shocks or other variables' fluctuations into interest rate fluctuations, which then strongly affect representative households' consumption via intertemporal substitution. In heterogeneous-agent models, however, households are less affected by intertemporal substitution and more affected by a precautionary saving motive. Thus, in addition to the financial frictions in the international financial market that only affect interest rates, I consider a financial friction shock that households face when trading assets so that it directly affects the precautionary saving motive.

[42] This discrepancy in output autocorrelation quickly dissipates from a two-quarter lag forward. Given that the discrepancy survives only one quarter and that output fluctuations mostly come from stationary productivity shocks (see the 'HASOE(z, g, μ, η) model' in Table 6), it is likely that replacing the conventional AR(1) process of stationary

The 'HASOE (z, g, μ, η) model' panel in Table 6 presents variance decomposition in the revised HASOE model. Most output fluctuations (91.8%) are driven by stationary productivity shocks, while trend shocks play only a limited role (7.8%). Consumption fluctuations are almost entirely driven by financial friction shocks (65.2%) and stationary productivity shocks (31.8%), while trend shocks play essentially no role.[43]

The addition of the financial friction shock is effective at reviving the HASOE model for two reasons. First, the η shock generates large consumption fluctuations without causing output fluctuations much (see Table 6), resolving the absence of excess consumption volatility in the initial HASOE model. Second, the η shock also generates large investment fluctuations (see Table 6), and importantly, the consumption and investment responses are in the opposite direction (see Figure L.8 in Online Appendix L.2), generating a negative correlation between consumption and investment and thus fixing the strongly positive $corr(\Delta \log C_t, \Delta \log I_t)$ in the initial HASOE model.[44]

To identify the driving mechanism of consumption fluctuations, I examine the consumption responses to financial friction shocks and stationary productivity shocks. Since $C_t = pC_t^W + (1-p)C_t^E$ in the revised HASOE model, the total consumption response can be decomposed into the responses of C_t^E and C_t^W. Moreover, since aggregate shocks affect workers' consumption by affecting $w_t\bar{l}_t$, r_t^a, r_t^b, and η_t in their budget constraints, the response of C_t^W can be further decomposed into the responses driven by each of them.

Figure 3a plots the total consumption response to a financial friction shock and decomposes it into entrepreneurs' consumption response and workers' responses driven by $w\bar{l}$, r^a, r^b, and η in their budget constraints. This figure shows that the total consumption response to a financial friction shock almost entirely comes from workers' consumption response to the change in η_t in their budget constraints. Workers reduce consumption when the asset trading cost increases for the following economic reasons. Workers facing a bad idiosyncratic earnings shock need to cash out their assets to smooth consumption. When the financial friction shock is realized, however, it becomes more costly to cash out their assets, and they fail to smooth consumption more significantly. For workers who do not face an immediate need to cash out their assets at the moment of

productivity shocks with an ARMA(1,1) process can fix this discrepancy. However, I do not impose this rather unconventional assumption because the model aims to minimize changes from conventional representative-agent models other than the heterogeneous household block with high MPCs.

[43]The 'HASOE (z, g, μ, η) model' panel in Table 6 also reports the variance decomposition of investment and trade-balance-to-output ratio fluctuations in the revised HASOE model. Notably, trend shocks play an important role in these fluctuations. When firms expect future productivity growth in the model, they can increase investment without a precautionary saving concern, unlike workers' consumption decisions. Moreover, given the limited output response to a trend shock, firms finance investment by rapidly increasing international debt through banks.

[44]Consumption and investment respond to an η shock in the opposite direction for the following reason. When financial friction is heightened, workers reduce consumption and increase saving due to either consumption smoothing disruption or enhanced precautionary saving, as will be discussed further in a later part of this section. As aggregate saving increases, the interest rate decreases, and the lower interest rate boosts investment.

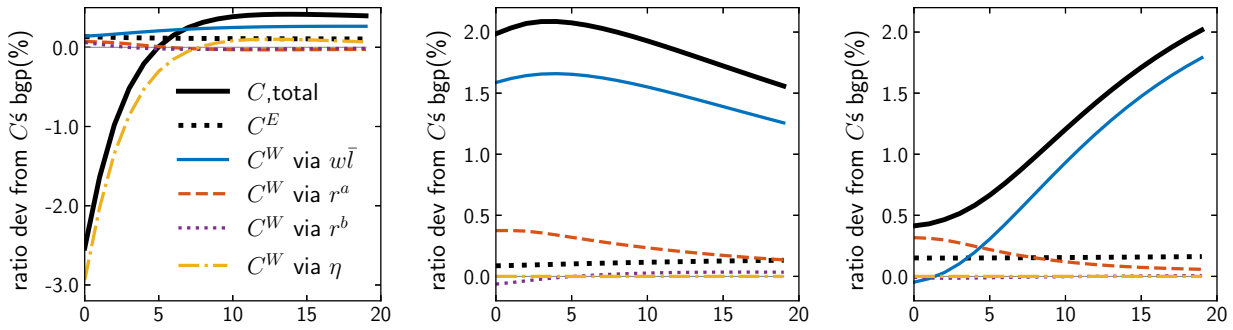

(a) Response to η Shock (b) Response to z Shock (c) Response to g Shock

Figure 3: Consumption Response Decomposition in the HASOE (z, g, μ, η) Model

Notes: Figures 3a, 3b, and 3c plot the impulse responses of consumption to one-standard-deviation η, z, and g shocks, respectively, in the revised HASOE model. In each figure, the consumption response is decomposed into entrepreneurs' consumption response and workers' responses driven by $w\bar{l}$, r^a, r^b, and η in their budget constraints. The model statistics are computed at each posterior draw, and their means across the posterior distribution are plotted. The unit of the y-axis is 'ratio dev from C's bgp(%),' which represents the deviation from the balanced growth path (b.g.p) of the variable of interest divided by the value of C_t on the b.g.p.

heightened financial friction, they recognize that it will be more expensive to cash out their assets for a while. Therefore, they prepare themselves by accumulating more buffer stocks and reducing consumption.

Figure 3b plots the total consumption response to a stationary productivity shock and its decomposed responses. This figure shows that the total consumption response mostly comes from workers' consumption response driven by aggregate earnings $w_t\bar{l}_t$. Workers' consumption response driven by r^a_t also nontrivially contributes to the total response. The economic mechanism behind this result is as follows. When a positive stationary productivity shock hits the economy, both labor and investment demands increase, and thus, aggregate earnings $(w_t\bar{l}_t,\ t \geq 0)$ and interest rates $(r_t = r^a_{t+1},\ t \geq 0)$ increase. Moreover, the asset price (q_0) jumps on impact (due to the higher future productivity), and so does the rate of asset return (r^a_0). As a result, workers' income, including their earnings and asset returns, increases. Importantly, because workers exhibit high MPC, they strongly translate these income fluctuations into consumption fluctuations.

In addition to the consumption responses to the main shocks (z and η), I also examine the consumption response to a trend shock. Figure 3c plots the total consumption response to a trend shock and its decomposed responses and reconfirms the economic intuition obtained in the previous section: the consumption response to a trend shock is muted in the HASOE model because in the face of a future growth of aggregate earnings, workers' precautionary saving becomes enhanced due to a greater future idiosyncratic risk.

5 Counterfactual Experiment

As discussed in the previous section, Peruvian households' high MPC and correspondingly strong precautionary saving play key roles in the transmission mechanism of η and z shocks to generate consumption volatility in the HASOE model. In this section, I quantify their role by running a counterfactual experiment under which household MPC is adjusted to the U.S. level, which is substantially lower than the Peruvian level (Hong, 2022).

For the counterfactual experiment, I recalibrate β, χ_1, and χ_2 by targeting U.S. MPC moments and workers' aggregate wealth. For the target MPC moments, I estimate U.S. MPC at each earnings decile by applying Blundell et al. (2008)'s method to the 2005–2017 waves of the Panel Study of Income Dynamics (PSID). Since the reference period of the PSID data is a year, I obtain annual U.S. MPC estimates, while my HASOE model is a quarterly model. Given the frequency mismatch between the model and data, I target the annual MPC estimates as follows: I first simulate individual workers' quarterly earnings and consumption series from the model; then, I convert the quarterly series to annual series by summing them over every four quarters; using the simulated annual data, I compute the model counterparts of the MPC estimates by applying the same MPC estimation procedure applied to the PSID; I calibrate β, χ_1, and χ_2 such that the model counterparts are as close as possible to the MPC moments.[45] For the workers' aggregate wealth, I target its value in the benchmark Peruvian economy ($(A^W + B^W)/Y = 6.658$, as reported in Table 3).

Table 7 reports the recalibrated parameter values. The value of χ_1 (0.716) in the counterfactual economy is markedly lower than the value (6.694) in the benchmark economy. This means that the U.S. MPC estimates discipline the model to exhibit lower MPC and weaker precautionary saving than the Peruvian MPC estimates do. The value of β (0.974) in the counterfactual economy is noticeably greater than the value (0.948) in the benchmark economy. This is because workers have a weaker precautionary saving motive in the counterfactual economy than in the benchmark economy and thus must be more patient to achieve the same amount of their aggregate wealth.

The joint recalibration again matches targets well, even though only three parameters are used to target eleven moments. First, workers' aggregate wealth $(A^W + B^W)/Y$ in the counterfactual economy is 6.564, which is close to the target, 6.658. Second, Figure 4a plots the annual MPC es-

Table 7: Recalibrated Parameters for the Counterfactual Economy

	Description	Value	Target / source
β	workers' discount factor	0.974	MPC estimates (from PSID) & $(A^W + B^W)/Y$ in Table 3
χ_1	scale parameter for illiquid asset adjustment cost	0.716	
χ_2	convexity parameter for illiquid asset adjustment cost	1.788	

[45] The same targeting method is used in Hong (2022) when comparing Peruvian and U.S. MPCs using a model.

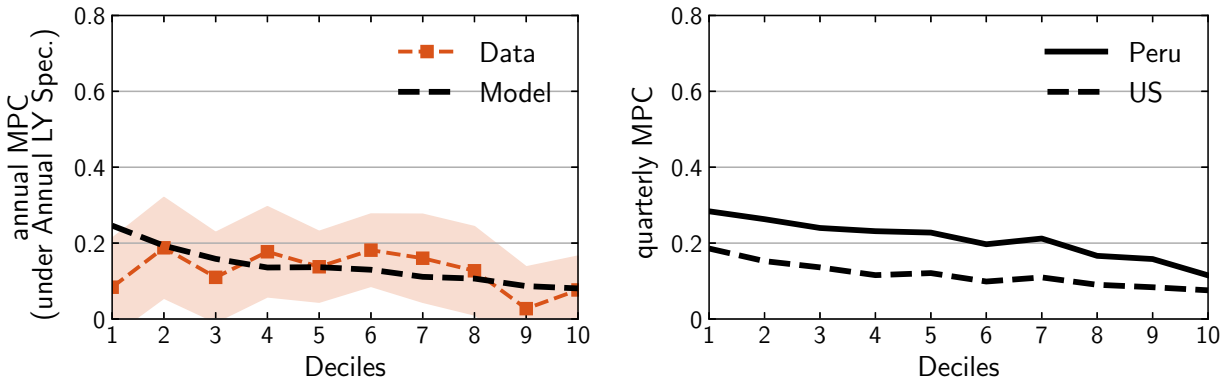

(a) U.S. Annual MPC Estimates: Data vs. Model (b) Model-Predicted Quarterly MPCs: Peru vs. U.S.

Figure 4: MPCs in the Counterfactual Economy

Notes: Figure 4a plots the annual MPC estimates obtained from the PSID (labeled 'Data') and its model counterpart in the counterfactual economy (labeled 'Model'). Shaded areas are 95% confidence intervals. Figure 4b plots the model-predicted quarterly MPC in the benchmark and counterfactual economies (labeled 'Peru' and 'US', respectively).

timates obtained from the PSID (labeled 'Data') and their model counterparts in the counterfactual economy (labeled 'Model') and shows that the latter tracks the former closely.

Figure 4b compares the model-predicted quarterly MPCs in the benchmark and counterfactual economies and shows that there is a substantial MPC gap between the two economies: the mean quarterly MPC across deciles in the benchmark economy is 0.209, which is approximately twice as large as that in the counterfactual economy, 0.117. This figure suggests that when we interpret the Peruvian and U.S. MPC estimates reflecting the different reference periods of the underlying surveys through the lens of the HASOE model, the estimates tell us that Peruvian households exhibit substantially higher MPCs than U.S. households.[46,47]

Now, we are ready to examine the business cycle implication of this MPC gap. In Figure 5, I plot the posterior distributions of output volatility $\sigma(\Delta \log Y_t)$, consumption volatility $\sigma(\Delta \log C_t)$, and their ratio in the benchmark economy and compare them with the corresponding distributions in the counterfactual economy, which are obtained by evaluating the recalibrated model at each parameter draw from the benchmark economy's posterior distribution. Figure 5a shows that the

[46]This result is consistent with the result of the model-based MPC comparison in Hong (2022), where I employ a standard one-asset incomplete-market model to interpret the MPC estimates reflecting different reference periods.

[47]Annual and quarterly MPCs mean a consumption response within a year and a quarter, respectively, after the realization of a shock. By definition, annual MPC should be greater than quarterly MPC. However, the annual MPC estimates (and their model counterparts) in Figure 4a are not much greater than the model-predicted quarterly MPC in Figure 4b. This is because the annual MPC estimates (and their model counterparts) in Figure 4a underestimate the true annual MPC in the model due to a 'time aggregation problem' noted by Crawley (2020): when households receive earnings shocks and make consumption decisions at a certain frequency while Blundell et al. (2008)'s method is applied to data aggregated over a longer time period, the method significantly underestimates the consumption sensitivity to transitory shocks. See Hong (2022) for a detailed discussion.

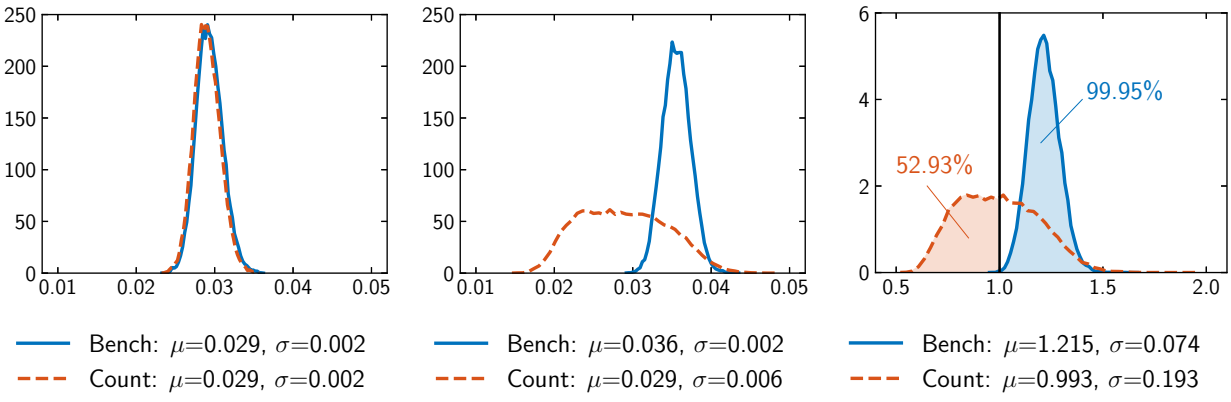

(a) $\sigma(\Delta \log Y_t)$ (b) $\sigma(\Delta \log C_t)$ (c) $\sigma(\Delta \log C_t)/\sigma(\Delta \log Y_t)$

Figure 5: Consumption and Output Volatilities and Their Ratio: Benchmark vs. Counterfactual

Notes: Figures 5a, 5b, and 5c plot the posterior distributions of $\sigma(\Delta \log Y_t)$, $\sigma(\Delta \log C_t)$, and $\frac{\sigma(\Delta \log C_t)}{\sigma(\Delta \log Y_t)}$ in the benchmark economy, respectively (labeled 'Bench'), and compare them with the corresponding distributions in the counterfactual economy (labeled 'Count'), which are obtained by evaluating the recalibrated model at each parameter draw from the benchmark economy's posterior distribution. The legend reports the mean and standard deviation of each distribution.

output volatility distribution is nearly identical between the two economies.[48] On the other hand, Figure 5b shows that the consumption volatility distribution changes substantially. In particular, the distribution in the counterfactual economy exhibits a lower mean (0.029) and greater standard deviation (0.006) than that in the benchmark economy (mean 0.036 and standard deviation 0.002). Figure 5c compares the distribution of the consumption-output volatility ratio. On average, the ratio is 1.215 in the benchmark economy (excess consumption volatility) and 0.993 in the counterfactual economy (the absence of excess consumption volatility). Moreover, unlike in the benchmark economy where consumption is more volatile than output in nearly the entire part (99.95%) of the posterior distribution, the excess consumption volatility disappears in the counterfactual economy in most (52.93%) of the posterior distribution, including the posterior median and mode.[49]

To understand the consumption volatility change, I compute consumption impulse responses in the counterfactual economy by evaluating the recalibrated model at each parameter draw from the benchmark economy's posterior distribution. Then, I decompose the consumption responses into entrepreneurs' responses and workers' responses driven by $w\bar{l}$, r^a, r^b, and η, as in Figure 3 for the benchmark economy. Figure 6 plots the mean responses across the posterior distribution.

[48] In the model, output is determined by firms' Cobb–Douglas production, $Y_t = z_t K_{t-1}^{\alpha}(X_t L_t)^{1-\alpha}$. Because K_{t-1} is a slow-moving variable and L_t is determined by z_t, X_t, X_{t-1}, and K_{t-1} (through labor supply (12) and labor demand (A.10)), aggregate shocks z_t and g_t almost entirely determine the output volatility. Given this supply-side feature of the model, it is not surprising that the two economies exhibit similar output volatilities.

[49] At the posterior mode, $\frac{\sigma(\Delta \log C_t)}{\sigma(\Delta \log Y_t)}$ is 1.232 and 0.746 in the benchmark and counterfactual economies, respectively.

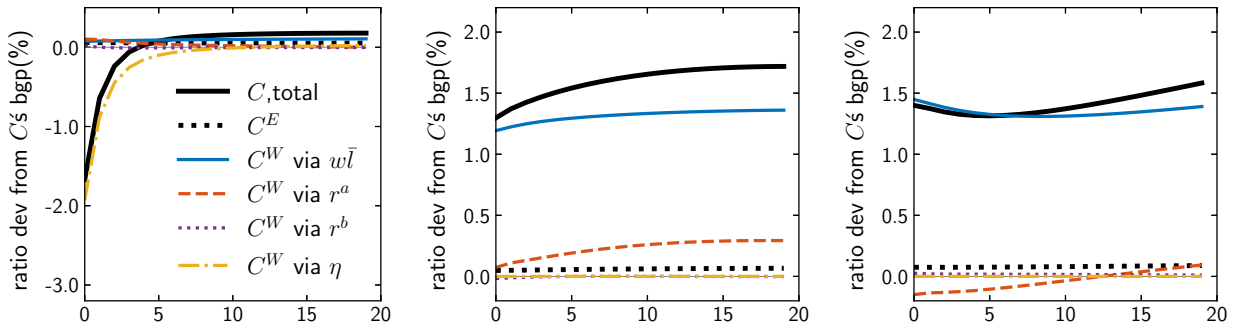

(a) Response to η Shock (b) Response to z Shock (c) Response to g Shock

Figure 6: Consumption Response Decomposition in the Counterfactual Economy

Notes: Figures 6a, 6b, and 6c plot the impulse responses of consumption to one-standard-deviation η, z, and g shocks, respectively, in the counterfactual economy evaluated at the parameter draws from the benchmark economy's posterior distribution. In each figure, the consumption response is decomposed into entrepreneurs' consumption response and workers' responses driven by $w\bar{l}$, r^a, r^b, and η in their budget constraints. The model statistics are computed at each posterior draw, and their means across the posterior distribution are plotted. The unit of the y-axis, 'ratio dev from C's bgp(%),' represents the deviation from the balanced growth path (b.g.p) of the variable of interest divided by C_t on the b.g.p.

Figure 6a shows that the mean consumption response to a financial friction shock is substantially weaker in the counterfactual economy than that in the benchmark economy (which is plotted in Figure 3a), and the weaker total response is driven by workers' weaker response to the change of η_t in their budget constraint. Economically, workers have a weaker precautionary saving motive in the counterfactual economy than in the benchmark economy, and thus, in the face of heightened financial friction, precautionary saving is also less enhanced in the counterfactual economy.

Figure 6b shows that the mean consumption response to a stationary productivity shock is also substantially weaker in the counterfactual economy than that in the benchmark economy (which is plotted in Figure 3b), and the weaker total response is driven by workers' weaker responses to $w_t\bar{l}_t$ and r^a_t in their budget constraint. However, as Online Appendix L.1 shows, the impulse responses of the drivers ($w_t\bar{l}_t$ and r^a_t) to a z shock are very similar between the two economies. This means that when a z shock is realized, workers face a similar degree of income fluctuations between the benchmark and counterfactual economies, but those in the counterfactual economy exhibit much smaller MPC and thus translate the income fluctuations far less into consumption fluctuations.

The weak consumption responses to η and z shocks observed in Figures 6a and 6b and the underlying economic mechanisms explain why the mean consumption volatility is smaller in the counterfactual economy than in the benchmark economy, as presented in Figure 5b.

In the rest of this section, I discuss two other interesting observations regarding the counterfactual economy. First, unlike η and z shocks, a trend shock generates more consumption fluctuations

in the counterfactual economy than in the benchmark economy.[50] Figures 6c and 3c reveal the reason why: the consumption response to a g shock is stronger in the counterfactual economy than in the benchmark economy. This is because a precautionary saving motive is weak in the counterfactual economy, and thus, Aguiar and Gopinath (2007)'s permanent income effect is revived.

Second, the consumption volatility distribution is more dispersed in the counterfactual economy than in the benchmark economy in Figure 5b for the following reason. The Bayesian estimation does not sharply pin down ρ_η and σ_η because both a relatively small but persistent η shock and a large but transitory η shock can generate a strong and sharp consumption response in the model (see Figure L.8 in Online Appendix L.2) and thus can explain macro data well. However, when these shocks are fed into the counterfactual economy, the consumption response varies substantially depending on the types of the η shock: the response becomes much weaker in the counterfactual economy than in the benchmark economy when the shock is relatively small but persistent (as in the posterior mode), while it becomes not much weaker (and sometimes becomes even stronger) when the shock is large but transitory. Economically, this is because the main transmission mechanism is different depending on the types of the η shock. As discussed in section 4, the financial friction shock generates consumption fluctuations through i) consumption smoothing disruption for those who face an immediate need to cash out their assets and ii) enhanced precautionary saving for those who do not. A relatively small but persistent η shock works more through enhanced precautionary saving for the future, while a large but transitory η shock works more through immediate consumption smoothing disruption. In the counterfactual economy, the enhanced precautionary saving effect becomes substantially weaker, while the consumption smoothing disruption does not.

6 Conclusion

This paper explains emerging market business cycles using a HASOE model disciplined by MPC estimates from Peruvian micro data. I find that a conventional mechanism through which the corresponding RASOE model explains emerging market business cycles does not operate in the HASOE model because it is hindered by household precautionary saving. Instead, the HASOE model explains emerging market business cycles through a new mechanism in which households' high MPC and correspondingly strong precautionary saving play important roles. When household MPCs are adjusted to the U.S. level, which is substantially lower than the Peruvian level, via recalibration, excess consumption volatility disappears in most of the posterior distribution.

[50] In Online Appendix I, I decompose the change in consumption variance (from the benchmark to the counterfactual economies) into the changes originating from each shock. In terms of the posterior mean, $\sigma^2(\Delta \log C_t)$ decreases by 32.2% in the counterfactual economy. Out of this -32.2% change, -27.9%p and -18.0%p come from η and z shocks generating fluctuations less, respectively, while +13.7%p comes from a g shock generating fluctuations more.

References

Aguiar, M. and G. Gopinath (2007). Emerging Market Business Cycles: The Cycle Is the Trend. *Journal of Political Economy 115*(1), 69–102.

Ahn, S., G. Kaplan, B. Moll, T. Winberry, and C. Wolf (2018). When Inequality Matters for Macro and Macro Matters for Inequality. *NBER Macroeconomics Annual 32*(1), 1–75.

Alvaredo, F., A. B. Atkinson, et al. (2021). Distributional National Accounts Guidelines: Methods and Concepts Used in the World Inequality Database. WID Working Paper No. 2016/2, revised June 2021.

Arellano, C. (2008). Default Risk and Income Fluctuations in Emerging Economies. *American Economic Review 98*(3), 690–712.

Atkeson, A. and L. E. Ohanian (2001). Are Phillips Curves Useful for Forecasting Inflation? *Federal Reserve Bank of Minneapolis Quarterly Review 25*(1), 2–11.

Auclert, A. (2019). Monetary Policy and the Redistribution Channel. *American Economic Review 109*(6), 2333–67.

Auclert, A., B. Bardóczy, and M. Rognlie (2021). MPCs, MPEs, and Multipliers: A Trilemma for New Keynesian Models. *The Review of Economics and Statistics*, 1–41.

Auclert, A., B. Bardóczy, M. Rognlie, and L. Straub (2021). Using the Sequence-Space Jacobian to Solve and Estimate Heterogeneous-Agent Models. *Econometrica 89*(5), 2375–2408.

Auclert, A., M. Rognlie, M. Souchier, and L. Straub (2021). Exchange Rates and Monetary Policy with Heterogeneous Agents: Sizing up the Real Income Channel. National Bureau of Economic Research Working Paper 28872.

Auclert, A., M. Rognlie, and L. Straub (2018). The Intertemporal Keynesian Cross. National Bureau of Economic Research Working Paper No. 25020.

Auclert, A., M. Rognlie, and L. Straub (2020). Micro Jumps, Macro Humps: Monetary Policy and Business Cycles in an Estimated HANK Model. National Bureau of Economic Research Working Paper No. 26647.

Bajard, F., L. Chancel, R. Moshrif, and T. Piketty (2022). Global Wealth Inequality on WID.world: Estimates and Imputations. World Inequality Lab Technical Note No. 2021/16, revised January 2022.

Bayer, C., B. Born, and R. Luetticke (2022). Shocks, Frictions, and Inequality in US Business Cycles. Working Paper.

Bayer, C. and R. Luetticke (2020). Solving Discrete Time Heterogeneous Agent Models with Aggregate Risk and Many Idiosyncratic States by Perturbation. *Quantitative Economics 11*(4), 1253–1288.

Bayer, C., R. Luetticke, L. Pham-Dao, and V. Tjaden (2019). Precautionary Savings, Illiquid

Assets, and the Aggregate Consequences of Shocks to Household Income Risk. *Econometrica 87*(1), 255–290.

Bianchi, J. (2011). Overborrowing and Systemic Externalities in the Business Cycle. *American Economic Review 101*(7), 3400–3426.

Blundell, R., L. Pistaferri, and I. Preston (2008). Consumption Inequality and Partial Insurance. *American Economic Review 98*(5), 1887–1921.

Boppart, T., P. Krusell, and K. Mitman (2018). Exploiting MIT Shocks in Heterogeneous-Agent Economies: the Impulse Response as a Numerical Derivative. *Journal of Economic Dynamics and Control 89*, 68–92.

Chang, R. and A. Fernández (2013). On the Sources of Aggregate Fluctuations in Emerging Economies. *International Economic Review 54*(4), 1265–1293.

Chen, K. and M. J. Crucini (2016). Trends and Cycles in Small Open Economies: Making the Case for a General Equilibrium Approach. *Journal of Economic Dynamics and Control 72*, 159–168.

Crawley, E. (2020). In Search of Lost Time Aggregation. *Economics Letters 189*, 108998.

De Ferra, S., K. Mitman, and F. Romei (2020). Household Heterogeneity and the Transmission of Foreign Shocks. *Journal of International Economics 124*, 103–303.

Diaz-Gimenez, J., V. Quadrini, and J.-V. Rios-Rull (1997). Dimensions of Inequality: Facts on the US Distribution of Earnings, Income and Wealth. *Federal Reserve Bank of Minneapolis Quarterly Review 21*(2), 3–21.

Feenstra, R. C., R. Inklaar, and M. P. Timmer (2015). The Next Generation of the Penn World Table. *American Economic Review 105*(10), 3150–82.

Fernández-Villaverde, J., P. Guerrón-Quintana, J. F. Rubio-Ramirez, and M. Uribe (2011). Risk Matters: The Real Effects of Volatility Shocks. *American Economic Review 101*(6), 2530–61.

Ferrante, F. and N. Gornemann (2022). Devaluations, Deposit Dollarization, and Household Heterogeneity. Working Paper.

Floden, M. and J. Lindé (2001). Idiosyncratic Risk in the United States and Sweden: Is There a Role for Government Insurance? *Review of Economic Dynamics 4*(2), 406–437.

Garcia-Cicco, J., R. Pancrazi, and M. Uribe (2010). Real Business Cycles in Emerging Countries? *American Economic Review 100*(5), 2510–31.

Greenwood, J., Z. Hercowitz, and G. W. Huffman (1988). Investment, Capacity Utilization, and the Real Business Cycle. *American Economic Review*, 402–417.

Guntin, R., P. Ottonello, and D. Perez (2022). The Micro Anatomy of Macro Consumption Adjustments. *The American Economic Review*, Forthcoming.

Guo, X., P. Ottonello, and D. Perez (2022). Monetary Policy and Redistribution in Open Economies. *Journal of Political Economy Macroeconomics*, Forthcoming.

Herbst, E. P. and F. Schorfheide (2015). *Bayesian Estimation of DSGE Models*. Princeton Univer-

sity Press.

Hong, S. (2022). MPCs in an Emerging Economy: Evidence from Peru. *Journal of International Economics*, Forthcoming.

Kaplan, G., B. Moll, and G. L. Violante (2018). Monetary Policy According to HANK. *American Economic Review 108*(3), 697–743.

Kaplan, G. and G. L. Violante (2018). Microeconomic Heterogeneity and Macroeconomic Shocks. *Journal of Economic Perspectives 32*(3), 167–194.

Krueger, D., K. Mitman, and F. Perri (2016). Macroeconomics and Household Heterogeneity. In *Handbook of Macroeconomics*, Volume 2, pp. 843–921. Elsevier.

Krueger, D. and F. Perri (2006). Does Income Inequality Lead to Consumption Inequality? Evidence and Theory. *The Review of Economic Studies 73*(1), 163–193.

McKay, A., E. Nakamura, and J. Steinsson (2016). The Power of Forward Guidance Revisited. *American Economic Review 106*(10), 3133–58.

Mendoza, E. G. (2010). Sudden Stops, Financial Crises, and Leverage. *American Economic Review 100*(5), 1941–66.

Mendoza, E. G. and V. Z. Yue (2012). A General Equilibrium Model of Sovereign Default and Business Cycles. *The Quarterly Journal of Economics 127*(2), 889–946.

Milesi-Ferretti, G. M. and P. R. Lane (2017). International Financial Integration in the Aftermath of the Global Financial Crisis. Working Paper 115, International Monetary Fund.

Neumeyer, P. A. and F. Perri (2005). Business Cycles in Emerging Economies: the Role of Interest Rates. *Journal of Monetary Economics 52*(2), 345–380.

Oh, H. and R. Reis (2012). Targeted Transfers and the Fiscal Response to the Great Recession. *Journal of Monetary Economics 59*, S50–S64.

Oskolkov, A. (2022). Exchange Rate Policy and Heterogeneity in Small Open Economies. Working Paper.

Reiter, M. (2009). Solving Heterogeneous-Agent Models by Projection and Perturbation. *Journal of Economic Dynamics and Control 33*(3), 649–665.

Sunel, E. (2018). Welfare Consequences of Gradual Disinflation in Emerging Economies. *Journal of Money, Credit and Banking 50*(4), 705–755.

Uribe, M. and S. Schmitt-Grohé (2017). *Open Economy Macroeconomics*. Princeton University Press.

Uribe, M. and V. Z. Yue (2006). Country Spreads and Emerging Countries: Who Drives Whom? *Journal of International Economics 69*(1), 6–36.

Villalvazo, S. (2021). Inequality and Asset Prices during Sudden Stops. Working Paper.

Winberry, T. (2018). A Method for Solving and Estimating Heterogeneous Agent Macro Models. *Quantitative Economics 9*(3), 1123–1151.

Zhou, H. (2021). Open Economy, Redistribution, and the Aggregate Impact of External Shocks. Working Paper.

[Online Appendix]

Emerging Market Business Cycles with Heterogeneous Agents

Seungki Hong

A Details of the RASOE Model

A.1 Equilibrium under Deterministic Paths of Aggregate Exogenous Variables

In this subsection, I characterize the complete set of equilibrium conditions of the RASOE model introduced in subsection 2.1 when the economy is subject to deterministic paths of aggregate exogenous variables $\{z_t, g_t, \mu_t\}_{t=0}^{\infty}$.

Households' optimality conditions are derived as follows.

$$\begin{aligned}\max_{\{C_t,A_t,L_t\}_{t=0}^{\infty}} & \sum_{t=0}^{\infty}(\beta_R)^t \frac{(C_t-\kappa_R X_{t-1}L_t^{1+\omega})^{1-\gamma}}{1-\gamma} \\ s.t. \quad & C_t + A_t = w_t L_t + (1+r_t^a)A_{t-1},\ t\geq 0, \text{ and} \\ & \lim_{j\to\infty} E_t\left[A_{t+j}\Big/\left(\prod_{s=1}^{j}(1+r_{t+s}^a)\right)\right]\geq 0.\end{aligned} \tag{A.1}$$

$$\mathfrak{L} = \sum_{t=0}^{\infty}(\beta_R)^t \frac{(C_t-\kappa_R X_{t-1}L_t^{1+\omega})^{1-\gamma}}{1-\gamma} + \sum_{t=0}^{\infty}(\beta_R)^t \lambda_t\left\{w_t L_t + (1+r_t^a)A_{t-1} - C_t - A_t\right\}.$$

$$(C_t-\kappa_R X_{t-1}L_t^{1+\omega})^{-\gamma} = \lambda_t, \quad t\geq 0, \tag{A.2}$$

$$\lambda_t = \beta_R(1+r_{t+1}^a)\lambda_{t+1}, \quad t\geq 0, \quad \text{and} \tag{A.3}$$

$$w_t = (1+\omega)\kappa_R X_{t-1}L_t^{\omega}, \quad t\geq 0. \tag{A.4}$$

Firms' optimality conditions are derived as follows.

$$\begin{aligned}\max_{\{K_t,F_t,L_t,Y_t,I_t,\Pi_t\}_{t=0}^{\infty}} & \sum_{t=0}^{\infty} Q_{0,t}\Pi_t \\ s.t. \quad & \Pi_t = Y_t - w_t L_t - I_t - \Phi(K_t,K_{t-1}) + F_t - (1+r_{t-1})F_{t-1}, && \text{(A.5)} \\ & Y_t = z_t K_{t-1}^{\alpha}(X_t L_t)^{1-\alpha}, && \text{(A.6)} \\ & I_t = K_t - (1-\delta)K_{t-1}, && \text{(A.7)} \\ & \Phi(K_t,K_{t-1}) = \frac{\phi}{2}\left(\frac{K_t}{K_{t-1}} - g^*\right)^2 K_{t-1},\end{aligned}$$

$$Q_{0,t} = \begin{cases} 1 & \text{if} \quad t = 0, \\ 1/(\prod_{s=1}^{t}(1+r_s^a)) & \text{if} \quad t \geq 1, \end{cases} \quad \text{and}$$

$$\lim_{j\to\infty} E_t\left[F_{t+j}\Big/(\prod_{s=1}^{j}(1+r_{t+s}^a))\right] \leq 0.$$

$$\Leftrightarrow \max_{\{K_t,F_t,L_t\}_{t=0}^{\infty}} \sum_{t=0}^{\infty} Q_{0,t}\Big[z_t K_{t-1}^{\alpha}(X_t L_t)^{1-\alpha} - w_t L_t - \big(K_t - (1-\delta)K_{t-1}\big) - \frac{\phi}{2}\left(\frac{K_t}{K_{t-1}} - g^*\right)^2 K_{t-1} + F_t - (1+r_{t-1})F_{t-1}\Big].$$

$$\begin{aligned}(1+r_{t+1}^a)\left\{1+\phi\left(\frac{K_t}{K_{t-1}}-g^*\right)\right\} &= \alpha z_{t+1}\left(\frac{K_t}{X_{t+1}L_{t+1}}\right)^{\alpha-1} \\ &+ \left\{1-\delta+\phi\left(\frac{K_{t+1}}{K_t}-g^*\right)\frac{K_{t+1}}{K_t} - \frac{\phi}{2}\left(\frac{K_{t+1}}{K_t}-g^*\right)^2\right\}, \quad t \geq 0, \end{aligned} \tag{A.8}$$

$$1 + r_{t+1}^a = 1 + r_t, \quad t \geq 0, \quad \text{and} \tag{A.9}$$

$$w_t = (1-\alpha) z_t X_t \left(\frac{K_{t-1}}{X_t L_t}\right)^{\alpha}. \tag{A.10}$$

Given the initial conditions on $X_{-1}, A_{-1}, K_{-1}, D_{-1}, F_{-1}$, and r_{-1} and deterministic paths of aggregate exogenous variables $\{z_t, g_t, \mu_t\}_{t=0}^{\infty}$, the equilibrium is characterized by equilibrium variables $\{C_t, A_t, L_t, \lambda_t, K_t, D_t, F_t, w_t, Y_t, I_t, \Pi_t, q_t, r_t^a, r_t\}_{t=0}^{\infty}$ satisfying equations (A.1) - (A.10), (2), (3), (5), and (6).

By Walras' law, we can derive the resource constraint (or, equivalently, the goods market clearing condition in the open economy) using equations (A.1), (2), (3), (A.5), and (5) as follows.

$$\begin{aligned} C_t &= w_t L_t + (1+r_t^a)A_{t-1} - A_t = w_t L_t + (1+r_t^a)q_{t-1} - q_t = w_t L_t + \Pi_t \\ &= Y_t - I_t - \Phi(K_t, K_{t-1}) + F_t - (1+r_{t-1})F_{t-1} = Y_t - I_t - \Phi(K_t, K_{t-1}) + D_t - (1+r_{t-1})D_{t-1}. \end{aligned}$$

$$\therefore C_t + I_t + \frac{\phi}{2}\left(\frac{K_t}{K_{t-1}} - g^*\right)^2 K_{t-1} = Y_t + D_t - (1+r_{t-1})D_{t-1}. \tag{A.11}$$

A.2 Detrended Equilibrium under Deterministic Paths of Aggregate Exogenous Variables

Since the equilibrium characterized in Online Appendix A.1 is nonstationary due to the stochastic trend $\{X_t\}_{t=0}^{\infty}$, we need to detrend the equilibrium to make it stationary. I detrend the equilibrium variables as follows.[1]

$$\tilde{C}_t := C_t/X_{t-1}, \quad \tilde{A}_t := A_t/X_t, \quad \tilde{\lambda}_t := \lambda_t/X_{t-1}^{-\gamma}, \quad \tilde{K}_t := K_t/X_t,$$

[1] Specifically, I detrend flow variables with X_{t-1} and stock variables with X_t.

$$\tilde{D}_t = D_t/X_t, \quad \tilde{F}_t = F_t/X_t, \quad \tilde{w}_t := w_t/X_{t-1}, \quad \tilde{Y}_t := Y_t/X_{t-1},$$

$$\tilde{I}_t := I_t/X_{t-1}, \quad \tilde{\Pi}_t := \Pi_t/X_{t-1}, \quad \tilde{q}_t := q_t/X_t, \quad \text{and} \quad \tilde{TB}_t = TB_t/X_{t-1}.$$

The equilibrium conditions are detrended as follows.

$$\tilde{C}_t + g_t\tilde{A}_t = \tilde{w}_t L_t + (1+r_t^a)\tilde{A}_{t-1}, \quad t \geq 0, \tag{A.12}$$

$$(\tilde{C}_t - \kappa_R L_t^{1+\omega})^{-\gamma} = \tilde{\lambda}_t, \quad t \geq 0, \tag{A.13}$$

$$\tilde{\lambda}_t = g_t^{-\gamma}\beta_R(1+r_t)\tilde{\lambda}_{t+1}, \quad t \geq 0, \tag{A.14}$$

$$\tilde{w}_t = (1+\omega)\kappa_R L_t^{\omega}, \quad t \geq 0, \tag{A.15}$$

$$\tilde{\Pi}_t = \tilde{Y}_t - \tilde{w}_t L_t - \tilde{I}_t - \frac{\phi}{2}\left(\frac{\tilde{K}_t}{\tilde{K}_{t-1}}g_t - g^*\right)^2 \tilde{K}_{t-1} + g_t\tilde{F}_t - (1+r_{t-1})\tilde{F}_{t-1}, \quad t \geq 0, \tag{A.16}$$

$$\tilde{Y}_t = z_t g_t^{1-\alpha}\tilde{K}_{t-1}^{\alpha} L_t^{1-\alpha}, \quad t \geq 0, \tag{A.17}$$

$$\tilde{I}_t = g_t\tilde{K}_t - (1-\delta)\tilde{K}_{t-1}, \quad t \geq 0, \tag{A.18}$$

$$\begin{aligned}(1+r_t)\left\{1+\phi\left(\frac{\tilde{K}_t}{\tilde{K}_{t-1}}g_t - g^*\right)\right\} &= \alpha z_{t+1} g_{t+1}^{1-\alpha}\left(\frac{\tilde{K}_t}{L_{t+1}}\right)^{\alpha-1} \\ &+ \left\{1-\delta+\phi\left(\frac{\tilde{K}_{t+1}}{\tilde{K}_t}g_{t+1} - g^*\right)\frac{\tilde{K}_{t+1}}{\tilde{K}_t}g_{t+1} - \frac{\phi}{2}\left(\frac{\tilde{K}_{t+1}}{\tilde{K}_t}g_{t+1} - g^*\right)^2\right\}, \quad t \geq 0,\end{aligned} \tag{A.19}$$

$$1 + r_{t+1}^a = 1 + r_t, \quad t \geq 0, \tag{A.20}$$

$$\tilde{w}_t = (1-\alpha) z_t g_t^{1-\alpha}\left(\frac{\tilde{K}_{t-1}}{L_t}\right)^{\alpha}, \quad t \geq 0, \tag{A.21}$$

$$\tilde{A}_t = \tilde{q}_t, \quad t \geq 0, \tag{A.22}$$

$$1 + r_t^a = \frac{\tilde{\Pi}_t + g_t\tilde{q}_t}{\tilde{q}_{t-1}}, \quad t \geq 0, \tag{A.23}$$

$$\tilde{F}_t = \tilde{D}_t, \quad t \geq 0, \quad \text{and} \tag{A.24}$$

$$r_t = r^* + \psi\left\{\exp\left(\frac{\tilde{D}_t - \tilde{D}^*}{\tilde{Y}^*}\right) - 1\right\} - \theta_z(z_t - 1) - \theta_g\left(\frac{g_t}{g^*} - 1\right) + \mu_t - 1, \quad t \geq 0. \tag{A.25}$$

Given the initial conditions on $\tilde{A}_{-1}, \tilde{K}_{-1}, \tilde{D}_{-1}, \tilde{F}_{-1}$, and r_{-1} and deterministic paths of aggregate exogenous variables $\{z_t, g_t, \mu_t\}_{t=0}^{\infty}$, the detrended equilibrium is characterized by equilibrium variables $\{\tilde{C}_t, \tilde{A}_t, L_t, \tilde{\lambda}_t, \tilde{K}_t, \tilde{D}_t, \tilde{F}_t, \tilde{w}_t, \tilde{Y}_t, \tilde{I}_t, \tilde{\Pi}_t, \tilde{q}_t, r_t^a, r_t\}_{t=0}^{\infty}$ satisfying equations (A.12) - (A.25).

The resource constraint and the equation for the trade balance are also detrended as follows.

$$\tilde{C}_t + \tilde{I}_t + \frac{\phi}{2}\left(\frac{\tilde{K}_t}{\tilde{K}_{t-1}}g_t - g^*\right)^2 \tilde{K}_{t-1} = \tilde{Y}_t + g_t\tilde{D}_t - (1+r_{t-1})\tilde{D}_{t-1}, \quad t \geq 0. \tag{A.26}$$

$$\tilde{TB}_t = -g_t \tilde{D}_t + (1 + r_{t-1})\tilde{D}_{t-1}, \quad t \geq 0. \tag{A.27}$$

A.3 Steady State of the Detrended Equilibrium

For any variable x_t, let x_{ss} denote its steady state value. In the steady state of the detrended equilibrium, the following equations hold.

$$z_{ss} = 1, \quad g_{ss} = g^*, \quad \text{and} \quad \mu_{ss} = 1.$$
$$\tilde{D}_{ss} = \tilde{D}^* \quad \text{and} \quad \tilde{Y}_{ss} = \tilde{Y}^* \quad \text{(by definition)}.$$

In the steady state, the detrended equilibrium conditions become

$$\tilde{C}_{ss} = \tilde{w}_{ss} L_{ss} + (1 + r^a_{ss} - g_{ss})\tilde{A}_{ss}, \tag{A.28}$$

$$(\tilde{C}_{ss} - \kappa_R L_{ss}^{1+\omega})^{-\gamma} = \tilde{\lambda}_{ss}, \tag{A.29}$$

$$g_{ss}^{-\gamma} \beta_R (1 + r_{ss}) = 1, \tag{A.30}$$

$$\tilde{w}_{ss} = (1 + \omega)\kappa_R L_{ss}^{\omega}, \tag{A.31}$$

$$\tilde{\Pi}_{ss} = \tilde{Y}_{ss} - \tilde{w}_{ss} L_{ss} - \tilde{I}_{ss} - (1 + r_{ss} - g_{ss})\tilde{F}_{ss}, \tag{A.32}$$

$$\tilde{Y}_{ss} = z_{ss} g_{ss}^{1-\alpha} \tilde{K}_{ss}^{\alpha} L_{ss}^{1-\alpha}, \tag{A.33}$$

$$\tilde{I}_{ss} = (g_{ss} - 1 + \delta)\tilde{K}_{ss}, \tag{A.34}$$

$$r_{ss} + \delta = \alpha(\tilde{Y}_{ss}/\tilde{K}_{ss}), \tag{A.35}$$

$$r^a_{ss} = r_{ss}, \tag{A.36}$$

$$\tilde{w}_{ss} = (1 - \alpha) z_{ss} g_{ss}^{1-\alpha} (\tilde{K}_{ss}/L_{ss})^{\alpha}, \tag{A.37}$$

$$\tilde{A}_{ss} = \tilde{q}_{ss}, \tag{A.38}$$

$$(1 + r^a_{ss} - g_{ss})\tilde{q}_{ss} = \tilde{\Pi}_{ss}, \tag{A.39}$$

$$\tilde{F}_{ss} = \tilde{D}_{ss}, \quad \text{and} \tag{A.40}$$

$$r_{ss} = r^*. \tag{A.41}$$

Moreover, the resource constraint and the equation for the trade balance become

$$\tilde{C}_{ss} + \tilde{I}_{ss} = \tilde{Y}_{ss} - (1 + r_{ss} - g_{ss})\tilde{D}_{ss}, \quad \text{and} \tag{A.42}$$

$$\tilde{TB}_{ss} = (1 + r_{ss} - g_{ss})\tilde{D}_{ss}. \tag{A.43}$$

Using equations (A.38), (A.39), (A.32), (A.37), (A.33), (A.35),(A.34), (A.40), and (A.36), we can derive a relationship among stock variables $\tilde{A}_{ss}$, $\tilde{K}_{ss}$, and $\tilde{D}_{ss}$ as follows.

$$\begin{aligned}(1+r^a_{ss}-g_{ss})\tilde{A}_{ss} &= (1+r^a_{ss}-g_{ss})\tilde{q}_{ss} = \tilde{\Pi}_{ss} = \tilde{Y}_{ss} - \tilde{w}_{ss}L_{ss} - \tilde{I}_{ss} - (1+r_{ss}-g_{ss})\tilde{F}_{ss} \\ &= \alpha\tilde{Y}_{ss} - \tilde{I}_{ss} - (1+r_{ss}-g_{ss})\tilde{F}_{ss} = (r_{ss}+\delta)\tilde{K}_{ss} - \tilde{I}_{ss} - (1+r_{ss}-g_{ss})\tilde{F}_{ss} \\ &= (r_{ss}+\delta)\tilde{K}_{ss} - (g_{ss}-1+\delta)\tilde{K}_{ss} - (1+r_{ss}-g_{ss})\tilde{F}_{ss} \\ &= (r_{ss}+\delta)\tilde{K}_{ss} - (g_{ss}-1+\delta)\tilde{K}_{ss} - (1+r_{ss}-g_{ss})\tilde{D}_{ss} \\ &= (1+r_{ss}-g_{ss})(\tilde{K}_{ss}-\tilde{D}_{ss}) = (1+r^a_{ss}-g_{ss})(\tilde{K}_{ss}-\tilde{D}_{ss}).\end{aligned}$$

$$\therefore \tilde{A}_{ss} = \tilde{K}_{ss} - \tilde{D}_{ss}.$$

A.4 An Equivalent, Centralized Economy

In subsection 2.1, I present a decentralized version of a stanrard RASOE model. In this subsection, I present an equivalent, centralized version of the RASOE model, which appears far more frequently in related studies.

Consider an economy composed of representative households. They produce output Y_t using capital K_{t-1} and their own labor L_t, make investment I_t to accumulate capital, and borrow debt D_t from the international financial market. They optimize the GHH preference subject to resource constraints and the no-Ponzi-game constraint as follows.

$$\max_{\{C_t,I_t,K_t,Y_t,D_t,L_t\}_{t=0}^{\infty}} E_0 \sum_{t=0}^{\infty} (\beta_R)^t \frac{(C_t - \kappa_R X_{t-1} L_t^{1+\omega})^{1-\gamma}}{1-\gamma}$$

$$s.t. \quad C_t + I_t + \frac{\phi}{2}\left(\frac{K_t}{K_{t-1}} - g^*\right)^2 K_{t-1} = Y_t + D_t - (1+r_{t-1})D_{t-1}, \tag{A.44}$$

$$Y_t = z_t K_{t-1}^{\alpha} (X_t L_t)^{1-\alpha}, \tag{A.45}$$

$$I_t = K_t - (1-\delta)K_{t-1}, \text{ and} \tag{A.46}$$

$$\lim_{j\to\infty} E_t\left[D_{t+j} \Big/ \left(\prod_{s=0}^{j-1}(1+r_{t+s})\right)\right] \leq 0.$$

The interest rate r_t in the international financial market is determined according to equation (6). As in Online Appendix A.1, I derive the complete set of equilibrium conditions when the

economy is subject to deterministic paths of aggregate exogenous variables $\{z_t, g_t, \mu_t\}_{t=0}^{\infty}$.

$$\mathfrak{L} = \sum_{t=0}^{\infty} (\beta_R)^t \frac{(C_t - \kappa_R X_{t-1} L_t^{1+\omega})^{1-\gamma}}{1-\gamma}$$
$$+ \sum_{t=0}^{\infty} (\beta_R)^t \lambda_t \left\{ z_t K_{t-1}^{\alpha} (X_t L_t)^{1-\alpha} + D_t - (1+r_{t-1}) D_{t-1} - C_t - (K_t - (1-\delta) K_{t-1}) - \frac{\phi}{2} \left(\frac{K_t}{K_{t-1}} - g^* \right)^2 K_{t-1} \right\}.$$

$$(C_t - \kappa_R X_{t-1} L_t^{1+\omega})^{-\gamma} = \lambda_t, \quad t \geq 0, \tag{A.47}$$

$$\lambda_t = \beta_R (1+r_t) \lambda_{t+1}, \quad t \geq 0, \tag{A.48}$$

$$(1-\alpha) z_t X_t \left(\frac{K_{t-1}}{X_t L_t} \right)^{\alpha} = (1+\omega) \kappa_R X_{t-1} L_t^{\omega}, \quad t \geq 0, \quad \text{and} \tag{A.49}$$

$$\begin{aligned} (1+r_t) \left\{ 1 + \phi \left(\frac{K_t}{K_{t-1}} - g^* \right) \right\} &= \alpha z_{t+1} \left(\frac{K_t}{X_{t+1} L_{t+1}} \right)^{\alpha-1} \\ &+ \left\{ 1 - \delta + \phi \left(\frac{K_{t+1}}{K_t} - g^* \right) \frac{K_{t+1}}{K_t} - \frac{\phi}{2} \left(\frac{K_{t+1}}{K_t} - g^* \right)^2 \right\}, \quad t \geq 0. \end{aligned} \tag{A.50}$$

Given the initial conditions on X_{-1}, K_{-1}, D_{-1}, and r_{-1} and deterministic paths of aggregate exogenous variables $\{z_t, g_t, \mu_t\}_{t=0}^{\infty}$, the equilibrium is characterized by equilibrium variables $\{C_t, L_t, \lambda_t, K_t, D_t, Y_t, I_t, r_t\}_{t=0}^{\infty}$ satisfying equations (A.44) - (A.50) and (6).

It is straightforward to verify that i) all the equilibrium conditions in the centralized economy are satisfied in the decentralized economy and that ii) $\{A_t, F_t, w_t, \Pi_t, q_t, r_t^a\}_{t=0}^{\infty}$ can be constructed in the centralized economy such that the equilibrium variables and the newly constructed variables of the centralized economy together satisfy all the equilibrium conditions of the decentralized economy. Therefore, the decentralized economy in subsection 2.1 and the centralized economy in this subsection yield the same equilibrium.

B Details of the HASOE Model

B.1 Equilibrium under Deterministic Paths of Aggregate Exogenous Variables

In this subsection, I characterize the complete set of equilibrium conditions of the HASOE model in subsection 4 when the economy is subject to deterministic paths of aggregate exogenous variables $\{z_t, g_t, \mu_t, \eta_t\}_{t=0}^{\infty}$. The HASOE model in subsection 2.2, which does not have a financial friction shock η_t, has the same equilibrium conditions except that η_t should be replaced with 1.

Workers' problem can be expressed as the following Bellman equation.

$$V_t^W(e_1,e_2,b_-,a_-;\Gamma) = \max_{c,b,a} \frac{c^{1-\gamma}}{1-\gamma} + \beta \sum_{e_1',e_2'} P(e_1',e_2'|e_1,e_2) V_{t+1}^W(e_1',e_2',b,a;\Gamma)$$

$$\begin{aligned} s.t. \quad & c+b+a+\eta_t\chi_t(a-(1+r_t^a)a_-,a_-;\Gamma) = w_t\Gamma e\bar{l}_t + (1-\xi)(1+r_t^b)b_- + (1+r_t^a)a_-, \\ & a \geq 0, \quad b \geq 0, \quad \text{and} \\ & \log e = \log e_1 + \log e_2. \end{aligned}$$

On the balanced growth path where $z_t = 1$, $g_t = g^*$, $\mu_t = 1$,and $\eta_t = 1$, V_t^W grows at the rate of $(g^*)^{1-\gamma}$ or, equivalently, $V_{t+1}^W = (g^*)^{1-\gamma} V_t^W$.

Under the parametrization of $\chi_t(v,a_-;\Gamma)$ in subsection 2.2, its first-order derivatives are

$$\begin{aligned} \chi_{1,t}(v,a_-;\Gamma) &= sign(v)\ \chi_1\chi_2 \left| \frac{v}{(1+r_t^a)a_- + \chi_0\Upsilon(\Gamma)X_{t-1}} \right|^{\chi_2-1}, \quad \text{and} \\ \chi_{2,t}(v,a_-;\Gamma) &= \chi_1(1-\chi_2) \left| \frac{v}{(1+r_t^a)a_- + \chi_0\Upsilon(\Gamma)X_{t-1}} \right|^{\chi_2} (1+r_t^a). \end{aligned}$$

Both $\chi_{1,t}(v,a_-;\Gamma)$ and $\chi_{2,t}(v,a_-;\Gamma)$ are continuous in (v,a_-) everywhere, including the area around $v=0$. Therefore, $\chi_t(v,a_-;\Gamma)$ is continuous and differentiable in (v,a_-) everywhere.

Workers' optimality conditions are derived as follows.

$$\begin{aligned} V_t^W(e_1,e_2,b_-,a_-;\Gamma) = \max_{c,b,a}\ & \frac{c^{1-\gamma}}{1-\gamma} + \beta \sum_{e_1',e_2'} P(e_1',e_2'|e_1,e_2) V_{t+1}^W(e_1',e_2',b,a;\Gamma) \\ & + \lambda\{w_t\Gamma e\bar{l}_t + (1-\xi)(1+r_t^b)b_- + (1+r_t^a)a_- \\ & \quad - c - b - a - \eta_t\chi_t(a-(1+r_t^a)a_-,a_-;\Gamma)\} + \varphi^b b + \varphi^a a. \end{aligned}$$

$$\lambda = c^{-\gamma}, \tag{B.1}$$

$$\lambda = \beta \sum_{e_1',e_2'} P(e_1',e_2'|e_1,e_2) V_{b,t+1}^W(e_1',e_2',b,a;\Gamma) + \varphi^b, \tag{B.2}$$

$$\lambda\{1+\eta_t\chi_{1,t}(a-(1+r_t^a)a_-,a_-;\Gamma)\} = \beta \sum_{e_1',e_2'} P(e_1',e_2'|e_1,e_2) V_{a,t+1}^W(e_1',e_2',b,a;\Gamma) + \varphi^a, \tag{B.3}$$

$$V_{b,t}^W(e_1,e_2,b_-,a_-;\Gamma) = (1-\xi)(1+r_t^b)\lambda, \tag{B.4}$$

$$\begin{aligned} V_{a,t}^W(e_1,e_2,b_-,a_-;\Gamma) = \lambda\{&(1+r_t^a) + (1+r_t^a)\eta_t\chi_{1,t}(a-(1+r_t^a)a_-,a_-;\Gamma) \\ &- \eta_t\chi_{2,t}(a-(1+r_t^a)a_-,a_-;\Gamma)\}, \end{aligned} \tag{B.5}$$

$$c+b+a+\eta_t\chi_t(a-(1+r_t^a)a_-,a_-;\Gamma) = w_t\Gamma e\bar{l}_t + (1-\xi)(1+r_t^b)b_- + (1+r_t^a)a_-, \tag{B.6}$$

$$\varphi^b \geq 0, \quad b \geq 0, \quad \varphi^b b = 0, \quad \text{and} \tag{B.7}$$

$$\varphi^a \geq 0, \quad a \geq 0, \quad \varphi^a a = 0. \tag{B.8}$$

Entrepreneurs' optimality conditions are derived as follows.

$$\begin{aligned} &\max_{\{C_t^E, A_t^E\}_{t=0}^{\infty}} \sum_{t=0}^{\infty} (\beta_E)^t \frac{(C_t^E)^{1-\gamma}}{1-\gamma} \\ s.t. \quad & C_t^E + A_t^E = R_t^E + (1+r_t^a)A_{t-1}^E, \quad \text{and} \\ & \lim_{j\to\infty} E_t \left[A_{t+j}^E \Big/ \left(\prod_{s=1}^{j} (1+r_{t+s}^a) \right) \right] \geq 0. \end{aligned} \tag{B.9}$$

$$\mathfrak{L} = \sum_{t=0}^{\infty} (\beta_E)^t \frac{(C_t^E)^{1-\gamma}}{1-\gamma} + \sum_{t=0}^{\infty} (\beta_E)^t \lambda_t^E \left\{ R_t^E + (1+r_t^a)A_{t-1}^E - C_t^E - A_t^E \right\}.$$

$$\lambda_t^E = (C_t^E)^{-\gamma}, \quad t \geq 0,$$

$$\lambda_t^E = \beta_E (1+r_{t+1}^a)\lambda_{t+1}^E, \quad t \geq 0$$

$$\Rightarrow (C_t^E)^{-\gamma} = \beta_E (1+r_{t+1}^a)(C_{t+1}^E)^{-\gamma}, \quad t \geq 0. \tag{B.10}$$

Firms' optimality conditions are the same as those derived in Online Appendix A.1.

Given the initial conditions on $\Psi_0(e_1, e_2, b_-, a_-|\Gamma)$, X_{-1}, A_{-1}, A_{-1}^E, K_{-1}, D_{-1}, B_{-1}, F_{-1}, and r_{-1} and deterministic paths of aggregate exogenous variables $\{z_t, g_t, \mu_t, \eta_t\}_{t=0}^{\infty}$, *(i)* individual workers' policy functions $\{c_t(e_1, e_2, b_-, a_-; \Gamma), b_t(e_1, e_2, b_-, a_-; \Gamma), a_t(e_1, e_2, b_-, a_-; \Gamma)\}_{t=0}^{\infty}$, first-order derivatives of the value functions $\{V_{b,t}^W(e_1, e_2, b_-, a_-; \Gamma), V_{a,t}^W(e_1, e_2, b_-, a_-; \Gamma)\}_{t=0}^{\infty}$, and Lagrangian multipliers $\{\lambda_t(e_1, e_2, b_-, a_-; \Gamma), \varphi_t^b(e_1, e_2, b_-, a_-; \Gamma), \varphi_t^a(e_1, e_2, b_-, a_-; \Gamma)\}_{t=0}^{\infty}$ that satisfy workers' optimality conditions (B.1) - (B.8), *(ii)* conditional cumulative distributions $\{\Psi_t(e_1, e_2, b_-, a_-|\Gamma)\}_{t=1}^{\infty}$ that evolve over time according to equation (13), and *(iii)* prices and aggregate variables $\{r_t^b, r_t^a, r_t, w_t, q_t, \bar{l}_t, L_t, \Pi_t, Y_t, I_t, K_t, F_t, D_t, TB_t, C_t, C_t^E, A_t, A_t^E, R_t^E, B_t, \chi_t^{agg}\}_{t=0}^{\infty}$ satisfying entrepreneurs' optimality conditions (B.9) and (B.10), firms' optimality conditions (A.5) - (A.10), aggregation equations (18), (19), (20), and (23), and other equilibrium conditions (2), (3), (6), (8), (11), (12), (15), (16), and (17) constitute the equilibrium of the economy.

By Walras' law, we can show that the resource constraint (A.11) (or, equivalently, the goods market clearing condition in the open economy) also holds in the HASOE model as follows. By aggregating workers' budget constraint (B.6), we obtain

$$C_t^W + B_t^W + A_t^W + \chi_t^W = w_t(L_t/p) + (1-\xi)(1+r_t^b)B_{t-1}^W + (1+r_t^a)A_{t-1}^W. \tag{B.11}$$

Combining equation (B.11) with equations (B.9), (17), (18), (19), (20), and (23), we can obtain

$$C_t + B_t + A_t = w_t L_t + (1 + r_t^b) B_{t-1} + (1 + r_t^a) A_{t-1}. \tag{B.12}$$

Combining equations (B.12), (2), (3), (A.5), (16), and (15), we can obtain

$$\begin{aligned} C_t &= w_t L_t + (1 + r_t^b) B_{t-1} - B_t + (1 + r_t^a) A_{t-1} - A_t = w_t L_t + (1 + r_t^b) B_{t-1} - B_t + (1 + r_t^a) q_{t-1} - q_t \\ &= w_t L_t + (1 + r_t^b) B_{t-1} - B_t + \Pi_t = Y_t - I_t - \Phi(K_t, K_{t-1}) + F_t - (1 + r_{t-1}) F_{t-1} + (1 + r_t^b) B_{t-1} - B_t \\ &= Y_t - I_t - \Phi(K_t, K_{t-1}) + D_t - (1 + r_{t-1}) D_{t-1}. \end{aligned}$$

$$\therefore C_t + I_t + \frac{\phi}{2} \left(\frac{K_t}{K_{t-1}} - g^* \right)^2 K_{t-1} = Y_t + D_t - (1 + r_{t-1}) D_{t-1}.$$

B.2 Detrended Equilibrium under Deterministic Paths of Aggregate Exogenous Variables

Since the equilibrium characterized in Online Appendix B.1 is nonstationary due to the stochastic trend $\{X_t\}_{t=0}^{\infty}$, we need to detrend the equilibrium to make it stationary. I detrend the variables and functions as follows.[2]

$$\tilde{c}_{i,t} := c_{i,t}/X_{t-1}, \quad \tilde{b}_{i,t} := b_{i,t}/X_t, \quad \tilde{a}_{i,t} := a_{i,t}/X_t,$$

$$\tilde{\lambda}_{i,t} := \lambda_{i,t}/X_{t-1}^{-\gamma}, \quad \tilde{\varphi}_{i,t}^b := \varphi_{i,t}^b/X_{t-1}^{-\gamma}, \quad \tilde{\varphi}_{i,t}^a := \varphi_{i,t}^a/X_{t-1}^{-\gamma},$$

$$\tilde{Y}_t := Y_t/X_{t-1}, \quad \tilde{C}_t := C_t/X_{t-1}, \quad \tilde{C}_t^E := C_t^E/X_{t-1}, \quad \tilde{C}_t^W := C_t^W/X_{t-1}, \quad \tilde{I}_t := I_t/X_{t-1}, \quad \tilde{R}_t^E := R_t^E/X_{t-1},$$

$$\tilde{\chi}_t^{agg} := \chi_t^{agg}/X_{t-1}, \quad \tilde{\chi}_t^W := \chi_t^W/X_{t-1}, \quad \tilde{w}_t := w_t/X_{t-1}, \quad \tilde{\Pi}_t := \Pi_t/X_{t-1}, \quad \tilde{TB}_t := TB_t/X_{t-1},$$

$$\tilde{B}_t := B_t/X_t, \quad \tilde{B}_t^W := B_t^W/X_t, \quad \tilde{A}_t := A_t/X_t, \quad \tilde{A}_t^E := A_t^E/X_t, \quad \tilde{A}_t^W := A_t^W/X_t,$$

$$\tilde{q}_t := q_t/X_t, \quad \tilde{D}_t := D_t/X_t, \quad \tilde{K}_t := K_t/X_t, \quad \text{and} \quad \tilde{F}_t := F_t/X_t.$$

$$\tilde{\Psi}_t(e_1, e_2, \tilde{b}_-, \tilde{a}_- | \Gamma) := \Psi_t(e_1, e_2, \tilde{b}_- X_{t-1}, \tilde{a}_- X_{t-1} | \Gamma),$$

$$\tilde{V}_{b,t}^W(e_1, e_2, \tilde{b}_-, \tilde{a}_-; \Gamma) := V_{b,t}^W(e_1, e_2, \tilde{b}_- X_{t-1}, \tilde{a}_- X_{t-1}; \Gamma)/X_{t-1}^{-\gamma},$$

$$\tilde{V}_{a,t}^W(e_1, e_2, \tilde{b}_-, \tilde{a}_-; \Gamma) := V_{a,t}^W(e_1, e_2, \tilde{b}_- X_{t-1}, \tilde{a}_- X_{t-1}; \Gamma)/X_{t-1}^{-\gamma},$$

$$\tilde{c}_t(e_1, e_2, \tilde{b}_-, \tilde{a}_-; \Gamma) := c_t(e_1, e_2, \tilde{b}_- X_{t-1}, \tilde{a}_- X_{t-1}; \Gamma)/X_{t-1},$$

$$\tilde{b}_t(e_1, e_2, \tilde{b}_-, \tilde{a}_-; \Gamma) := b_t(e_1, e_2, \tilde{b}_- X_{t-1}, \tilde{a}_- X_{t-1}; \Gamma)/X_t,$$

$$\tilde{a}_t(e_1, e_2, \tilde{b}_-, \tilde{a}_-; \Gamma) := a_t(e_1, e_2, \tilde{b}_- X_{t-1}, \tilde{a}_- X_{t-1}; \Gamma)/X_t,$$

[2] As in Online Appendix A.2, I detrend flow variables with X_{t-1} and stock variables with X_t.

$$\tilde{\lambda}_t(e_1,e_2,\tilde{b}_-,\tilde{a}_-;\Gamma) := \lambda_t(e_1,e_2,\tilde{b}_- X_{t-1},\tilde{a}_- X_{t-1};\Gamma)/X_{t-1}^{-\gamma},$$

$$\tilde{\varphi}_t^b(e_1,e_2,\tilde{b}_-,\tilde{a}_-;\Gamma) := \varphi_t^b(e_1,e_2,\tilde{b}_- X_{t-1},\tilde{a}_- X_{t-1};\Gamma)/X_{t-1}^{-\gamma},$$

$$\tilde{\varphi}_t^a(e_1,e_2,\tilde{b}_-,\tilde{a}_-;\Gamma) := \varphi_t^a(e_1,e_2,\tilde{b}_- X_{t-1},\tilde{a}_- X_{t-1};\Gamma)/X_{t-1}^{-\gamma}, \quad \text{and}$$

$$\tilde{\chi}_t(\tilde{v},\tilde{a}_-;\Gamma) := \chi_1 \left| \frac{\tilde{v}}{(1+r_t^a)\tilde{a}_- + \chi_0 \Upsilon(\Gamma)} \right|^{\chi_2} \big((1+r_t^a)\tilde{a}_- + \chi_0 \Upsilon(\Gamma) \big), \quad \text{where} \quad \Upsilon(\Gamma) = \tilde{w}_{ss} \Gamma \bar{e} \bar{l}_{ss}.$$

($\tilde{w}_{ss}$ and $\bar{l}_{ss}$ are the steady state values of $\tilde{w}_t$ and $\bar{l}_t$, respectively.)

The first-order derivatives of $\tilde{\chi}_t(\tilde{v},\tilde{a}_-;\Gamma)$ are

$$\tilde{\chi}_{1,t}(\tilde{v},\tilde{a}_-;\Gamma) = sign(\tilde{v}) \chi_1 \chi_2 \left| \frac{\tilde{v}}{(1+r_t^a)\tilde{a}_- + \chi_0 \Upsilon(\Gamma)} \right|^{\chi_2 - 1}, \quad \text{and}$$

$$\tilde{\chi}_{2,t}(\tilde{v},\tilde{a}_-;\Gamma) = \chi_1 (1-\chi_2) \left| \frac{\tilde{v}}{(1+r_t^a)\tilde{a}_- + \chi_0 \Upsilon(\Gamma)} \right|^{\chi_2} (1+r_t^a).$$

When $v_{i,t} = a_{i,t} - (1+r_t^a) a_{i,t-1}$ and $\tilde{v}_{i,t} := v_{i,t}/X_{t-1} = g_t \tilde{a}_{i,t} - (1+r_t^a)\tilde{a}_{i,t-1}$, we have

$$\begin{aligned}
&\tilde{\chi}_t(\tilde{v}_{i,t},\tilde{a}_{i,t-1};\Gamma) = \chi_t(v_{i,t},a_{i,t-1};\Gamma)/X_{t-1}, \\
&\tilde{\chi}_{1,t}(\tilde{v}_{i,t},\tilde{a}_{i,t-1};\Gamma) = \chi_{1,t}(v_{i,t},a_{i,t-1};\Gamma), \quad \text{and} \\
&\tilde{\chi}_{2,t}(\tilde{v}_{i,t},\tilde{a}_{i,t-1};\Gamma) = \chi_{2,t}(v_{i,t},a_{i,t-1};\Gamma).
\end{aligned}$$

Workers' optimality conditions are detrended as follows.

$$\tilde{\lambda} = \tilde{c}^{-\gamma}, \tag{B.13}$$

$$\tilde{\lambda} = \beta g_t^{-\gamma} \sum_{e_1',e_2'} P(e_1',e_2'|e_1,e_2) \tilde{V}_{\tilde{b},t+1}^W(e_1',e_2',\tilde{b},\tilde{a};\Gamma) + \tilde{\varphi}^b, \tag{B.14}$$

$$\begin{aligned}
&\tilde{\lambda}\{1+\eta_t \tilde{\chi}_{1,t}(g_t\tilde{a} - (1+r_t^a)\tilde{a}_-,\tilde{a}_-;\Gamma)\} \\
&\quad = \beta g_t^{-\gamma} \sum_{e_1',e_2'} P(e_1',e_2'|e_1,e_2) \tilde{V}_{\tilde{a},t+1}^W(e_1',e_2',\tilde{b},\tilde{a};\Gamma) + \tilde{\varphi}^a,
\end{aligned} \tag{B.15}$$

$$\tilde{V}_{\tilde{b},t}^W(e_1,e_2,\tilde{b}_-,\tilde{a}_-;\Gamma) = (1-\xi)(1+r_t^b)\tilde{\lambda}, \tag{B.16}$$

$$\begin{aligned}
\tilde{V}_{\tilde{a},t}^W(e_1,e_2,\tilde{b}_-,\tilde{a}_-;\Gamma) = \tilde{\lambda}\{&(1+r_t^a) + (1+r_t^a)\eta_t \tilde{\chi}_{1,t}(g_t\tilde{a} - (1+r_t^a)\tilde{a}_-,\tilde{a}_-;\Gamma) \\
&- \eta_t \tilde{\chi}_{2,t}(g_t\tilde{a} - (1+r_t^a)\tilde{a}_-,\tilde{a}_-;\Gamma)\},
\end{aligned} \tag{B.17}$$

$$\tilde{c} + g_t\tilde{b} + g_t\tilde{a} + \eta_t \tilde{\chi}_t(g_t\tilde{a} - (1+r_t^a)\tilde{a}_-,\tilde{a}_-;\Gamma) = \tilde{w}_t \Gamma e \bar{l}_t + (1-\xi)(1+r_t^b)\tilde{b}_- + (1+r_t^a)\tilde{a}_-, \tag{B.18}$$

$$\tilde{\varphi}^b \geq 0, \quad \tilde{b} \geq 0, \quad \tilde{\varphi}^b \tilde{b} = 0, \quad \text{and} \tag{B.19}$$

$$\tilde{\varphi}^a \geq 0, \quad \tilde{a} \geq 0, \quad \tilde{\varphi}^a \tilde{a} = 0. \tag{B.20}$$

The law of motion for $\Psi_t(e_1,e_2,b_-,a_-|\Gamma)$ (or, equivalently, equation (13)) is detrended to the law of motion for $\tilde{\Psi}_t(e_1,e_2,\tilde{b}_-,\tilde{a}_-|\Gamma)$ as follows.

$$\tilde{\Psi}_{t+1}(e_1',e_2',\tilde{b},\tilde{a}|\Gamma) = \int_{e_1,e_2,\tilde{b}_-,\tilde{a}_-} \Big[P(e_{1,t+1}\leq e_1'|e_{1,t}=e_1)\,P(e_{2,t+1}\leq e_2') \\ I_{\{\tilde{b}_t(e_1,e_2,\tilde{b}_-,\tilde{a}_-;\Gamma)\leq\tilde{b},\ \tilde{a}_t(e_1,e_2,\tilde{b}_-,\tilde{a}_-;\Gamma)\leq\tilde{a}\}}(e_1,e_2,\tilde{b}_-,\tilde{a}_-)\Big]\, d\tilde{\Psi}_t(e_1,e_2,\tilde{b}_-,\tilde{a}_-|\Gamma). \tag{B.21}$$

Entrepreneurs' optimality conditions are detrended as follows.

$$\tilde{C}_t^E + g_t\tilde{A}_t^E = \tilde{R}_t^E + (1+r_t^a)\tilde{A}_{t-1}^E, \quad t\geq 0, \quad \text{and} \tag{B.22}$$

$$(\tilde{C}_t^E)^{-\gamma} = g_t^{-\gamma}\beta_E(1+r_{t+1}^a)(\tilde{C}_{t+1}^E)^{-\gamma}, \quad t\geq 0. \tag{B.23}$$

Firms' detrended optimality conditions are the same as those derived in Online Appendix A.2. The aggregation equations (18), (19), (20), and (23) are detrended as follows.

$$\tilde{C}_t = p\tilde{C}_t^W + (1-p)\tilde{C}_t^E, \quad \tilde{C}_t^W = \int_\Gamma\int_{e_1,e_2,\tilde{b}_-,\tilde{a}_-} \tilde{c}_t(e_1,e_2,\tilde{b}_-,\tilde{a}_-;\Gamma)\, d\tilde{\Psi}_t dG. \tag{B.24}$$

$$\tilde{A}_t = p\tilde{A}_t^W + (1-p)\tilde{A}_t^E, \quad \tilde{A}_t^W = \int_\Gamma\int_{e_1,e_2,\tilde{b}_-,\tilde{a}_-} \tilde{a}_t(e_1,e_2,\tilde{b}_-,\tilde{a}_-;\Gamma)\, d\tilde{\Psi}_t dG. \tag{B.25}$$

$$\tilde{B}_t = p\tilde{B}_t^W, \quad \tilde{B}_t^W = \int_\Gamma\int_{e_1,e_2,\tilde{b}_-,\tilde{a}_-} \tilde{b}_t(e_1,e_2,\tilde{b}_-,\tilde{a}_-;\Gamma)\, d\tilde{\Psi}_t dG. \tag{B.26}$$

$$\tilde{\chi}_t^{agg} = p\tilde{\chi}_t^W, \ \ \tilde{\chi}_t^W = \int_\Gamma\int_{e_1,e_2,\tilde{b}_-,\tilde{a}_-} \eta_t\tilde{\chi}_t\left(g_t\tilde{a}_t(e_1,e_2,\tilde{b}_-,\tilde{a}_-;\Gamma) - (1+r_t^a)\tilde{a}_-,\tilde{a}_-;\Gamma\right) d\tilde{\Psi}_t dG. \tag{B.27}$$

Equations (12), (15), and (17) are detrended as follows.

$$\tilde{w}_t(p\bar{\Gamma}\bar{e})^{1+\omega} = \kappa L_t^\omega, \quad t\geq 0. \tag{B.28}$$

$$\tilde{F}_t = \tilde{D}_t + \tilde{B}_t, \quad t\geq 0. \tag{B.29}$$

$$(1-p)\tilde{R}_t^E = \xi(1+r_t^b)\tilde{B}_{t-1} + \tilde{\chi}_t^{agg}. \tag{B.30}$$

Equations (11) and (16) do not need to be detrended. The rest of the equilibrium conditions (*i.e.*, equations (2), (3), (6), and (8)) are detrended in Online Appendix A.2.

Given the initial conditions on $\tilde{\Psi}_0(e_1,e_2,\tilde{b}_-,\tilde{a}_-|\Gamma)$, $\tilde{A}_{-1}$, $\tilde{A}_{-1}^E$, $\tilde{K}_{-1}$, $\tilde{D}_{-1}$, $\tilde{B}_{-1}$, $\tilde{F}_{-1}$, and r_{-1} and deterministic paths of aggregate exogenous variables $\{z_t,g_t,\mu_t,\eta_t\}_{t=0}^\infty$, *(i)* individual workers' detrended policy functions $\{\tilde{c}_t(e_1,e_2,\tilde{b}_-,\tilde{a}_-;\Gamma),\tilde{b}_t(e_1,e_2,\tilde{b}_-,\tilde{a}_-;\Gamma),\tilde{a}_t(e_1,e_2,\tilde{b}_-,\tilde{a}_-;\Gamma)\}_{t=0}^\infty$, first-order derivatives of the detrended value functions $\{\tilde{V}_{\tilde{b},t}^W(e_1,e_2,\tilde{b}_-,\tilde{a}_-;\Gamma),\tilde{V}_{\tilde{a},t}^W(e_1,e_2,\tilde{b}_-,\tilde{a}_-;\Gamma)\}_{t=0}^\infty$, and detrended Lagrangian multipliers $\{\tilde{\lambda}_t(e_1,e_2,\tilde{b}_-,\tilde{a}_-;\Gamma),\tilde{\varphi}_t^b(e_1,e_2,\tilde{b}_-,\tilde{a}_-;\Gamma),\tilde{\varphi}_t^a(e_1,e_2,\tilde{b}_-,\tilde{a}_-;\Gamma)\}_{t=0}^\infty$

that satisfy workers' detrended optimality conditions (B.13) - (B.20), *(ii)* conditional cumulative distributions $\{\tilde{\Psi}_t(e_1,e_2,\tilde{b}_-,\tilde{a}_-|\Gamma)\}_{t=1}^{\infty}$ that evolve over time according to equation (B.21), and *(iii)* prices and aggregate variables $\{r_t^b, r_t^a, r_t, \tilde{w}_t, \tilde{q}_t, \bar{l}_t, L_t, \tilde{\Pi}_t, \tilde{Y}_t, \tilde{I}_t, \tilde{K}_t, \tilde{F}_t, \tilde{D}_t, \tilde{TB}_t, \tilde{C}_t, \tilde{C}_t^E, \tilde{A}_t, \tilde{A}_t^E, \tilde{R}_t^E, \tilde{B}_t, \tilde{\chi}_t^{agg}\}_{t=0}^{\infty}$ satisfying entrepreneurs' detrended optimality conditions (B.22) and (B.23), firms' detrended optimality conditions (A.16) - (A.21), detrended aggregation equations (B.24) - (B.27), and other detrended equilibrium conditions (A.22), (A.23), (A.25), (A.27), (11), (B.28), (B.29), (16), and (B.30) constitute the detrended equilibrium of the economy.

Since the resource constraint (A.11) holds in the undetrended HASOE equilibrium, the detrended resource consstraint (A.26) also holds in the detrended HASOE equilibrium.

B.3 Workers' Detrended and Normalized Optimality Conditions

Workers' detrended optimality conditions (B.13) - (B.20) can be normalized such that the predictable component of idiosyncratic productivity Γ is irrelevant under the normalized conditions. Let

$$\hat{w}_t := \tilde{w}_t/\tilde{w}_{ss}, \quad \hat{e}_{i,t} := e_{i,t}/\bar{e}, \quad \hat{l}_t := \bar{l}_t/\bar{l}_{ss},$$

$$\bar{e}_1 := E[e_{1,i,t}], \quad \hat{e}_{1,i,t} := e_{1,i,t}/\bar{e}_1, \quad \bar{e}_2 := E[e_{2,i,t}], \quad \hat{e}_{2,i,t} := e_{2,i,t}/\bar{e}_2,$$

$$\hat{c}_{i,t} := \tilde{c}_{i,t}/\Upsilon(\Gamma), \quad \hat{b}_{i,t} := \tilde{b}_{i,t}/\Upsilon(\Gamma), \quad \hat{a}_{i,t} := \tilde{a}_{i,t}/\Upsilon(\Gamma),$$

$$\hat{\lambda}_{i,t} := \tilde{\lambda}_{i,t}/\Upsilon(\Gamma)^{-\gamma}, \quad \hat{\varphi}_{i,t}^b := \tilde{\varphi}_{i,t}^b/\Upsilon(\Gamma)^{-\gamma}, \quad \hat{\varphi}_{i,t}^a := \tilde{\varphi}_{i,t}^a/\Upsilon(\Gamma)^{-\gamma},$$

$$\hat{C}_t^W := \tilde{C}_t^W/\Upsilon(\bar{\Gamma}), \quad \hat{B}_t^W := \tilde{B}_t^W/\Upsilon(\bar{\Gamma}), \quad \hat{A}_t^W := \tilde{A}_t^W/\Upsilon(\bar{\Gamma}), \quad \hat{\chi}_t^W := \tilde{\chi}_t^W/\Upsilon(\bar{\Gamma}),$$

$$\hat{\Psi}_t(\hat{e}_1,\hat{e}_2,\hat{b}_-,\hat{a}_-) := \tilde{\Psi}_t(\bar{e}_1\hat{e}_1,\bar{e}_2\hat{e}_2,\Upsilon(\Gamma)\hat{b}_-,\Upsilon(\Gamma)\hat{a}_-|\Gamma),$$

$$\hat{V}_{\hat{b},t}^W(\hat{e}_1,\hat{e}_2,\hat{b}_-,\hat{a}_-) := \tilde{V}_{\tilde{b},t}^W(\bar{e}_1\hat{e}_1,\bar{e}_2\hat{e}_2,\Upsilon(\Gamma)\hat{b}_-,\Upsilon(\Gamma)\hat{a}_-;\Gamma) \;/\; \Upsilon(\Gamma)^{-\gamma},$$

$$\hat{V}_{\hat{a},t}^W(\hat{e}_1,\hat{e}_2,\hat{b}_-,\hat{a}_-) := \tilde{V}_{\tilde{a},t}^W(\bar{e}_1\hat{e}_1,\bar{e}_2\hat{e}_2,\Upsilon(\Gamma)\hat{b}_-,\Upsilon(\Gamma)\hat{a}_-;\Gamma) \;/\; \Upsilon(\Gamma)^{-\gamma},$$

$$\hat{c}_t(\hat{e}_1,\hat{e}_2,\hat{b}_-,\hat{a}_-) := \tilde{c}_t(\bar{e}_1\hat{e}_1,\bar{e}_2\hat{e}_2,\Upsilon(\Gamma)\hat{b}_-,\Upsilon(\Gamma)\hat{a}_-;\Gamma)/\Upsilon(\Gamma),$$

$$\hat{b}_t(\hat{e}_1,\hat{e}_2,\hat{b}_-,\hat{a}_-) := \tilde{b}_t(\bar{e}_1\hat{e}_1,\bar{e}_2\hat{e}_2,\Upsilon(\Gamma)\hat{b}_-,\Upsilon(\Gamma)\hat{a}_-;\Gamma)/\Upsilon(\Gamma),$$

$$\hat{a}_t(\hat{e}_1,\hat{e}_2,\hat{b}_-,\hat{a}_-) := \tilde{a}_t(\bar{e}_1\hat{e}_1,\bar{e}_2\hat{e}_2,\Upsilon(\Gamma)\hat{b}_-,\Upsilon(\Gamma)\hat{a}_-;\Gamma)/\Upsilon(\Gamma),$$

$$\hat{\lambda}_t(\hat{e}_1,\hat{e}_2,\hat{b}_-,\hat{a}_-) := \tilde{\lambda}_t(\bar{e}_1\hat{e}_1,\bar{e}_2\hat{e}_2,\Upsilon(\Gamma)\hat{b}_-,\Upsilon(\Gamma)\hat{a}_-;\Gamma)/\Upsilon(\Gamma)^{-\gamma},$$

$$\hat{\varphi}_t^b(\hat{e}_1,\hat{e}_2,\hat{b}_-,\hat{a}_-) := \tilde{\varphi}_t^b(\bar{e}_1\hat{e}_1,\bar{e}_2\hat{e}_2,\Upsilon(\Gamma)\hat{b}_-,\Upsilon(\Gamma)\hat{a}_-;\Gamma)/\Upsilon(\Gamma)^{-\gamma},$$

$$\hat{\varphi}_t^a(\hat{e}_1,\hat{e}_2,\hat{b}_-,\hat{a}_-) := \tilde{\varphi}_t^a(\bar{e}_1\hat{e}_1,\bar{e}_2\hat{e}_2,\Upsilon(\Gamma)\hat{b}_-,\Upsilon(\Gamma)\hat{a}_-;\Gamma)/\Upsilon(\Gamma)^{-\gamma}, \quad \text{and}$$

$$\hat{\chi}_t(\hat{v},\hat{a}_-) := \chi_1\left|\frac{\hat{v}}{(1+r_t^a)\hat{a}_- + \chi_0}\right|^{\chi_2}\big((1+r_t^a)\hat{a}_- + \chi_0\big).$$

(In the first line of the equations, $\tilde{w}_{ss}$ and $\bar{l}_{ss}$ are the steady state values of $\tilde{w}_t$ and $\bar{l}_t$, respectively.)

The first-order derivatives of $\hat{\chi}_t(\hat{v},\hat{a}_-)$ are

$$\hat{\chi}_{1,t}(\hat{v},\hat{a}_-) = sign(\hat{v})\chi_1\chi_2\left|\frac{\hat{v}}{(1+r_t^a)\hat{a}_- + \chi_0}\right|^{\chi_2-1}, \quad \text{and}$$
$$\hat{\chi}_{2,t}(\hat{v},\hat{a}_-) = \chi_1(1-\chi_2)\left|\frac{\hat{v}}{(1+r_t^a)\hat{a}_- + \chi_0}\right|^{\chi_2}(1+r_t^a).$$

When $\tilde{v}_{i,t} = g_t\tilde{a}_{i,t} - (1+r_t^a)\tilde{a}_{i,t-1}$ and $\hat{v}_{i,t} := \tilde{v}_{i,t}/\Upsilon(\Gamma) = g_t\hat{a}_{i,t} - (1+r_t^a)\hat{a}_{i,t-1}$, we have

$$\hat{\chi}_t(\hat{v}_{i,t},\hat{a}_{i,t-1}) = \tilde{\chi}_t(\tilde{v}_{i,t},\tilde{a}_{i,t-1};\Gamma)/\Upsilon(\Gamma),$$
$$\hat{\chi}_{1,t}(\hat{v}_{i,t},\hat{a}_{i,t-1}) = \tilde{\chi}_{1,t}(\tilde{v}_{i,t},\tilde{a}_{i,t-1};\Gamma), \quad \text{and}$$
$$\hat{\chi}_{2,t}(\hat{v}_{i,t},\hat{a}_{i,t-1}) = \tilde{\chi}_{2,t}(\tilde{v}_{i,t},\tilde{a}_{i,t-1};\Gamma).$$

Workers' detrended optimality conditions (B.13) - (B.20) are normalized as follows.

$$\hat{\lambda} = \hat{c}^{-\gamma}, \tag{B.31}$$

$$\hat{\lambda} = \beta g_t^{-\gamma}\sum_{\hat{e}_1',\hat{e}_2'} P(\hat{e}_1',\hat{e}_2'|\hat{e}_1,\hat{e}_2)\hat{V}^W_{\hat{b},t+1}(\hat{e}_1',\hat{e}_2',\hat{b},\hat{a}) + \hat{\varphi}^b, \tag{B.32}$$

$$\begin{aligned}\hat{\lambda}\{1+&\eta_t\hat{\chi}_{1,t}(g_t\hat{a} - (1+r_t^a)\hat{a}_-,\hat{a}_-)\}\\ &= \beta g_t^{-\gamma}\sum_{\hat{e}_1',\hat{e}_2'} P(\hat{e}_1',\hat{e}_2'|\hat{e}_1,\hat{e}_2)\hat{V}^W_{\hat{a},t+1}(\hat{e}_1',\hat{e}_2',\hat{b},\hat{a}) + \hat{\varphi}^a,\end{aligned} \tag{B.33}$$

$$\hat{V}^W_{\hat{b},t}(\hat{e}_1,\hat{e}_2,\hat{b}_-,\hat{a}_-) = (1-\xi)(1+r_t^b)\hat{\lambda}, \tag{B.34}$$

$$\begin{aligned}\hat{V}^W_{\hat{a},t}(\hat{e}_1,\hat{e}_2,\hat{b}_-,\hat{a}_-) = \hat{\lambda}\{&(1+r_t^a) + (1+r_t^a)\eta_t\hat{\chi}_{1,t}(g_t\hat{a} - (1+r_t^a)\hat{a}_-,\hat{a}_-)\\ &- \eta_t\hat{\chi}_{2,t}(g_t\hat{a} - (1+r_t^a)\hat{a}_-,\hat{a}_-)\},\end{aligned} \tag{B.35}$$

$$\hat{c} + g_t\hat{b} + g_t\hat{a} + \eta_t\hat{\chi}_t(g_t\hat{a} - (1+r_t^a)\hat{a}_-,\hat{a}_-) = \hat{w}_t\hat{e}\hat{l}_t + (1-\xi)(1+r_t^b)\hat{b}_- + (1+r_t^a)\hat{a}_-, \tag{B.36}$$

$$\hat{\varphi}^b \geq 0, \quad \hat{b} \geq 0, \quad \hat{\varphi}^b\hat{b} = 0, \quad \text{and} \tag{B.37}$$

$$\hat{\varphi}^a \geq 0, \quad \hat{a} \geq 0, \quad \hat{\varphi}^a\hat{a} = 0. \tag{B.38}$$

Note that Γ does not appear in the normalized equations (B.31) - (B.38).

The law of motion for $\tilde{\Psi}_t(e_1,e_2,\tilde{b}_-,\tilde{a}_-|\Gamma)$ (or, equivalently, equation (B.21)) is normalized to

the law of motion for $\hat{\Psi}_t(\hat{e}_1,\hat{e}_2,\hat{b}_-,\hat{a}_-)$ as follows.

$$\hat{\Psi}_{t+1}(\hat{e}_1',\hat{e}_2',\hat{b},\hat{a}) = \int_{\hat{e}_1,\hat{e}_2,\hat{b}_-,\hat{a}_-} \Big[P(\hat{e}_{1,t+1} \leq \hat{e}_1' | \hat{e}_{1,t} = \hat{e}_1)\, P(\hat{e}_{2,t+1} \leq \hat{e}_2') \\ I_{\{\hat{b}_t(\hat{e}_1,\hat{e}_2,\hat{b}_-,\hat{a}_-)\leq \hat{b},\ \hat{a}_t(\hat{e}_1,\hat{e}_2,\hat{b}_-,\hat{a}_-)\leq \hat{a}\}}(\hat{e}_1,\hat{e}_2,\hat{b}_-,\hat{a}_-)\Big]\, d\hat{\Psi}_t(\hat{e}_1,\hat{e}_2,\hat{b}_-,\hat{a}_-). \tag{B.39}$$

Using the normalized variables and functions, the detreded aggregation equations (B.24) - (B.27) can be rewritten as follows.

$$\tilde{C}_t = p\tilde{C}_t^W + (1-p)\tilde{C}_t^E, \quad \tilde{C}_t^W = \Upsilon(\bar{\Gamma})\hat{C}_t^W, \quad \hat{C}_t^W = \int_{\hat{e}_1,\hat{e}_2,\hat{b}_-,\hat{a}_-} \hat{c}_t(\hat{e}_1,\hat{e}_2,\hat{b}_-,\hat{a}_-)\, d\hat{\Psi}_t. \tag{B.40}$$

$$\tilde{A}_t = p\tilde{A}_t^W + (1-p)\tilde{A}_t^E, \quad \tilde{A}_t^W = \Upsilon(\bar{\Gamma})\hat{A}_t^W, \quad \hat{A}_t^W = \int_{\hat{e}_1,\hat{e}_2,\hat{b}_-,\hat{a}_-} \hat{a}_t(\hat{e}_1,\hat{e}_2,\hat{b}_-,\hat{a}_-)\, d\hat{\Psi}_t. \tag{B.41}$$

$$\tilde{B}_t = p\tilde{B}_t^W, \quad \tilde{B}_t^W = \Upsilon(\bar{\Gamma})\hat{B}_t^W, \quad \hat{B}_t^W = \int_{\hat{e}_1,\hat{e}_2,\hat{b}_-,\hat{a}_-} \hat{b}_t(\hat{e}_1,\hat{e}_2,\hat{b}_-,\hat{a}_-)\, d\hat{\Psi}_t. \tag{B.42}$$

$$\tilde{\chi}_t^{agg} = p\tilde{\chi}_t^W, \ \ \tilde{\chi}_t^W = \Upsilon(\bar{\Gamma})\hat{\chi}_t^W, \ \ \hat{\chi}_t^W = \int_{\hat{e}_1,\hat{e}_2,\hat{b}_-,\hat{a}_-} \eta_t\hat{\chi}_t\big(g_t\hat{a}_t(\hat{e}_1,\hat{e}_2,\hat{b}_-,\hat{a}_-) - (1+r_t^a)\hat{a}_-,\hat{a}_-\big)\, d\hat{\Psi}_t. \tag{B.43}$$

Using the normalized variables, functions, and equations, the detrended equilibrium of the HASOE economy in Online Appendix B.2 can be rewritten as follows.

Given the initial conditions on $\hat{\Psi}_0(e_1,e_2,\tilde{b}_-,\tilde{a}_-)$, $\tilde{A}_{-1}$, $\tilde{A}_{-1}^E$, $\tilde{K}_{-1}$, $\tilde{D}_{-1}$, $\tilde{B}_{-1}$, $\tilde{F}_{-1}$, and r_{-1} and deterministic paths of aggregate exogenous variables $\{z_t,g_t,\mu_t,\eta_t\}_{t=0}^{\infty}$, *(i)* individual workers' detrended and normalized policy functions $\{\hat{c}_t(\hat{e}_1,\hat{e}_2,\hat{b}_-,\hat{a}_-),\hat{b}_t(\hat{e}_1,\hat{e}_2,\hat{b}_-,\hat{a}_-),\hat{a}_t(\hat{e}_1,\hat{e}_2,\hat{b}_-,\hat{a}_-)\}_{t=0}^{\infty}$, first-order derivatives of the detrended and normalized value functions $\{\hat{V}_{\hat{b},t}^W(\hat{e}_1,\hat{e}_2,\hat{b}_-,\hat{a}_-)$, $\hat{V}_{\hat{a},t}^W(\hat{e}_1,\hat{e}_2,\hat{b}_-,\hat{a}_-)\}_{t=0}^{\infty}$, and detrended and normalized Lagrangian multipliers $\{\hat{\lambda}_t(\hat{e}_1,\hat{e}_2,\hat{b}_-,\hat{a}_-)$, $\hat{\varphi}_t^b(\hat{e}_1,\hat{e}_2,\hat{b}_-,\hat{a}_-),\hat{\varphi}_t^a(\hat{e}_1,\hat{e}_2,\hat{b}_-,\hat{a}_-)\}_{t=0}^{\infty}$ that satisfy workers' detrended and normalized optimality conditions (B.31) - (B.38), *(ii)* cumulative distributions $\{\hat{\Psi}_t(\hat{e}_1,\hat{e}_2,\hat{b}_-,\hat{a}_-)\}_{t=1}^{\infty}$ that evolve over time according to equation (B.39), and *(iii)* prices and aggregate variables $\{r_t^b,r_t^a,r_t,\tilde{w}_t,\tilde{q}_t,\bar{l}_t,L_t,\tilde{\Pi}_t$, $\tilde{Y}_t,\tilde{I}_t,\tilde{K}_t,\tilde{F}_t,\tilde{D}_t,T\tilde{B}_t,\tilde{C}_t,\tilde{C}_t^E,\tilde{A}_t,\tilde{A}_t^E,\tilde{R}_t^E,\tilde{B}_t,\tilde{\chi}_t^{agg}\}_{t=0}^{\infty}$ satisfying entrepreneurs' detrended optimality conditions (B.22) and (B.23), firms' detrended optimality conditions (A.16) - (A.21), detrended aggregation equations (B.40) - (B.43), and other detrended equilibrium conditions (A.22), (A.23), (A.25), (A.27), (11), (B.28), (B.29), (16), and (B.30) constitute the detrended equilibrium of the economy.

When I numerically solve workers' problem, I use their detrended and normalized optimality conditions (B.31) - (B.38).

B.4 Steady State of the Detrended Equilibrium

For any variable x_t and any function $f_t(\cdot)$, let x_{ss} and $f_{ss}(\cdot)$ denote their steady state values, respectively. In the steady state of the detrended equilibrium, the following equations hold.

$$\begin{aligned} z_{ss} = 1, \quad g_{ss} = g^*, \quad \mu_{ss} = 1, \quad \text{and} \quad \eta_{ss} = 1. \\ \tilde{D}_{ss} = \tilde{D}^* \quad \text{and} \quad \tilde{Y}_{ss} = \tilde{Y}^* \quad \text{(by definition)}. \end{aligned}$$

In the steady state, workers' detrended and normalized policy functions $\hat{c}_{ss}(\hat{e}_1, \hat{e}_2, \hat{b}_-, \hat{a}_-)$, $\hat{b}_{ss}(\hat{e}_1, \hat{e}_2, \hat{b}_-, \hat{a}_-)$, and $\hat{a}_{ss}(\hat{e}_1, \hat{e}_2, \hat{b}_-, \hat{a}_-)$, first-order derivatives of the detrended and normalized value functions $\hat{V}^W_{\hat{b},ss}(\hat{e}_1, \hat{e}_2, \hat{b}_-, \hat{a}_-)$ and $\hat{V}^W_{\hat{a},ss}(\hat{e}_1, \hat{e}_2, \hat{b}_-, \hat{a}_-)$, and detrended and normalized Lagrangian multipliers $\hat{\lambda}_{ss}(\hat{e}_1, \hat{e}_2, \hat{b}_-, \hat{a}_-)$, $\hat{\varphi}^b_{ss}(\hat{e}_1, \hat{e}_2, \hat{b}_-, \hat{a}_-)$, and $\hat{\varphi}^a_{ss}(\hat{e}_1, \hat{e}_2, \hat{b}_-, \hat{a}_-)$ solve the following optimality conditions.

$$\hat{\lambda} = \hat{c}^{-\gamma}, \tag{B.44}$$

$$\hat{\lambda} = \beta g_{ss}^{-\gamma} \sum_{\hat{e}'_1, \hat{e}'_2} P(\hat{e}'_1, \hat{e}'_2 | \hat{e}_1, \hat{e}_2) \hat{V}^W_{\hat{b},ss}(\hat{e}'_1, \hat{e}'_2, \hat{b}, \hat{a}) + \hat{\varphi}^b, \tag{B.45}$$

$$\begin{aligned} &\hat{\lambda}\{1 + \hat{\chi}_{1,ss}(g_{ss}\hat{a} - (1 + r^a_{ss})\hat{a}_-, \hat{a}_-)\} \\ &\quad = \beta g_{ss}^{-\gamma} \sum_{\hat{e}'_1, \hat{e}'_2} P(\hat{e}'_1, \hat{e}'_2 | \hat{e}_1, \hat{e}_2) \hat{V}^W_{\hat{a},ss}(\hat{e}'_1, \hat{e}'_2, \hat{b}, \hat{a}) + \hat{\varphi}^a, \end{aligned} \tag{B.46}$$

$$\hat{V}^W_{\hat{b},ss}(\hat{e}_1, \hat{e}_2, \hat{b}_-, \hat{a}_-) = (1 - \xi)(1 + r^b_{ss})\hat{\lambda}, \tag{B.47}$$

$$\begin{aligned} \hat{V}^W_{\hat{a},ss}(\hat{e}_1, \hat{e}_2, \hat{b}_-, \hat{a}_-) = \hat{\lambda}\{&(1 + r^a_{ss}) + (1 + r^a_{ss})\hat{\chi}_{1,ss}(g_{ss}\hat{a} - (1 + r^a_{ss})\hat{a}_-, \hat{a}_-) \\ &- \hat{\chi}_{2,ss}(g_{ss}\hat{a} - (1 + r^a_{ss})\hat{a}_-, \hat{a}_-)\}, \end{aligned} \tag{B.48}$$

$$\hat{c} + g_{ss}\hat{b} + g_{ss}\hat{a} + \hat{\chi}_{ss}(g_{ss}\hat{a} - (1 + r^a_{ss})\hat{a}_-, \hat{a}_-) = \hat{w}_{ss}\hat{e}\hat{l}_{ss} + (1 - \xi)(1 + r^b_{ss})\hat{b}_- + (1 + r^a_{ss})\hat{a}_-, \tag{B.49}$$

$$\hat{\varphi}^b \geq 0, \quad \hat{b} \geq 0, \quad \hat{\varphi}^b \hat{b} = 0, \quad \text{and} \tag{B.50}$$

$$\hat{\varphi}^a \geq 0, \quad \hat{a} \geq 0, \quad \hat{\varphi}^a \hat{a} = 0. \tag{B.51}$$

In the steady state, the evolution equation for $\hat{\Psi}_t(\hat{e}_1, \hat{e}_2, \hat{b}_-, \hat{a}-)$ becomes

$$\begin{aligned} \hat{\Psi}_{ss}(\hat{e}'_1, \hat{e}'_2, \hat{b}, \hat{a}) = \int_{\hat{e}_1, \hat{e}_2, \hat{b}_-, \hat{a}_-} &\left[P(\hat{e}_{1,t+1} \leq \hat{e}'_1 | \hat{e}_{1,t} = \hat{e}_1)\, P(\hat{e}_{2,t+1} \leq \hat{e}'_2)\right. \\ &\left. I_{\{\hat{b}_{ss}(\hat{e}_1, \hat{e}_2, \hat{b}_-, \hat{a}_-) \leq \hat{b},\ \hat{a}_{ss}(\hat{e}_1, \hat{e}_2, \hat{b}_-, \hat{a}_-) \leq \hat{a}\}}(\hat{e}_1, \hat{e}_2, \hat{b}_-, \hat{a}_-)\right] d\hat{\Psi}_{ss}(\hat{e}_1, \hat{e}_2, \hat{b}_-, \hat{a}_-). \end{aligned} \tag{B.52}$$

In the steady state, entrepreneurs' detrended optimality conditions become

$$\tilde{C}^E_{ss} = \tilde{R}^E_{ss} + (1 + r^a_{ss} - g_{ss})\tilde{A}^E_{ss}, \quad \text{and} \tag{B.53}$$

$$g_{ss}^{-\gamma}\beta_E(1+r_{ss}^a)=1. \tag{B.54}$$

In the steady state, firms' detrended optimality conditions become (A.32) - (A.37).

In the steady state, the detrended aggregation equations become

$$\tilde{C}_{ss}=p\Upsilon(\bar{\Gamma})\hat{C}_{ss}^W+(1-p)\tilde{C}_{ss}^E,\quad \hat{C}_{ss}^W=\int_{\hat{e}_1,\hat{e}_2,\hat{b}_-,\hat{a}_-}\hat{c}_{ss}(\hat{e}_1,\hat{e}_2,\hat{b}_-,\hat{a}_-)\,d\hat{\Psi}_{ss}, \tag{B.55}$$

$$\tilde{A}_{ss}=p\Upsilon(\bar{\Gamma})\hat{A}_{ss}^W+(1-p)\tilde{A}_{ss}^E,\quad \hat{A}_{ss}^W=\int_{\hat{e}_1,\hat{e}_2,\hat{b}_-,\hat{a}_-}\hat{a}_{ss}(\hat{e}_1,\hat{e}_2,\hat{b}_-,\hat{a}_-)\,d\hat{\Psi}_{ss}, \tag{B.56}$$

$$\tilde{B}_{ss}=p\Upsilon(\bar{\Gamma})\hat{B}_{ss}^W,\quad \hat{B}_{ss}^W=\int_{\hat{e}_1,\hat{e}_2,\hat{b}_-,\hat{a}_-}\hat{b}_{ss}(\hat{e}_1,\hat{e}_2,\hat{b}_-,\hat{a}_-)\,d\hat{\Psi}_{ss},\quad \text{and} \tag{B.57}$$

$$\tilde{\chi}_{ss}^{agg}=p\Upsilon(\bar{\Gamma})\hat{\chi}_{ss}^W,\ \ \hat{\chi}_{ss}^W=\int_{\hat{e}_1,\hat{e}_2,\hat{b}_-,\hat{a}_-}\hat{\chi}_{ss}\left(g_{ss}\hat{a}_{ss}(\hat{e}_1,\hat{e}_2,\hat{b}_-,\hat{a}_-)-(1+r_{ss}^a)\hat{a}_-,\hat{a}_-\right)d\hat{\Psi}_{ss}. \tag{B.58}$$

In the steady state, equilibrium conditions (A.22), (A.23), (A.25), and (A.27) become (A.38), (A.39), (A.41), and (A.43), respectively, and equilibrium conditions (11), (B.28), (B.29), (16), and (B.30) become

$$L_{ss}=p\bar{\Gamma}\bar{e}\bar{l}_{ss}, \tag{B.59}$$

$$\tilde{w}_{ss}(p\bar{\Gamma}\bar{e})^{1+\omega}=\kappa L^{\omega}, \tag{B.60}$$

$$\tilde{F}_{ss}=\tilde{D}_{ss}+\tilde{B}_{ss}, \tag{B.61}$$

$$r_{ss}^b=r_{ss},\quad \text{and} \tag{B.62}$$

$$(1-p)\tilde{R}_{ss}^E=\xi(1+r_{ss}^b)\tilde{B}_{ss}+\tilde{\chi}_{ss}^{agg}. \tag{B.63}$$

Using equations (A.38), (A.39), (A.32), (A.37), (A.33), (A.35),(A.34), (B.61), and (A.36), we can derive a relationship among stock variables $\tilde{A}_{ss}$, $\tilde{B}_{ss}$, $\tilde{K}_{ss}$, and $\tilde{D}_{ss}$ as follows.

$$\begin{aligned}(1+r_{ss}^a-g_{ss})\tilde{A}_{ss}&=(1+r_{ss}^a-g_{ss})\tilde{q}_{ss}=\tilde{\Pi}_{ss}=\tilde{Y}_{ss}-\tilde{w}_{ss}L_{ss}-\tilde{I}_{ss}-(1+r_{ss}-g_{ss})\tilde{F}_{ss}\\&=\alpha\tilde{Y}_{ss}-\tilde{I}_{ss}-(1+r_{ss}-g_{ss})\tilde{F}_{ss}=(r_{ss}+\delta)\tilde{K}_{ss}-\tilde{I}_{ss}-(1+r_{ss}-g_{ss})\tilde{F}_{ss}\\&=(r_{ss}+\delta)\tilde{K}_{ss}-(g_{ss}-1+\delta)\tilde{K}_{ss}-(1+r_{ss}-g_{ss})\tilde{F}_{ss}\\&=(r_{ss}+\delta)\tilde{K}_{ss}-(g_{ss}-1+\delta)\tilde{K}_{ss}-(1+r_{ss}-g_{ss})(\tilde{D}_{ss}+\tilde{B}_{ss})\\&=(1+r_{ss}-g_{ss})(\tilde{K}_{ss}-\tilde{D}_{ss}-\tilde{B}_{ss})=(1+r_{ss}^a-g_{ss})(\tilde{K}_{ss}-\tilde{D}_{ss}-\tilde{B}_{ss}).\end{aligned}$$

$$\therefore\tilde{A}_{ss}+\tilde{B}_{ss}=\tilde{K}_{ss}-\tilde{D}_{ss}. \tag{B.64}$$

C Solution Method

I solve the detrended equilibrium of the RASOE and HASOE models (characterized in Online Appendices A.2 and B.2, respectively) using Auclert et al. (2021)'s method. In this section, I discuss how this method is applied to solve the models.

C.1 Steady State

The first step is to solve the steady state. The steady state of the (detrended) RASOE economy is straightforward to compute using equations (A.28) - (A.43). To compute the steady state of the (detrended) HASOE economy, I solve workers' (detrended and normalized) policy functions and stationary distribution that satisfy equations (B.44) - (B.52). Auclert et al. (2021) develop a fast algorithm that extends Carroll (2006)'s method of endogenous gridpoints to a two-asset environment in order to solve the steady state of their two-asset HANK model. Since the worker block of my model is almost identical to the household block of their model, I closely follow this algorithm to solve the workers' problem in the steady state. See Appendix E.1 of Auclert et al. (2021) for details of this algorithm.[3]

C.2 Sequence Space Approach

Once the steady state is pinned down, Auclert et al. (2021)'s method computes the Jacobians of 'blocks'. Here, a 'block' is a function that maps the sequences of input variables $\{x_{1,t},\cdots,x_{n_x,t}\}_{t=0}^{\infty}$ into the sequences of output variables $\{y_{1,t},\cdots,y_{n_y,t}\}_{t=0}^{\infty}$ using a subset of equilibrium conditions. The Jacobian of each block is a matrix composed of $(\partial y_{j,s}/\partial x_{i,t})_{1\leq i\leq n_x,\ 1\leq j\leq n_y,\ s,t\geq 0}$. For example, the worker block in my HASOE model maps the sequences of input variables $\{\tilde{w}_t, r_t^a, r_t^b, g_t, \bar{l}_t, \eta_t\}_{t=0}^{\infty}$ into the sequences of output variables $\{\tilde{C}_t^W, \tilde{B}_t^W, \tilde{A}_t^W, \tilde{\chi}_t^W\}_{t=0}^{\infty}$ using equilibrium conditions (B.31) - (B.43).[4] The Jacobian of the worker block is composed of $(\partial y_s/\partial x_t)_{x\in\{\tilde{w},r^a,r^b,g,\bar{l},\eta\},\ y\in\{\tilde{C}^W,\tilde{B}^W,\tilde{A}^W,\tilde{\chi}^W\},\ s,t\geq 0}$.

Figure C.1 is a directed acyclical graph (DAG) representation of the detrended equilibrium of the HASOE model, in which blocks, input variables, and output variables are indicated. Both the blue rectangles and red ellipses represent blocks of the equilibrium. For each block, variables coming into the block and variables coming out of the block (indicated by arrows connecting

[3] For grids, I use 10 gridpoints for $\hat{e}_1$ and $\hat{e}_2$, respectively, 50 gridpoints for $\hat{b}_-$, and 70 gridpoints for $\hat{a}_-$.

[4] Since I use normalized optimality conditions (B.31) - (B.38) to solve workers' problem, I first compute the Jacobian for normalized variables and then scale it to the one for unnormalized variables. For example, to compute $(\partial\tilde{C}_s^W/\partial\tilde{w}_t)$, I first compute $(\partial\hat{C}_s^W/\partial\hat{w}_t)$, and then scale it using the following equation:

$$\frac{\partial\tilde{C}_s^W}{\partial\tilde{w}_t} = \frac{\partial\left(\Upsilon(\bar{\Gamma})\hat{C}_s^W\right)}{\partial\left(\tilde{w}_{ss}\hat{w}_t\right)} = \frac{\Upsilon(\bar{\Gamma})}{\tilde{w}_{ss}}\frac{\partial\hat{C}_s^W}{\partial\hat{w}_{ss}}.$$

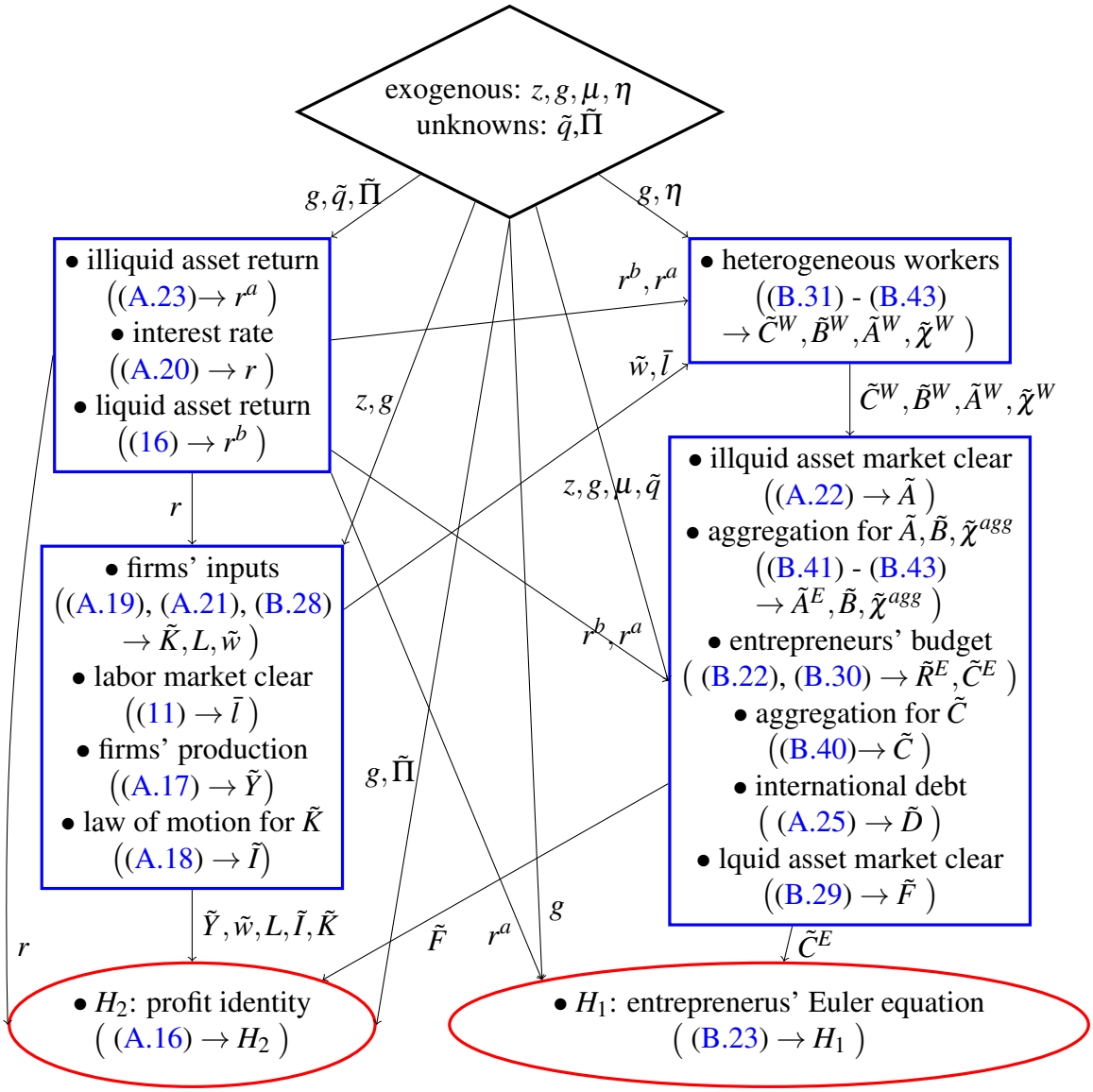

Figure C.1: DAG Representation of the Detrended Equilibrium of the HASOE Model

blocks) are input and output variables of the block, respectively. Within each block, the bullet points and following parentheses indicate the names of the equilibrium conditions, corresponding equation numbers, and output variables pinned down by the equilibrium conditions.

Following Auclert et al. (2021)'s notations, let Z denote a stacked vector of the sequences of exogenous variables and U be a stacked vector of the sequences of unknown variables (indicated in the black diamond box in Figure C.1). Moreover, let $H(U,Z)$ be a function that maps U and Z into a stacked vector of the sequences of target variables $\{H_{1,t}, H_{2,t}\}_{t=0}^{\infty}$, which are the output

variables of the red ellipses in Figure C.1 and are defined as

$$H_{1,t} = g_t^{-\gamma}\beta_E(1+r^a_{t+1})(\tilde{C}^E_{t+1})^{-\gamma} - (\tilde{C}^E_t)^{-\gamma}, \quad \text{and}$$
$$H_{2,t} = \tilde{Y}_t - \tilde{w}_t L_t - \tilde{I}_t - \frac{\phi}{2}\left(\frac{\tilde{K}_t}{\tilde{K}_{t-1}}g_t - g^*\right)^2 \tilde{K}_{t-1} + g_t\tilde{F}_t - (1+r_{t-1})\tilde{F}_{t-1} - \tilde{\Pi}_t.$$

Under this formulation, 'solving the model' boils down to finding U that satisfies

$$H(U,Z) = 0$$

for a given Z. Under the first-order approximation regarding U and Z, this equation becomes

$$\begin{aligned} H_U dU + H_Z dZ &= 0 \\ \Leftrightarrow dU &= -H_U^{-1} H_Z dZ. \end{aligned} \tag{C.1}$$

By combining the Jacobians of the blocks through the Chain Rule, Auclert et al. (2021)'s method computes H_U and H_Z. Then, the method solves dU using equation (C.1) and recovers the linearized dynamics of other variables by combining the Jacobians again along the directed acyclical graph in Figure C.1.

In the whole procedure of solving the HASOE model, i) computing the steady state and ii) computing the Jacobian of the heterogeneous worker block are the most time-consuming steps. In particular, calibrating β, χ_1, and χ_2 requires solving the steady state multiple times, and this step takes longer than a day. However, once these parameters are calibrated and I have both the computed steady state and Jacobian of the worker block in my hand, the rest of the steps required to solve the model are very fast. This is why Bayesian estimation of the model is possible as long as the parameters to be estimated do not affect the steady state and the Jacobian of the worker block.

As Auclert et al. (2021) notes, this method can also be used to solve representative-agent models. In this paper, I also solve my RASOE model using this method. Figure C.2 presents a DAG representation of the detrended equilibrium of the RASOE model.

In implementation of the sequence space approach, sequences of the equilibrium variables over an infinite horizon must be truncated to a finite horizon. In this paper, I truncate sequences at $T = 700$ when solving models and drop the last seven periods further when evaluating moments. In Online Appendix E, I verify that under this implementation, the truncation errors barely affect model statistics at the posterior mode.

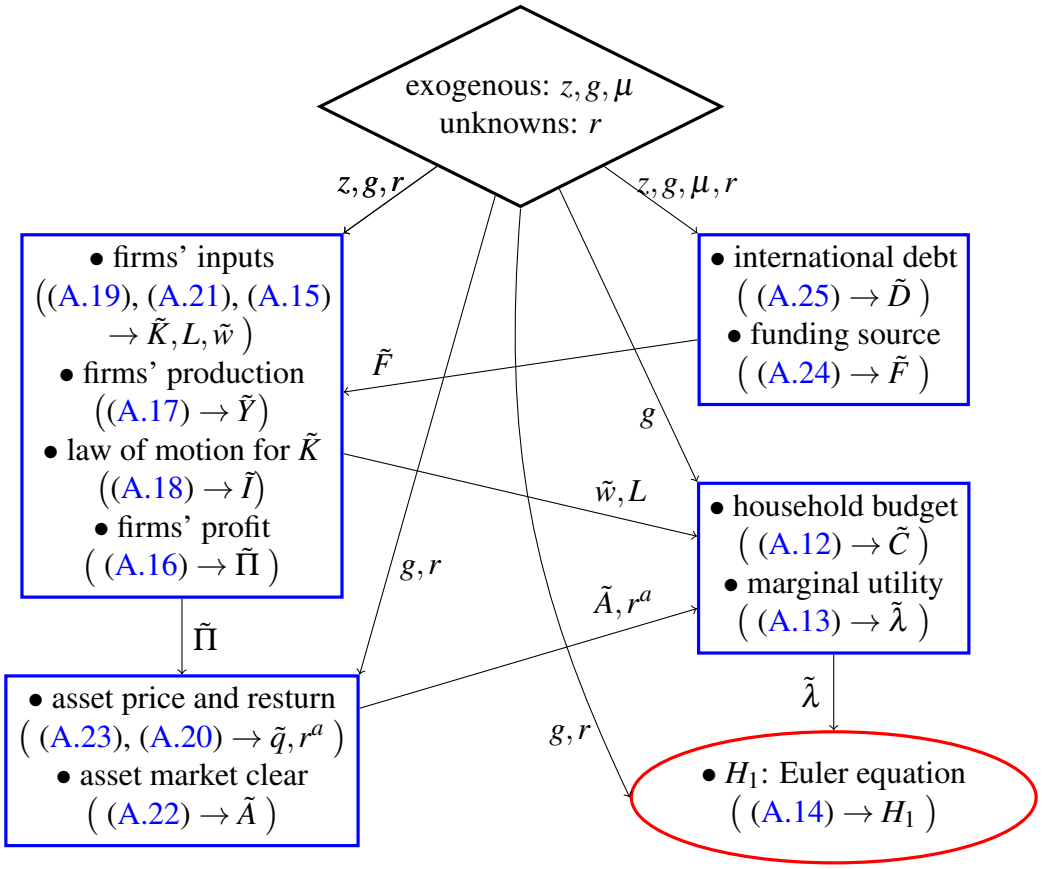

Figure C.2: DAG Representation of the Detrended Equilibrium of the RASOE Model

D Recovering the Original Equilibrium

Once the detrended equilibrium is solved, we can recover the original equilibrium. There are three types of variables in the original equilibrium that I must recover: i) observable variables ($\Delta \log Y_t$, $\Delta \log C_t$, $\Delta \log I_t$, and $\Delta(TB_t/Y_t)$), which do not exhibit a stochastic trend, ii) flow variables, which exhibit a stochastic trend and are detrended by X_{t-1} in the detrended equilibrium, and iii) stock variables, which exhibit a stochastic trend and are detrended by X_t in the detrended equilibrium. In this section, I discuss how I recover their impulse responses.

D.1 Observable Variables ($\Delta \log Y_t$, $\Delta \log C_t$, $\Delta \log I_t$, and $\Delta(TB_t/Y_t)$)

The observable variables in the original equilibrium can be described with variables in the detrended equilibrium as follows.

$$\begin{aligned}
\Delta \log Y_t &= \Delta \log \tilde{Y}_t - \Delta \log \tilde{Y}_{t-1} + \log g_{t-1}, \\
\Delta \log C_t &= \Delta \log \tilde{C}_t - \Delta \log \tilde{C}_{t-1} + \log g_{t-1}, \\
\Delta \log I_t &= \Delta \log \tilde{I}_t - \Delta \log \tilde{I}_{t-1} + \log g_{t-1}, \quad \text{and} \\
\Delta(TB_t/Y_t) &= (\tilde{TB}_t/\tilde{Y}_t) - (\tilde{TB}_{t-1}/\tilde{Y}_{t-1}).
\end{aligned} \tag{D.1}$$

For the purpose of this paper, I must compute the impulse responses of observable variables in terms of their *level* deviation. By solving the detrended equilibrium using Auclert et al. (2021)'s method, for any variable $\tilde{M}_t$ in the detrended equilibrium, I obtain $d(\tilde{M}_t) := \tilde{M}_t - \tilde{M}_{ss}$, where $\tilde{M}_{ss}$ is the steady state value of $\tilde{M}_t$. Using the relationships described in equation (D.1), I compute the observable variables' impulse responses as follows.

$$\begin{aligned}
IRF^{level}_{\Delta \log Y}(t) &= d(\Delta \log \tilde{Y}_t) - d(\Delta \log \tilde{Y}_{t-1}) + d(\log g_{t-1}), \\
IRF^{level}_{\Delta \log C}(t) &= d(\Delta \log \tilde{C}_t) - d(\Delta \log \tilde{C}_{t-1}) + d(\log g_{t-1}), \\
IRF^{level}_{\Delta \log I}(t) &= d(\Delta \log \tilde{I}_t) - d(\Delta \log \tilde{I}_{t-1}) + d(\log g_{t-1}), \quad \text{and} \\
IRF^{level}_{\Delta(TB/Y)}(t) &= d\left(\frac{\tilde{TB}_t}{\tilde{Y}_t}\right) - d\left(\frac{\tilde{TB}_{t-1}}{\tilde{Y}_{t-1}}\right).
\end{aligned}$$

D.2 Flow Variables

Flow variables in the original equilibrium, such as Y_t, C_t, I_t, Π_t, and w_t, exhibit a stochastic trend and are detrended by X_{t-1} in the detrended equilibrium. For the purpose of this paper, I must compute the impulse responses of the flow variables in terms of their *ratio* deviation from the balanced growth path. To this end, I first define the 'constant growth trend of the balanced growth path' X^*_t as follows. Given that a shock hits the economy at period 0,

$$X^*_t := (g^*)^{t+1} X_{-1}.$$

Let M^f_t denote one of the flow variables in the original equilibrium, $\tilde{M}^f_t := M^f_t / X_{t-1}$ denote its detrended variable, and $\tilde{M}^f_{ss}$ denote the steady state value of $\tilde{M}^f_t$ in the detrended equilibrium. M^f_t on the balanced growth path, which I denote as M^{f*}_t, is determined by

$$M^{f*}_t = \tilde{M}^f_{ss} X^*_{t-1}, \quad t \geq 0.$$

This is the path of M_t^f when there is no shock. The impulse response of M_t^f in terms of their ratio deviation from the balanced growth path can now be written as

$$IRF_{M^f}^{ratio}(t) = \frac{M_t^f - M_t^{f*}}{M_t^{f*}} = \frac{M_t^f / X_{t-1}^* - \tilde{M}_{ss}^f}{\tilde{M}_{ss}^f}.$$

I compute this impulse response as follows. By solving the detrended equilibrium using Auclert et al. (2021)'s method, I obtain $d\tilde{M}_t^f = \tilde{M}_t^f - \tilde{M}_{ss}^f$, where the d-operator on the left-hand side means the level deviation from the steady state in the detrended equilibrium (as defined in Online Appendix D.1). Then, I use the following equation, which holds under the first-order approximation, to obtain $d(M_t^f / X_{t-1}^*) = M_t^f / X_{t-1}^* - \tilde{M}_{ss}^f$.

$$\begin{aligned} d(M_t^f / X_{t-1}^*) &= d(\tilde{M}_t^f (X_{t-1} / X_{t-1}^*)) \\ &= d\tilde{M}_t^f + \tilde{M}_{ss}^f \, d(X_{t-1} / X_{t-1}^*) \\ &= d\tilde{M}_t^f + \tilde{M}_{ss}^f \, d\left(\frac{g_0}{g^*} \frac{g_1}{g^*} \cdots \frac{g_{t-1}}{g^*} \right) \\ &= d\tilde{M}_t^f + \frac{\tilde{M}_{ss}^f}{g^*} \left(\sum_{j=0}^{t-1} dg_j \right). \end{aligned}$$

By dividing $d(M_t^f / X_{t-1}^*)$ with $\tilde{M}_{ss}^f$, I obtain $IRF_{M^f}^{ratio}(t)$.

D.3 Stock Variables

Stock variables in the original equilibrium, such as K_t, A_t, B_t, D_t, and F_t, exhibit a stochastic trend and are detrended by X_t in the detrended equilibrium. For the purpose of this paper, I must also compute the impulse responses of the stock variables in terms of their *ratio* deviation from the balanced growth path.

The impulse responses of the stock variables can be computed in a similar way as those of the flow variables. Let M_t^s denote one of the stock variables in the original equilibrium, $\tilde{M}_t^s := M_t^s / X_t$ denote its detrended variable, and $\tilde{M}_{ss}^s$ denote the steady state value of $\tilde{M}_t^s$ in the detrended equilibrium. M_t^s on the balanced growth path, which I denote as M_t^{s*}, is determined by

$$M_t^{s*} = \tilde{M}_{ss}^s X_t^*, \quad t \geq 0.$$

(See Online Appendix D.2 for the definition of X_t^*.) The impulse response of M_t^s in terms of their ratio deviation from the balanced growth path can now be written as

$$IRF_{M^s}^{ratio}(t) = \frac{M_t^s - M_t^{s*}}{M_t^{s*}} = \frac{M_t^s / X_t^* - \tilde{M}_{ss}^s}{\tilde{M}_{ss}^s}.$$

After obtaining $d\tilde{M}_t^s = \tilde{M}_t^s - \tilde{M}_{ss}^s$ by solving the detrended equilibrium with Auclert et al. (2021)'s method, I compute $d(M_t^s/X_t^*) = M_t^s/X_t^* - \tilde{M}_{ss}^s$ using the following first-order-approximated equation.

$$d(M_t^s/X_t^*) = d\tilde{M}_t^s + \frac{\tilde{M}_{ss}^s}{g^*}\left(\sum_{j=0}^{t} dg_j\right).$$

By dividing $d(M_t^s/X_t^*)$ with $\tilde{M}_{ss}^s$, I obtain $IRF_{M^s}^{ratio}(t)$.

E Truncation Errors

Auclert et al. (2021)'s sequence space approach requires a truncation of sequences, and truncation errors can be nontrivial when the economy is extremely persistent. In this section, I inspect truncation errors and verify that at the posterior mode, the truncation errors are negligible in the model statistics used in this paper.

In this paper, I truncate sequences at $T = 700$ when solving models and drop the last seven periods further when evaluating moments. I start by comparing the impulse response sequences (at the posterior mode) obtained under truncation at $T = 700$ with those under truncation at $T = 1500$. Three observations emerge from this comparison: i) in each model (*i.e.*, each of RASOE (z, g, μ), HASOE (z, g, μ), and HASOE (z, g, μ, η) models), all impulse responses reach a balanced growth path before $t = 1499$; ii) there are some impulse responses that have not reached a balanced growth path in $t = 699$; iii) even in such cases, the impulse response sequences obtained under truncation at $T = 700$ are distorted only in the last few periods compared to those under truncation at $T = 1500$.

As an example, in Figure E.1, I plot the impulse responses of Y_t, C_t, I_t, and TB_t/Y_t to a trend shock in the RASOE model evaluated at its posterior mode, where the trend shock is very persistent ($\rho_g = 0.988$). All the impulse responses in this figure reach a new balanced growth path before $t = 1499$ (observation i)). The impulse responses of Y and C have already reached a balanced growth

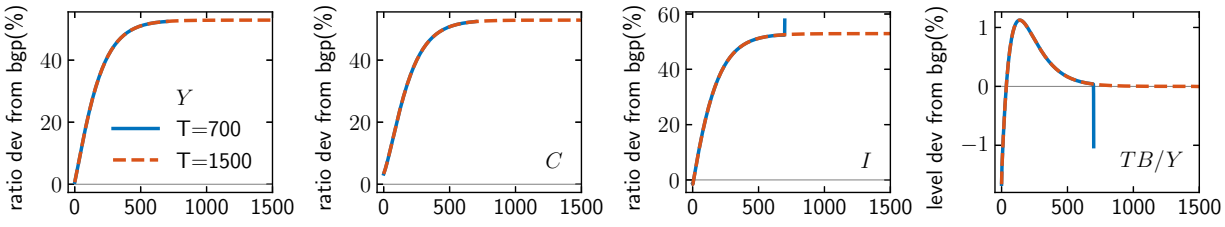

Figure E.1: Truncation Errors on the Impulse Responses to g Shock in the RASOE (z, g, μ) Model

Notes: This figure plots the impulse responses of Y, C, I, and TB/Y to a one-standard-deviation g shock in the RASOE (z, g, μ) model evaluated at the posterior mode. In particular, the model is solved under two different truncation lengths, $T = 700$ and $T = 1500$.

path before $t = 699$, while those of I and TB/Y have not (observation ii)). By truncating sequences at $T = 700$ in which I and TB/Y have not reached a balanced growth path yet, a truncation error occurs in their impulse responses. Importantly, however, the truncation error occurs only in the last few periods (observation iii)).

Based on these observations, when I evaluate model moments, I drop the last $0.01T$ periods from the length-T sequences and use only the first $0.99T$ periods. In the rest of the section, I evaluate the model statistics used in this paper at the posterior mode of each model under two different truncation lengths, $T = 700$ and 1500, and compare them. Specifically, I compare the following model statistics: i) Figures E.2, E.3, and E.4 compare the autocovarinaces of observable time series $[\Delta \log Y_t, \Delta \log C_t, \Delta \log I_t, \Delta TB_t/Y_t]$ (which are used when evaluating a likelihood in the Bayesian estimation); ii) Table E.1 compares business cycle moments; and iii) Table E.2 compares the variance decomposition result. From these comparisons, I find that truncation errors on these model statistics are negligible.

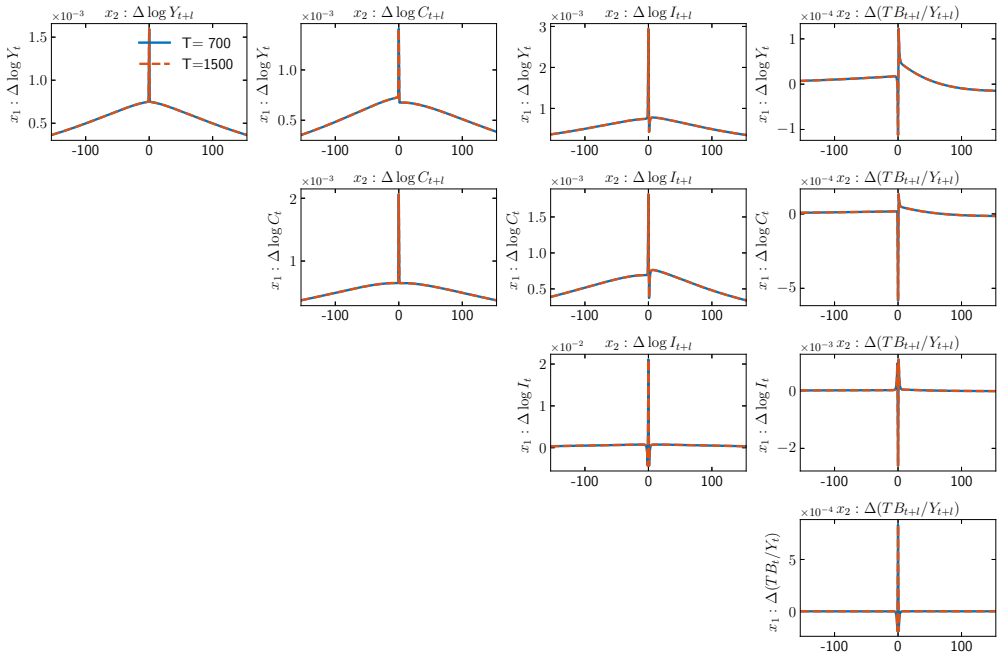

Figure E.2: Truncation Errors on the Autocovariances of Observables: RASOE (z, g, μ) Model

Notes: The RASOE (z, g, μ) model is evaluated at the posterior mode and solved at two different truncation lengths, $T = 700$ and 1500. The moments are evaluated using the first $0.99T$ periods of the length-T sequences.

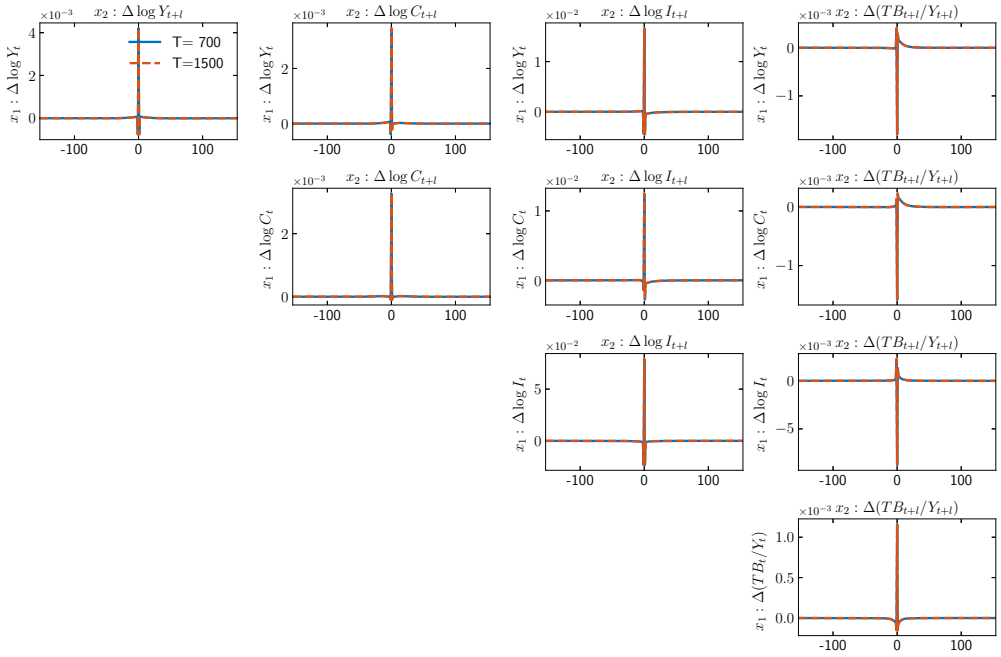

Figure E.3: Truncation Errors on the Autocovariances of Observables: HASOE (z, g, μ) Model

Notes: The HASOE (z, g, μ) model is evaluated at the posterior mode and solved at two different truncation lengths, $T = 700$ and 1500. The moments are evaluated using the first $0.99T$ periods of the length-T sequences.

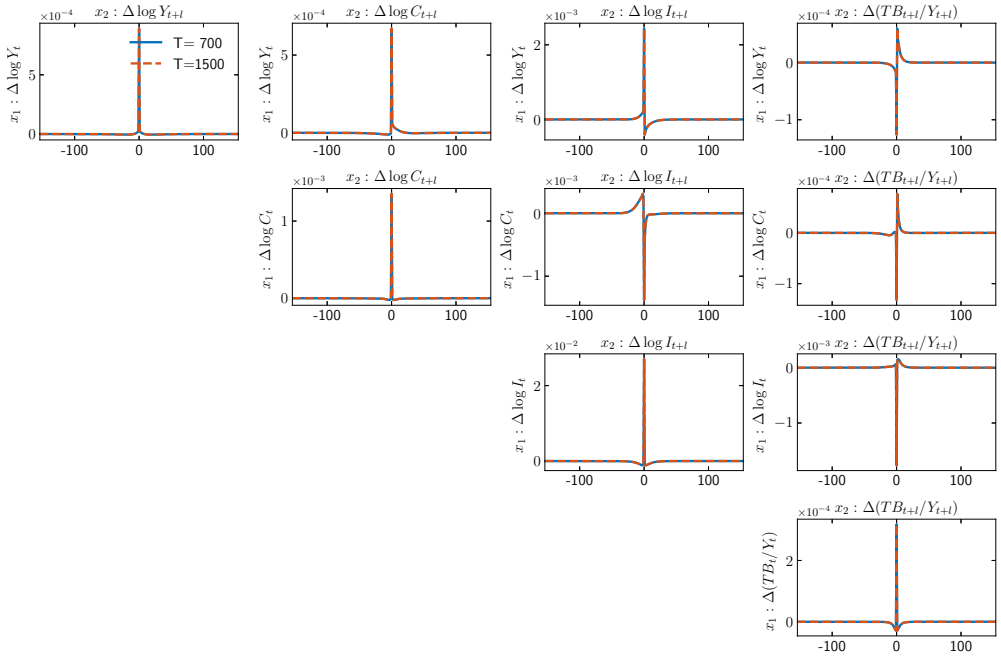

Figure E.4: Truncation Errors on the Autcovariances of Observables: HASOE (z, g, μ, η) Model

Notes: The HASOE (z, g, μ, η) model is evaluated at the posterior mode and solved at two different truncation lengths, $T = 700$ and 1500. The moments are evaluated using the first $0.99T$ periods of the length-T sequences.

Table E.1: Truncation errors on business cycle moments

			$\Delta\log Y_t$	$\Delta\log C_t$	$\Delta\log I_t$	$\Delta(TB_t/Y_t)$
Standard deviation						
	RASOE (z,g,μ) model	$T=700$	0.040	0.045	0.145	0.029
		$T=1500$	0.040	0.045	0.145	0.029
	HASOE (z,g,μ) model	$T=700$	0.065	0.057	0.281	0.034
		$T=1500$	0.065	0.057	0.281	0.034
	HASOE (z,g,μ,η) model	$T=700$	0.030	0.037	0.164	0.018
		$T=1500$	0.030	0.037	0.164	0.018
Contemporaneous correlation						
with $\Delta\log Y_t$	RASOE (z,g,μ) model	$T=700$		0.776	0.507	-0.097
		$T=1500$		0.776	0.507	-0.097
	HASOE (z,g,μ) model	$T=700$		0.932	0.911	-0.814
		$T=1500$		0.932	0.912	-0.815
	HASOE (z,g,μ,η) model	$T=700$		0.611	0.497	-0.237
		$T=1500$		0.611	0.497	-0.237
with $\Delta(TB_t/Y_t)$	RASOE (z,g,μ) model	$T=700$		-0.443	-0.620	
		$T=1500$		-0.443	-0.620	
	HASOE (z,g,μ) model	$T=700$		-0.811	-0.913	
		$T=1500$		-0.812	-0.913	
	HASOE (z,g,μ,η) model	$T=700$		-0.202	-0.603	
		$T=1500$		-0.202	-0.603	
with $\Delta\log C_t$	RASOE (z,g,μ) model	$T=700$			0.275	
		$T=1500$			0.275	
	HASOE (z,g,μ) model	$T=700$			0.776	
		$T=1500$			0.776	
	HASOE (z,g,μ,η) model	$T=700$			-0.228	
		$T=1500$			-0.228	
Autocorrelation						
with lag 1	RASOE (z,g,μ) model	$T=700$	0.472	0.314	-0.204	-0.228
		$T=1500$	0.472	0.314	-0.204	-0.228
	HASOE (z,g,μ) model	$T=700$	-0.180	-0.029	-0.292	-0.126
		$T=1500$	-0.180	-0.030	-0.295	-0.132
	HASOE (z,g,μ,η) model	$T=700$	0.026	-0.002	-0.027	-0.091
		$T=1500$	0.026	-0.002	-0.027	-0.091
with lag 2	RASOE (z,g,μ) model	$T=700$	0.469	0.314	-0.051	-0.082
		$T=1500$	0.469	0.315	-0.051	-0.082
	HASOE (z,g,μ) model	$T=700$	0.008	0.009	-0.029	-0.050
		$T=1500$	0.008	0.008	-0.030	-0.054
	HASOE (z,g,μ,η) model	$T=700$	0.020	-0.013	-0.040	-0.079
		$T=1500$	0.020	-0.013	-0.040	-0.079
with lag 3	RASOE (z,g,μ) model	$T=700$	0.468	0.315	0.004	-0.029
		$T=1500$	0.468	0.315	0.004	-0.029
	HASOE (z,g,μ) model	$T=700$	0.015	0.001	-0.014	-0.045
		$T=1500$	0.015	0.001	-0.016	-0.049
	HASOE (z,g,μ,η) model	$T=700$	0.014	-0.016	-0.042	-0.068
		$T=1500$	0.014	-0.016	-0.042	-0.068

Notes: Each model is evaluated at its posterior mode and solved at two different truncation lengths, $T=700$ and 1500. The moments are evaluated using the first $0.99T$ periods of the length-T sequences.

Table E.2: Truncation errors on variance decomposition

		$\Delta \log Y_t$	$\Delta \log C_t$	$\Delta \log I_t$	$\Delta(TB_t/Y_t)$
RASOE (z, g, μ) *model*					
stationary productivity shock (z)	$T = 700$	0.498	0.164	0.319	0.013
	$T = 1500$	0.498	0.164	0.319	0.013
trend shock (g)	$T = 700$	0.502	0.835	0.053	0.344
	$T = 1500$	0.502	0.835	0.053	0.344
interest rate shock (μ)	$T = 700$	0.001	0.000	0.628	0.642
	$T = 1500$	0.001	0.000	0.628	0.642
HASOE (z, g, μ) *model*					
stationary productivity shock (z)	$T = 700$	0.526	0.824	0.215	0.352
	$T = 1500$	0.526	0.824	0.213	0.348
trend shock (g)	$T = 700$	0.473	0.166	0.729	0.385
	$T = 1500$	0.473	0.166	0.730	0.387
interest rate shock (μ)	$T = 700$	0.000	0.010	0.057	0.264
	$T = 1500$	0.000	0.010	0.057	0.265
HASOE (z, g, μ, η) *model*					
stationary productivity shock (z)	$T = 700$	0.924	0.325	0.173	0.008
	$T = 1500$	0.924	0.325	0.173	0.008
trend shock (g)	$T = 700$	0.069	0.032	0.352	0.946
	$T = 1500$	0.069	0.032	0.352	0.946
interest rate shock (μ)	$T = 700$	0.000	0.000	0.009	0.036
	$T = 1500$	0.000	0.000	0.009	0.036
financial friction shock (η)	$T = 700$	0.007	0.643	0.466	0.009
	$T = 1500$	0.007	0.643	0.466	0.009

Notes: Each model is evaluated at its posterior mode and solved at two different truncation lengths, $T = 700$ and 1500. The moments are evaluated using the first $0.99T$ periods of the length-T sequences.

F MPC Estimation using Micro Data

F.1 Method

Following Hong (2022), I estimate MPC out of transitory income shocks using an extended version of Blundell et al. (2008). Let the individual earnings $Y_{i,t}$ be specified as follows.

$$\begin{aligned}\log Y_{i,t} &= Z_{i,t}'\varphi_t + P_{i,t} + \varepsilon_{i,t},\\ P_{i,t} &= \rho P_{i,t-1} + \zeta_{i,t},\\ \zeta_{i,t} \sim_{iid} (0,\sigma_{ps}^2), \quad \varepsilon_{i,t} &\sim_{iid} (0,\sigma_{tr}^2), \quad \text{and} \quad (\zeta_{i,t})_t \perp (\varepsilon_{i,t})_t,\end{aligned}$$

where $(x_t)_t$ represents time series $(\cdots, x_{t-1}, x_t, x_{t+1}, \cdots)$. $Z_{i,t}'\varphi_t$ represents the predictable component of log earnings $\log Y_{i,t}$, where $Z_{i,t}$ denotes a vector of dummy variables for observable characteristics of household i.[5] The unpredictable components of log earnings, $y_{i,t} (:= \log Y_{i,t} - Z_{i,t}'\varphi_t)$, is composed of a persistent component $P_{i,t}$, which follows an AR(1) process, and a transitory component, which is an *i.i.d.* shock. This earnings process specification is consistent with the model in subsection 2.2 such that $Z_{i,t}'\varphi_t$, $P_{i,t}$, and $\varepsilon_{i,t}$ correspond to $\log(w_t\Gamma_i\bar{l}_t)$, $e_{1,i,t}$, and $e_{2,i,t}$, respectively.

Let $c_{i,t}$ be the unpredictable component of consumption (*i.e.,* $c_{i,t} := \log C_{i,t} - Z_{i,t}'\varphi_t^c$, where $C_{i,t}$ is consumption and $Z_{i,t}'\varphi_t^c$ is the predictable component of $\log C_{i,t}$). Blundell et al. (2008)'s partial insurance parameter to transitory shocks for a group G, which I denote by ψ_G, is defined as follows.

$$\psi_G = \frac{cov[\Delta c_{i,t}, \varepsilon_{i,t} | (i,t) \in G]}{cov[\Delta y_{i,t}, \varepsilon_{i,t} | (i,t) \in G]}.$$

In other words, ψ_G is the elasticity of consumption with respect to earnings when the earnings change is caused by an idiosyncratic transitory shock.

As in Online Appendix G.6 of Hong (2022), I estimate ψ_G adopting Kaplan and Violante (2010)'s identification strategy for Blundell et al. (2008)'s partial insurance parameters under the 'AR(1)+*i.i.d.*' specification of the earnings process. Specifically, let $\tilde{\Delta}^K y_{i,t}$ and $\Delta^K c_{i,t}$ be

$$\begin{aligned}\tilde{\Delta}^K y_{i,t} &:= y_{i,t} - \rho^K y_{i,t-K}, \quad K \geq 1, \quad \text{and}\\ \Delta^K c_{i,t} &:= c_{i,t} - c_{i,t-K}, \quad K \geq 1.\end{aligned}$$

[5] The observable characteristics of households include education, ethnicity, employment status, region, cohort, household size, number of children, urban area, the existence of members other than heads and spouses earning income, and the existence of persons who do not live with but are financially supported by the household. Among these characteristics, education, ethnicity, employment status, and region are allowed to have time-varying effects.

Then, we have

$$\tilde{\Delta}^K y_{i,t} = \sum_{s=0}^{K-1} \rho^s \zeta_{i,t-s} + \varepsilon_{i,t} - \rho^K \varepsilon_{i,t-K}.$$

When the grouping of observations is independent of $(\zeta_{i,t+j}, \varepsilon_{i,t+j})_{j\geq 0}$ and $\Delta c_{i,t}$ is independent of $(\zeta_{i,t+j}, \varepsilon_{i,t+j})_{j\geq 1}$, we can derive

$$\psi_G = \frac{cov[\Delta^K c_{i,t}, \tilde{\Delta}^K y_{i,t+K} | (i,t) \in G]}{cov[\tilde{\Delta}^K y_{i,t}, \tilde{\Delta}^K y_{i,t+K} | (i,t) \in G]}. \tag{F.1}$$

To identify ψ_G using equation (F.1), we need the value of ρ. Adopting Floden and Lindé (2001)'s identification strategy, parameter ρ is estimated using the following moment conditions for the autocovariances of $y_{i,t}$.[6]

$$E[y_{i,t}^2] = \frac{\sigma_{ps}^2}{1-\rho^2} + \sigma_{tr}^2,$$
$$E[y_{i,t}, y_{i,t+nK}] = \frac{\sigma_{ps}^2}{1-\rho^2}\rho^{nK}, \quad n \geq 1.$$

Once ρ is estimated, I estimate ψ_G using equation (F.1). Since ψ_G is an elasticity, I transform it to MPC by multiplying a group-level consumption-income ratio as follows.

$$MPC_G = \psi_G \frac{E[C_{i,t} | (i,t) \in G]}{E[Y_{i,t} | (i,t) \in G]}. \tag{F.2}$$

ENAHO provides the year-over-year growth of quarterly income and consumption, and thus, I set one period as a quarter and $K = 4$ for the Peruvian sample. As a result, I obtain quarterly MPCs of Peruvian households. On the other hand, the PSID provides the two-year-over-two-year growth of annual income and consumption, and thus, I set one period as a year and $K = 2$ for the U.S. sample. As a result, I obtain annual MPCs of U.S. households.

F.2 Revisions on Hong (2022)

Compared to Hong (2022), I make three revisions to the MPC estimation procedure, which are necessary to maintain consistency between micro moments and macro data or model. First, I change the consumption measure from non-durable consumption to total consumption (including both non-durable and durable consumption). Once the model is calibrated by targeting the MPC moments, I estimate the model using macro data. In this step, I use total consumption series (as studies on emerging market business cycles typically do) because non-durable consumption is not

[6] In this estimation, I obtain the estimates of ρ, σ_{ps}, and σ_{tr}. These estimates for Peruvian households are also used in subsection 3.1 to calibrate the earnings process in the HASOE model.

available in the Peruvian national accounts. To make the consumption concept consistent between micro and macro data, I use the total consumption measure when analyzing the micro data, too.

Second, the sample periods are changed for both ENAHO and the PSID because some of the key durable expenses are available only after certain years in both surveys. Specifically, I use the 2011-2018 waves of ENAHO and the 2005-2017 waves of the PSID.[7]

Third, the earnings process specification is revised to be consistent with the HASOE model. Blundell et al. (2008)'s method requires a structural specification of the earnings process. In its baseline specification, Hong (2022) assumes that the unpredictable component of earnings is composed of a permanent component and a transitory component, where the permanent component follows a random walk as in the original specification of Blundell et al. (2008). In this paper, I replace the random walk component with a component following an AR(1) process so that the earnings process specification imposed in the MPC estimation is consistent with the model.[8]

F.3 Variable Construction

The consumption measure in MPC estimation is total consumption, which includes both non-durable and durable consumption. I construct such consumption by aggregating the following expenses in each of ENAHO and the PSID: non-durable expenses including 1) food, 2) clothing (including clothing services, footwear, watches and jewelry), 3) housing rent, rental equivalence of owned or donated housing, 4) utilities (heat, electricity, water, etc.), 5) telephone and cable, 6) vehicle repairs and maintenance, 7) gasoline and oil, 8) parking, 9) public transportation, 10) household repairs and maintenance, 11) recreation, 12) insurance (home insurance, car insurance, health insurance, etc.), 13) childcare, 14) domestic services and other home services, 15) personal care, 16) alcohol, 17) tobacco, and 18) daily non-durables (laundry items, bathroom items, matches, candle, stationeries, etc.), and durable expenses including 19) vehicles, 20) furnishings and equipment (textiles, furniture, floor coverings, appliances, housewares, etc.), 21) health, and

[7] My ENAHO sample starts from 2011 for the following reason. ENAHO is conducted continuously (*i.e.*, households are interviewed in different months) and the reference periods of income and expense items are usually in the format of a 'specified period before the interview' (such as 'previous n months') rather than a fixed calender period (such as 'during 2014'). Accordingly, I set the reference periods of my consumption and income measures using the same format (*i.e.*, a specified period before the interview such as 'previous n months'). One exception is Questionnaire 612. This questionnaire collects information on household furnishings, equipment, and vehicles, which take a sizable portion of durable goods. Until 2010, this questionnaire asks which calendar year each item is acquired, and thus it is impossible to aggregate this questionnaire's expense items with other expense items under a consistent reference period format. From 2011 onward, Questionnaire 612 asks the acquisition month instead of the acquisition year, which makes it possible to recover this questionnaire's expense items during a specified period before the interview (such as 'previous n months') and to aggregate these expense items with other expense items under a consistent reference period format. My PSID sample starts from 2005 because the survey began to collect expenses on household furnishings and equipment since then. Moreover, some non-durable items including clothing and recreation are also collected from 2005 onward.

[8] Hong (2022) also considers the 'AR(1) + *i.i.d.*' specification during a robustness check in his Appendix G.6.

22) education.[9] Among the listed expenses, ENAHO does not have expenses on 13) childcare, and the PSID does not have expenses on 14) domestic services and other home services, 15) personal care, 16) alcohol, 17) tobacco, and 18) daily non-durables (laundry items, bathroom items, matches, candle, stationeries, etc.). Nonpurchased consumption, such as donations, food stamps, in-kind income, and self-production, is excluded.

The income measure in MPC estimation is the sum of disposable labor income and transfers, as in Blundell et al. (2008). Capital income is excluded in order not to falsely attribute endogenous capital income changes as income shocks. In ENAHO, capital income and labor income are not distinguishable in self-employment income. As in Diaz-Gimenez et al. (1997), Krueger and Perri (2006), and Hong (2022), I split the self-employment income into labor income and capital income parts using the ratio between unambiguous capital and labor incomes in the sample.[10] In ENAHO, imputed components of missing income are distinguishable, and I exclude them from Peruvian incomes, as in Hong (2022). For the PSID sample, I closely follow Kaplan et al. (2014) in constructing U.S. incomes. Specifically, U.S. households' disposable labor income and transfers are constructed by i) estimating federal income taxes for total income (including labor income, transfers, and capital income) by TAXSIM program, ii) splitting proportionately the estimated federal taxes into the labor income and transfers part and the capital income part, and iii) subtracting the federal taxes on labor income and transfers from gross labor income and transfers.

In ENAHO, reference periods vary across income and expense items. Importantly, Peruvian households report 97.5% of income items and 92.9% of expense items (in value) under reference periods shorter than or equal to the previous three months, on average. Given this feature of the data, I set the reference period of Peruvian income and consumption as the previous three months. Expense and income items reported under a different reference period than the previous three months are scaled to three-month expenses and incomes, respectively. (For example, a monthly tobacco expense is scaled up by a factor of three.)[11] Moreover, to remove any comovement between income and consumption that occurs prior to the previous three months, I exclude income items with reference periods longer than the previous three months from Peruvian incomes.

In the PSID, the reference periods of income items are firmly fixed to a calendar year, while the reference periods of expense items can depend on interpretation, as Crawley (2020) notes. For example, food expenses in the PSID can be interpreted either as the last week's expense or

[9] In listing the expenses, I categorize expenses on 21) health and 22) education as durable expenses because of their durable nature. In national accounts, however, they are categorized as non-durable consumption. Since I use total consumption, how they are categorized between durable and non-durable consumption does not have any effect.

[10] As noted in footnote 24, the ratio of (unambiguous labor income) / (unambiguous labor income + unambiguous capital income) is 0.817 in ENAHO, and this ratio is close to the ratio that Diaz-Gimenez et al. (1997) and Krueger and Perri (2006) use for their U.S. sample, 0.864.

[11] Online Appendix B.2 of Hong (2022) describes how one can achieve such scaling effectively using certain variables in the ENAHO data.

the average weekly expense during the calendar year. I adopt the latter interpretation, as related studies often do, and treat the reference periods of expense items as being synchronized with those of income items. Accordingly, I set the reference period of U.S. income and consumption as the corresponding calender year.

ENAHO is conducted annually, and I use the 2011-2018 waves. This ENAHO sample provides seven years of the year-over-year growth of quarterly income and consumption. For the PSID, I use the 2005-2017 waves, and the survey is conducted biannually during the sample period. This PSID sample provides six years of the two-year-over-two-year growth of annual income and consumption.

In both the ENAHO and the PSID samples, nominal income and consumption are deflated with the Consumer Price Index (CPI) series.[12]

F.4 Sample Selection

The sample selection for ENAHO closely follows Hong (2022) and proceeds as follows. First, I drop observations when households appear only once in the survey. Second, I drop observations when households are interviewed in different months between two consecutive surveys or when household heads are changed. I also drop observations when it is likely that two different households are linked as panel observations by failing to distinguish an old household moving out and a new household moving into the same address.[13] Third, I drop observations classified as 'incomplete' by pollsters. Fourth, I drop observations when household heads are younger than 25 and older than 65. Fifth, I drop observations when observable characteristics used to control for the predictable components of income and consumption are missing. Sixth, I drop observations reporting nonpositive income or consumption. Seventh, I drop observations with too much imputed value or too much value reported under a longer reference period than the previous three months in their income.[14] Eighth, I drop income outliers.[15] As a result, I obtain a sample composed of 36,292 observations, 18,479 pairs of two consecutive observations, and 7,241 triplets of three consecutive observations. The panel A of Table F.1 reports the number of remaining observations in each step.

[12] Unlike the reference periods in the PSID sample, the reference periods in the ENAHO sample are not fixed to a calendar period. For example, the three-month reference period of households surveyed in January, 2015 starts one-month earlier than that of households surveyed in February, 2015. Fortunately, this feature of the data does not complicate the deflation procedure, as ENAHO provides variables recording within-year-deflated values of income and expense items. Online Appendix B.2 of Hong (2022) provides a detailed deflation procedure using these variables.

[13] Hong (2022) defines such panel observations as 'potentially fake panel observations.' The potentially fake panel observations can be effectively detected and dropped by using household-member-level information. See Online Appendix B.4 of Hong (2022) for a detailed discussion.

[14] 'Too much value' is defined as follows. For each $(x, y) \in \{$(imputed value, baseline income) (value reported under a reference period longer than the previous three months, baseline income)$\}$, I drop observations when $\frac{x}{x+y} > 0.05$.

[15] Income outliers are defined as households exhibiting an extreme income growth, which falls in the range of extreme 1 % (0.5% at the top and 0.5% at the bottom) in a calendar-year subsample at least once.

Table F.1: Sample Selection

	N_1	N_2	N_3
A. ENAHO			
households appearing only once	87,305	59,691	32,077
months not matched, fake panel obs., or head changed	73,248	47,950	22,652
incomplete survey	63,410	38,343	17,386
age restriction, 25-65	48,636	28,983	12,971
observable characteristics missing	48,403	28,904	12,955
nonpositive Y and C	48,052	28,522	12,732
too much imputation or 3ml in Y	36,805	18,808	7,398
income outliers	36,292	18,479	7,241
B. The PSID			
households appearing only once or head changed	57,560	45,553	33,546
SEO sample 1968 and Latino sample 1990/1992	39,660	31,523	23,386
topcoded obs.	39,650	31,507	23,369
age restriction, 25-65	31,447	24,380	17,711
observable characteristics missing	30,225	23,277	16,805
non-positive Y and C	30,028	23,021	16,570
income outliers	29,145	22,345	16,092

Notes: In the penultimate line of panel A, '3ml' is an abbreviation for 'items with reference periods longer than the previous three months.' The columns labeled N_1, N_2, and N_3 report the number of remaining observations, pairs of two consecutive observations, and triplets of three consecutive observations, respectively, in each step.

The sample selection for the PSID proceeds similarly to the sample selection for ENAHO as follows. First, I drop observations when households appear only once in the survey. I also drop observations when household heads are changed. Second, I drop observations if they belong to the sample from Survey of Economic Opportunities (SEO) (added to the PSID in 1968) or to the Latino sample (added to the PSID in 1990 and 1992). Third, I drop observations when their income or consumption include topcoded values. Fourth, I drop observations when household heads are younger than 25 and older than 65. Fifth, I drop observations when observable characteristics used to control for the predictable components of income and consumption are missing. Sixth, I drop observations reporting nonpositive income or consumption. Seventh, I drop income outliers, which are defined in the same way as in the Peruvian sample selection. As a result, I obtain a sample composed of 29,145 observations, 22,345 pairs of two consecutive observations, and 16,092 triplets of three consecutive observations. The panel B of Table F.1 reports the number of remaining observations in each step.

F.5 Earnings Grouping

When disciplining the HASOE model, I use MPC estimated within each decile of residual earnings, which is $e_{i,t}$ in the model and $y_{i,t}$ in the MPC estimation procedure described in Online Appendix F.1. In particular, I do not group observations by total earnings, which is $w_t\Gamma_i e_{i,t}\bar{l}_t$ in the model and $Y_{i,t}$ in the MPC estimation procedure in Online Appendix F.1, because $e_{i,t}$ bears risk and thus induces precautionary saving and MPC heterogeneity, while Γ_i does not.

When estimating the MPC moments, I construct residual earnings deciles in the same way as in Hong (2022). See section 3.4 of the paper for details.

G The Market Value of Wealth

In subsection 3.1, I calibrate parameter p such that the entrepreneurs' wealth share matches top $100(1-p)\%$ share of wealth in data. For this purpose, I use wealth inequality data from World Inequality Database (WID). As Alvaredo et al. (2021) note, WID's wealth concept is a market-value of wealth, which includes financial assets yielding nonproductive pure rents, such as entrepreneurs' claims to rents R^E_t in the model. Thus, I evaluate the market value of the claims assuming that entrepreneurs can trade the claims among themselves and include this value as part of entrepreneurs' wealth. Specifically, the market value of the claims is evaluated as follows.

$$\begin{aligned} U^E_t &:= \sum_{s=1}^{\infty} (\beta^E)^s \frac{\lambda^E_{t+s}}{\lambda^E_t} R^E_{t+s} \\ &= \sum_{s=1}^{\infty} \frac{Q_{0,t+s}}{Q_{0,t}} \frac{\chi^{agg}_{t+s} + \xi(1+r^b_{t+s})B_{t+s-1}}{1-p}. \end{aligned}$$

Let $\tilde{U}^E_t := U^E_t / X_t$. Then, we have

$$\tilde{U}^E_t = \sum_{s=1}^{\infty} \frac{Q_{0,t+s}}{Q_{0,t}} \frac{\tilde{\chi}^{agg}_{t+s} + \xi(1+r^b_{t+s})\tilde{B}_{t+s-1}}{1-p} \frac{X_{t+s-1}}{X_t}.$$

In the steady state of the detrended equilibrium, $\tilde{U}^E_t$ becomes

$$\begin{aligned} \tilde{U}^E_{ss} &= \sum_{s=1}^{\infty} \frac{1}{(1+r_{ss})^s} \frac{\tilde{\chi}^{agg}_{ss} + \xi(1+r_{ss})\tilde{B}_{ss}}{1-p} (g_{ss})^{s-1} \\ &\Leftrightarrow \tilde{U}^E_{ss} = \frac{\tilde{\chi}^{agg}_{ss} + \xi(1+r_{ss})\tilde{B}_{ss}}{1+r_{ss}-g_{ss}} \frac{1}{1-p}. \end{aligned} \tag{G.1}$$

In the detrended steady state, the market value of entrepreneurs' wealth, $\tilde{\mathscr{W}}^E_{ss}$, and that of workers'

wealth, $\tilde{\mathscr{W}}_{ss}^{W}$, are determined as follows.

$$\tilde{\mathscr{W}}_{ss}^{E} = \tilde{U}_{ss}^{E} + \tilde{A}_{ss}^{E}, \quad \text{and} \tag{G.2}$$

$$\tilde{\mathscr{W}}_{ss}^{W} = \tilde{B}_{ss}^{W} + \tilde{A}_{ss}^{W}. \tag{G.3}$$

The market value of the total wealth in this economy, $\tilde{\mathscr{W}}_{ss}$, is characterized as follows.

$$\begin{aligned}\tilde{\mathscr{W}}_{ss} = & \underbrace{p\tilde{\mathscr{W}}_{ss}^{W}}_{\text{workers' portion}} + \underbrace{(1-p)\tilde{\mathscr{W}}_{ss}^{E}}_{\text{entreprenerus' portion}} \\ = & \tilde{A}_{ss} + \tilde{B}_{ss} + (1-p)\tilde{U}_{ss}^{E} \\ = & \tilde{K}_{ss} - \tilde{D}_{ss} + (1-p)\tilde{U}_{ss}^{E} \quad \text{(by equation (B.64))}.\end{aligned}$$

$$\tilde{\mathscr{W}}_{ss} = \tilde{K}_{ss} - \tilde{D}_{ss} + \frac{\tilde{\chi}_{ss}^{agg} + \xi(1+r_{ss})\tilde{B}_{ss}}{1+r_{ss}-g_{ss}}. \tag{G.4}$$

Parameter p is calibrated such that the fraction $(1-p)\tilde{\mathscr{W}}_{ss}^{E}/\tilde{\mathscr{W}}_{ss}$ in the model under a given value of p is equal to the top $100(1-p)\%$ share of wealth in the data (WID).

H Consumption Response Decomposition in the RASOE Model

In Figure 2a, I decompose the response of GHH_t to a trend shock (g) in the RASOE model into the response driven by w_t and $h_t(\cdot)$ and the response driven by r_t^a. This consumption response decomposition, however, cannot be obtained directly from the sequence space approach. This is because I must write the DAG representation of the RASOE model (presented in Figure C.2) such that households' partial equilibrium problem does not form a separate block for the following reason: if the DAG representation of the RASOE model were written such that representative households' partial equilibrium problem form a separate block, the Jacobian of the block contains $(\partial GHH_s/r_t^a)_{s,t\geq 0}$, which, for any t, never dies out when $s \to \infty$.[16]

Thus, I obtain the consumption response decomposition in the RASOE model using the conventional state space approach developed by Blanchard and Kahn (1980) as follows. Let

$$dy_t = d\tilde{C}_t, \quad dx_t = [d\tilde{A}_{t-1}, dg_t, d\tilde{w}_t, dr_t^a]', \quad \text{and} \quad d\varepsilon_t = [dg_t, d\tilde{w}_t, dr_t^a]'.$$

The households' partial equilibrium is characterized by detrended equilibrium conditions (A.12),

[16] Workers' partial equilibrium problem in the HASOE model does not have this issue, and thus, the DAG representation of the HASOE model (presented in Figure C.1) is written such that workers' problem forms a separate block. As a result, workers' consumption response decomposition across driving factors are obtained directly from the sequence space approach in the HASOE model.

(A.13), (A.14), and (A.15). After substituting out L_t and $\tilde{\lambda}_t$ from the equilibrium conditions, the households' partial equilibrium can be described by the following VAR representation.

$$A \cdot \begin{bmatrix} dy_{t+1} \\ dx_{t+1} \end{bmatrix} = B \cdot \begin{bmatrix} dy_t \\ dx_t \end{bmatrix} + C \cdot d\varepsilon_{t+1},$$

where A and B are 5-by-5 matrices and C is a 5-by-3 matrix. Note that dy_t is a control variable, dx_t is a vector of state variables, and $d\varepsilon_t$ is a vector of exogenous variables in this system. A is invertible under any posterior parameter draws, and thus, this equation can be rewritten as follows.

$$\begin{bmatrix} dy_{t+1} \\ dx_{t+1} \end{bmatrix} = M \cdot \begin{bmatrix} dy_t \\ dx_t \end{bmatrix} + A^{-1}C \cdot d\varepsilon_{t+1},$$

where $M := A^{-1}B$. Let $M = W^{-1}JW$ be the Jordan decomposition of M under which the diagonal vector of J, $(\lambda_1, \cdots, \lambda_5)$, satisfies $|\lambda_1| \geq \cdots \geq |\lambda_5|$. I find that there is only one explosive eigenvalue (*i.e.*, $|\lambda_1| > 1 \geq |\lambda_2| \geq \cdots \geq |\lambda_5|$) under any posterior parameter draws, and thus, Blanchard and Kahn (1980)'s stationarity condition is always satisfied. For notational convenience, I introduce submatrices of J, W, and $WA^{-1}C$ as follows.

$$J = \begin{bmatrix} \underbrace{J_1}_{1\times1} & \underbrace{0}_{1\times4} \\ \underbrace{0}_{4\times1} & \underbrace{J_2}_{4\times4} \end{bmatrix}, \quad W = \begin{bmatrix} \underbrace{W_{11}}_{1\times1} & \underbrace{W_{12}}_{1\times4} \\ \underbrace{W_{21}}_{4\times1} & \underbrace{W_{22}}_{4\times4} \end{bmatrix}, \quad \text{and} \quad WA^{-1}C = \begin{bmatrix} \underbrace{T_1}_{1\times3} \\ \underbrace{T_2}_{4\times1} \end{bmatrix}.$$

Let

$$\begin{bmatrix} dz_{1,t} \\ dz_{2,t} \end{bmatrix} := W \begin{bmatrix} dy_t \\ dx_t \end{bmatrix} = \begin{bmatrix} W_{11} \cdot dy_t + W_{12} \cdot dx_t \\ W_{21} \cdot dy_t + W_{22} \cdot dx_t \end{bmatrix}. \tag{H.1}$$

Then, we have

$$\begin{bmatrix} dz_{1,t+1} \\ dz_{2,t+1} \end{bmatrix} = J \cdot \begin{bmatrix} dz_{1,t} \\ dz_{2,t} \end{bmatrix} + WA^{-1}C \cdot d\varepsilon_{t+1}$$

$$\Leftrightarrow \begin{cases} dz_{1,t+1} = J_1 dz_{1,t} + T_1 d\varepsilon_{t+1}, \\ dz_{2,t+1} = J_2 dz_{1,t} + T_2 d\varepsilon_{t+1}. \end{cases} \tag{H.2}$$

Now, we can solve $dz_{1,t}$ and $dz_{2,t}$ as follows. From the first equation in (H.2), we can obtain

$$dz_{1,t} = -\sum_{j=1}^{\infty} J_1^{-j} T_1 d\varepsilon_{t+j}, \quad t \geq 0. \tag{H.3}$$

From equation (H.1), we can obtain

$$dz_{2,0} = [W_{22} - W_{21}W_{11}^{-1}W_{12}]dx_0 + W_{21}W_{11}^{-1}dz_{1,0}, \tag{H.4}$$

where $dx_0 = [0, dg_0, d\tilde{w}_0, d\tilde{r}_0^a]'$. From the second equation in (H.2), we have

$$dz_{2,t} = J_2 dz_{1,t-1} + T_2 d\varepsilon_t, \quad t \geq 1. \tag{H.5}$$

With the solved $dz_{1,t}$ and $dz_{2,t}$, we can solve dx_t and dy_t using equation (H.1) as follows.

$$\begin{aligned} dx_t &= [W_{22} - W_{21}W_{11}^{-1}W_{12}]^{-1}\{dz_{2,t} - W_{21}W_{11}^{-1}dz_{1,t}\}, \quad \text{and} \\ dy_t &= W_{11}^{-1}(dz_{1,t} - W_{12}dx_t). \end{aligned} \tag{H.6}$$

Once we substitute $d\varepsilon_t$ with the impulse responses of $[dg_t, d\tilde{w}_t, dr_t^a]'$ to a trend shock in equations (H.3), (H.4), (H.5), and (H.6), we obtain the impulse responses of $dy_t (= d\tilde{C}_t)$ and $dx_t (= [d\tilde{A}_{t-1}, dg_t, d\tilde{w}_t, dr_t^a]')$. The consumption response can be decomposed into the response driven by w_t and $h_t(\cdot)$ and the response driven by r_t^a by substituting $d\varepsilon_t$ with $[dg_t, d\tilde{w}_t, 0]'$ and $[0, 0, dr_t^a]'$, respectively, instead of $[dg_t, d\tilde{w}_t, dr_t^a]'$. Lastly, the response of GHH_t to a trend shock (and its decomposition) can be recovered by using the following equilibrium relationship.

$$d\tilde{GHH}_t (:= d(GHH_t / X_{t-1})) = d\tilde{C}_t - \frac{L_{ss}}{\omega} d\tilde{w}_t. \tag{H.7}$$

I Decomposition of the Consumption Variance Change from the Benchmark to the Counterfactual Economies

In section 5, I show that in the counterfactual economy, excess consumption volatility disappears in most of the posterior distribution, including the posterior mean, median, and mode. Moreover, such a change is driven by the volatility change of consumption (rather than that of income). In this section, I decompose the change of consumption variance (from the benchmark to the counterfactual economies) into the changes originating from each shock.

Let $V(\Delta \log C_t)^{\mathfrak{B}}$ be the consumption variance in the benchmark economy, and $V(\Delta \log C_t)_s^{\mathfrak{B}}$, $s \in \{z, g, \mu, \eta\}$ be its decomposed variances across shocks. Similarly, let $V(\Delta \log C_t)^{\mathfrak{C}}$ be the consumption variance in the counterfactual economy, and $V(\Delta \log C_t)_s^{\mathfrak{C}}$, $s \in \{z, g, \mu, \eta\}$ be its decomposed variances across shocks. The variance change (in ratio) is decomposed as follows.

$$\frac{V(\Delta \log C_t)^{\mathfrak{C}} - V(\Delta \log C_t)^{\mathfrak{B}}}{V(\Delta \log C_t)^{\mathfrak{B}}} = \sum_{s \in \{z,g,\mu,\eta\}} \frac{V(\Delta \log C_t)_s^{\mathfrak{C}} - V(\Delta \log C_t)_s^{\mathfrak{B}}}{V(\Delta \log C_t)^{\mathfrak{B}}}. \tag{I.1}$$

Table I.1: Decomposition of the consumption variance change

total	z	g	μ	η
-0.322	-0.180	0.137	-0.000	-0.279
(0.247)	(0.023)	(0.073)	(0.000)	(0.252)

Notes: The consumption variance change decomposition (I.1) is conducted under each posterior draw, and the mean and standard deviation (in parentheses) of each decomposed component over the posterior distribution are reported.

I conduct the variance change decomposition (I.1) under each posterior draw. Table I.1 reports the mean and standard deviation of each decomposed component over the posterior distribution. In terms of the posterior mean, consumption variance decreases by 32.2% in the counterfactual economy. Out of this -32.2% change, -27.9%p and -18.0%p come from η and z shocks generating fluctuations less, respectively, while +13.7%p comes from a g shock generating fluctuations more. As discussed in section 5, η and z shocks generate less consumption fluctuations in the counterfactual economy because households exhibit lower MPC and a correspondingly weaker precautionary saving behavior. On the other hand, a g shock generates more consumption fluctuations in the counterfactual economy because the permanent income effect the shock revives as the counteracting precautionary saving effect becomes weak.

Another noteworthy observation is that the large posterior standard deviation of the total consumption variance change inherits from that of the consumption variance change generated by an η shock. As discussed in the last paragraph of 5, a relatively small but persistent η shock and a large but transitory η shock can both generate a strong and sharp consumption response in the benchmark economy and thus are not well distinguished by a posterior likelihood in the Bayesian estimation. However, these shocks generate very different consumption responses in the counterfactual economy: the consumption response becomes much weaker in the counterfactual economy than in the benchmark economy when the shock is relatively small but persistent, while it becomes not much weaker (and sometimes becomes even stronger) when the shock is large but transitory.

J A Debate: What Drives Large Consumption Swings?

My paper is most closely related to Guntin et al. (2022). These two papers share the view that micro data, when interpreted through a heterogeneous-agent model, provide important information about what drives large consumption fluctuations. However, they come to different conclusions: Guntin et al. (2022) find that the permanent income effect of a trend shock drives large consumption swings, while I find that a financial friction shock and a stationary productivity shock mainly drive consumption fluctuations. In this sense, a long-standing debate on what drives consumption

fluctuations in emerging economies, particularly between a trend shift and financial frictions[17], continues in the heterogeneous-agent open economy landscape. In this section, I discuss key differences between the two papers and how they come to different conclusions.

Micro Moments. The two papers use different information from micro data. Guntin et al. (2022) use a group-level consumption-income elasticity between the peak and trough around a crisis episode, $\hat{\varepsilon}^G_{GOP} := \frac{\log \bar{c}^G_{t+h} - \log \bar{c}^G_t}{\log \bar{y}^G_{t+h} - \log \bar{y}^G_t}$, where $\bar{c}^G_t$ and $\bar{y}^G_t$ are the group-average (residualized) consumption and income, and t and $t+h$ are the peak and trough around a crisis, respectively. On the other hand, I use an MPC out of idiosyncratic transitory income shocks obtained by using Blundell et al. (2008)'s method.

The two micro moments exhibit two important differences. First, the source of income variation is different. Guntin et al. (2022)'s elasticity washes out all the idiosyncratic income risk by group-averaging consumption and income and exploits only aggregate income risk borne by each group. In contrast, my MPC moment exploits idiosyncratic income risk only.[18] Given that individual households face much greater idiosyncratic risk than aggregate risk[19], the MPC moment may capture household consumption smoothing disruption better than the group-level elasticity.

Second, Guntin et al. (2022)'s elasticity is determined by two periods, the peak and trough around a crisis, and thus can be sensitive to timing identification. They identify the peak and trough around the 2008 Peruvian recession as 2007 and 2010, respectively, based on the aggregated individual consumption from ENAHO (rather than based on national accounts). This identification can be affected by time-varying measurement errors in the survey. Indeed, the first two panels of Figure J.1 plot the output and consumption in national accounts and suggest that the Peruvian economy was not in the trough during 2010.[20] On the other hand, my MPC moments are relatively free from the timing issue, as they are based on all periods in which data are available.

Models. Both papers interpret micro moments using a heterogeneous-agent small-open-economy model, but their models also exhibit two important differences. First, the aggregate precautionary savings correspond to liquid wealth in Guntin et al. (2022)'s model, while it corresponds to total wealth in my model.[21] As a result, households in my model exhibit much stronger precautionary saving behavior than those in Guntin et al. (2022)'s model. For this reason, a trend shock cannot

[17] For a trend shift, see Aguiar and Gopinath (2007). For financial frictions, see Neumeyer and Perri (2005), Garcia-Cicco et al. (2010), Chang and Fernández (2013), Mendoza (2010), and Bianchi (2011).

[18] The effect of aggregate income risk is removed when extracting a predictable component of income and consumption, which includes a time-fixed effect.

[19] To have a quantitative sense of their relative magnitude, one can compare the log growth dispersion between aggregate and idiosyncratic incomes. $\sigma(\Delta \log e_{i,t})$ is 0.689 in ENAHO, where $\log e_{i,t}$ is the unpredictable component of log earnings. This number is 25.2 times as large as $\sigma(\Delta \log Y_t) = 0.027$, where Y_t is aggregate income.

[20] An expert diagnosis shares this view: Economic Commission for Latin America and the Caribbean (2010) notes on page 79 that "[t]he Peruvian economy was strong in 2010, driven by growing domestic demand."

[21] To be precise, the aggregate precautionary savings correspond to the workers' share (52.2%) of the total wealth.

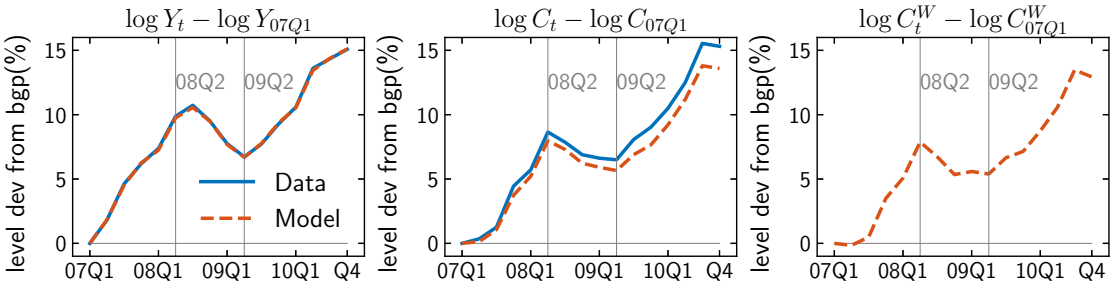

Figure J.1: What Happens in 2007–2010

Notes: The first two panels plot i) output and consumption from national accounts in logs after seasonal adjustment and log-linear detrending (labeled 'Data') and ii) their model counterparts simulated using smoothed shocks at the posterior mode (labeled 'Model'). The third panel plots the smoothed average workers' consumption.

generate large consumption fluctuations in my model, while it can in Guntin et al. (2022)'s model; a consumption response to a trend shock is muted in my model because an enhanced precautionary saving effect offsets the permanent income effect; in Guntin et al. (2022)'s model, the enhanced precautionary saving effect is far weaker, and thus, the permanent income effect can dominate.

Second, when examining whether a model can explain a micro data pattern, Guntin et al. (2022) simulate a crisis by hitting the economy with a one-time, single-type shock. In the data, they find a flat or upward-sloping graph of their elasticity over income deciles (*i.e.*, higher-income households exhibit higher elasticity). In the model, they consider two scenarios: i) a trend shock hits the economy where households face constant borrowing constraints, and ii) a stationary productivity shock hits the economy where households face aggregate-income-dependent borrowing constraints. They find that the first scenario can explain the flat or upward-sloping elasticity graph, while the second scenario cannot, as it produces a downward-sloping graph. Based on the simulation results, they conclude that a trend shock drives large consumption swings during a crisis.

My model allows different types of shocks to hit the economy at different times and, as a result, depicts a quite different story about what happened during the 2008 Peruvian recession. Importantly, I obtain an upward-sloping graph of Guntin et al. (2022)'s elasticity in the model although heightened financial friction plays a major role in the story, suggesting that the upward-sloping graph does not necessarily favor trend shift theory over financial friction theory in my model.

To see how my model depicts the 2008 Peruvian recession, I smooth aggregate shocks at the posterior mode.[22] As the first two panels of Figure J.1 show, the simulated output and consumption using smoothed shocks in the model closely track the data counterparts in 2007–2010.[23] The

[22] I thank Nils Gornemann for suggesting the smoothing analysis.

[23] Figure K.1 in Online Appendix K plots all the simulated observable variables using smoothed shocks in the

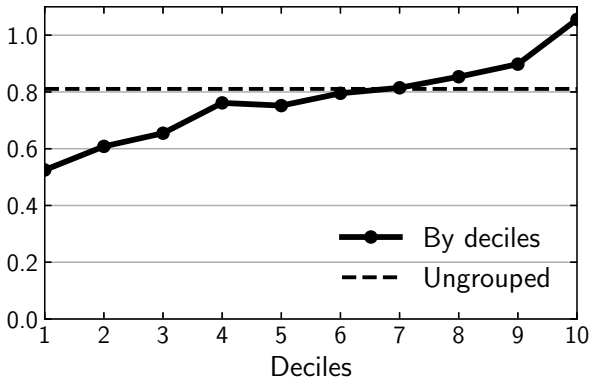

Figure J.2: Guntin et al. (2022)'s Group-Level Consumption-Income Elasticity in My Model

third panel plots smoothed workers' consumption, showing similar dynamics as total consumption. Using the smoothed shocks, I compute Guntin et al. (2022)'s elasticity around the recession. Based on the consumption and output dynamics in Figure J.1, I define the peak and trough as 2008Q2 and 2009Q2, respectively (which are indicated by gray vertical lines).[24] Figure J.2 plots the elasticity at each earnings decile, exhibiting an upward-sloping graph.

Figures J.3 and J.4 show what happened during the recession according to the simulation with smoothed shocks. As Figure J.3 shows, a large financial friction shock (η) hits the economy first in 2008Q3, while productivities (z and g) remain stable. Afterwards, large z and g shocks hit the economy in the following quarters (2008Q4 and 2009Q1, respectively). The financial friction (η) is at its peak in 2008Q4 and then comes back close to a precrisis level in 2009Q1, while productiv-

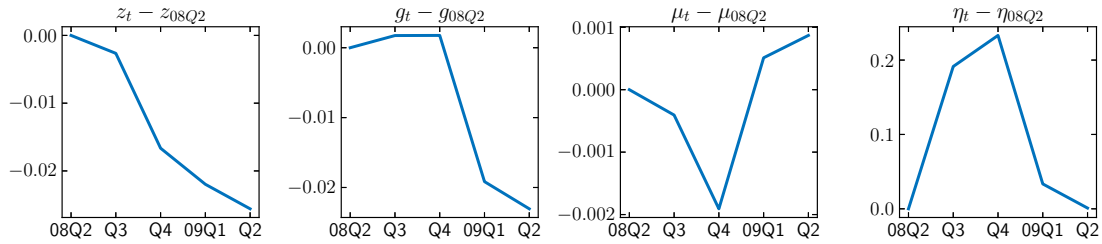

Figure J.3: Smoothed Shocks around the 2008 Peruvian Recession

model and their data counterparts throughout the data period (1980–2018), showing that the model and data track each other very closely. As explained in the Online Appendix, they are not exactly equal only because measurement errors are not included in the simulation.

[24] Additional details regarding the elasticity calculation are worth noting: i) my model is evaluated at the posterior mode; ii) the elasticity is measured for a synthetic group (*i.e.*, not for a fixed group), as in Guntin et al. (2022); iii) earnings are used as the income measure, following Guntin et al. (2022)'s treatment of the ENAHO data; and iv) the sample is composed of workers only, reflecting Guntin et al. (2022)'s sample selection, where only observations reporting positive income (which is positive earnings in ENAHO) are used.

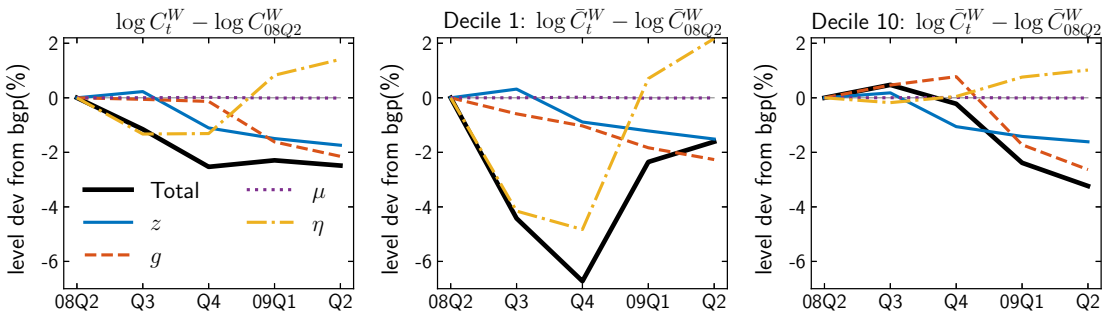

Figure J.4: Decomposition of Smoothed Workers' Consumption Fluctuations across Shocks

Notes: The three panels in Figure J.4 plot the smoothed average workers' consumption fluctuations in the whole economy and in the bottom and top earnings deciles and decompose them into fluctuations driven by each shock.

ities are still very low.[25] The first panel in Figure J.4 shows how these different shocks at different times drive consumption fluctuations during the recession. The heightened financial friction (η) drives a consumption plunge in 2008Q3. Afterwards, the stationary productivity (z) drags consumption down further in 2008Q4, and both productivities (z and g) maintain consumption at a depressed level in 2009Q1-Q2 despite alleviated financial friction. The consumption recovery due to alleviated financial friction in 2009Q1-Q2 itself goes beyond the precrisis level because of an expectation that the financial condition will be favorable for a while.

The second and third panels of Figure J.4 show how these shocks affect the group-average consumption of the bottom and top deciles differently. The heightened financial friction (η) in 2008Q3 generates a disproportionately large consumption plunge in the bottom decile, while the top decile consumption barely responds to it.[26] The consumption recovery due to alleviated financial friction in 2009Q1-Q2 is also much stronger in the bottom decile than in the top decile. The stationary productivity (z) drags consumption down during 2008Q4-2009Q2 to a similar degree between the top and bottom deciles, while the nonstationary productivity (g) drags consumption down during 2009Q1-Q2 more strongly in the top decile than in the bottom decile.[27]

In terms of a (log) consumption change between the peak (08Q2) and trough (09Q2), the bottom decile experiences a smaller change than the top decile, and this is what Guntin et al. (2022)'s elasticity captures. However, it misses a large consumption swing driven by heightened financial friction and borne disproportionately more by lower income deciles between the peak and trough.

[25] Gilchrist and Zakrajšek (2012) empirically find that a financial disruption leads a slowdown in real activities. Although their finding is for the U.S. economy, this empirical pattern is consistent with the story my model delivers about the 2008 Peruvian recession.

[26] This model behavior is in fact consistent with Guntin et al. (2022)'s model prediction that under the second scenario, where financial friction plays a major role, the elasticity graph is downward-sloping.

[27] Figure K.2 in Online Appendix K presents the decomposition of consumption fluctuations for other deciles and shows that the graphs change gradually across deciles.

K Smoothing

In Online Appendix J, I smooth aggregate shocks at the posterior mode to see how my model depicts the 2008 Peruvian recession. This section explains how the smoothing is actually implemented under the sequence space approach. This section also provides additional figures from the smoothing analysis that are omitted from Online Appendix J for brevity.

For any n-by-m matrix A, let $ravel(A)$ be an (nm)-by-1 vector defined as follows:

$$ravel(A) := \begin{bmatrix} [A]_1, [A]_2, \cdots, [A]_n \end{bmatrix}',$$

where $[A]_i$ is the i-th row of matrix A.

Let T be the truncation length used when solving the model under the sequence space approach, and $T_c(:= 0.99T)$ be the truncation length used when evaluating model statistics.[28] Moreover, let $T_{obs}(:= 155)$ be the time length of the observed time series $[\Delta \log Y_t, \Delta \log C_t, \Delta \log I_t, \Delta TB_t/Y_t]$ during 1980Q2-2018Q4. Let $n_{exo}(:= 4)$ be the number of aggregate exogenous variables (*i.e.*, z_t, g_t, μ_t, and η_t), and $n_{obs}(:= 4)$ be the number of the observable variables (*i.e.*, $\Delta \log Y_t, \Delta \log C_t, \Delta \log I_t$, $\Delta TB_t/Y_t$]). I define an $\big(n_{exo} \times (T_c + T_{obs} - 1)\big)$-by-1 vector $\mathbf{E}$ and an $(n_{obs} \times T_{obs})$-by-1 vector $\mathbf{Y}$ as follows.

$$\mathbf{E} := ravel\left(\begin{bmatrix} \varepsilon^z_{-T_c+1}, & \varepsilon^g_{-T_c+1}, & \varepsilon^\mu_{-T_c+1}, & \varepsilon^\eta_{-T_c+1} \\ \varepsilon^z_{-T_c+2}, & \varepsilon^g_{-T_c+2}, & \varepsilon^\mu_{-T_c+2}, & \varepsilon^\eta_{-T_c+2} \\ \vdots & \vdots & \vdots & \vdots \\ \varepsilon^z_0, & \varepsilon^g_0, & \varepsilon^\mu_0, & \varepsilon^\eta_0 \\ \vdots & \vdots & \vdots & \vdots \\ \varepsilon^z_{T_{obs}-1}, & \varepsilon^g_{T_{obs}-1}, & \varepsilon^\mu_{T_{obs}-1}, & \varepsilon^\eta_{T_{obs}-1} \end{bmatrix} \right), \quad \text{and}$$

$$\mathbf{Y} := ravel\left(\begin{bmatrix} d\Delta \log Y_0, & d\Delta \log C_0, & d\Delta \log I_0, & d\Delta(TB_0/Y_0) \\ d\Delta \log Y_1, & d\Delta \log C_1, & d\Delta \log I_1, & d\Delta(TB_1/Y_1) \\ \vdots & \vdots & \vdots & \vdots \\ d\Delta \log Y_{T_{obs}-1}, & d\Delta \log C_{T_{obs}-1}, & d\Delta \log I_{T_{obs}-1}, & d\Delta(TB_{T_{obs}-1}/Y_{T_{obs}-1}) \end{bmatrix} \right),$$

where d is a demeaning operator (*i.e.*, for an observable variable OBS_t and its long-run average $\overline{OBS}_t$, $dOBS_t := OBS_t - \overline{OBS}_t$).

Because each aggregate shock is assumed to follow a normal distribution, a concatenated vector

[28] See Online Appendix E for a related discussion.

$[\mathbf{E}', \mathbf{Y}']'$ follows a multivariate normal distribution. Specifically,

$$\begin{bmatrix} \mathbf{E} \\ \mathbf{Y} \end{bmatrix} \sim N\left(\begin{bmatrix} 0 \\ 0 \end{bmatrix}, \begin{bmatrix} \Sigma_{\mathbf{EE}}, & \Sigma_{\mathbf{EY}} \\ \Sigma_{\mathbf{YE}}, & \Sigma_{\mathbf{YY}} \end{bmatrix} \right),$$

where $\Sigma_{\mathbf{EE}}$ and $\Sigma_{\mathbf{YY}}$ are the variance-covariance matrices of $\mathbf{E}$ and $\mathbf{Y}$, respectively, and $\Sigma_{\mathbf{EY}}$ and $\Sigma_{\mathbf{YE}} (= \Sigma'_{\mathbf{EY}})$ are the covariance matrices between $\mathbf{Y}$ and $\mathbf{E}$.

The relationship between $\mathbf{E}$ and $\mathbf{Y}$ can be described as follows.

$$\mathbf{Y} = \Phi \cdot \mathbf{E} + \mathbf{W}, \quad \mathbf{W} \sim N(0, \Sigma_{\mathbf{WW}}), \tag{K.1}$$

where Φ is an $(n_{obs} \times T_{obs})$-by-$\big(n_{exo} \times (T_c + T_{obs} - 1)\big)$ matrix whose elements are impulse response coefficients, and $\mathbf{W}$ is an $(n_{obs} \times T_{obs})$-by-1 vector whose elements are measurement errors assumed in the Bayesian estimation. $\Sigma_{\mathbf{WW}}$ is the variance-covariance matrix of $\mathbf{W}$.

Given the parameter values at the posterior mode, we know $\Sigma_{\mathbf{EE}}$ and $\Sigma_{\mathbf{WW}}$. By solving the model at the posterior mode, we obtain the impulse response matrix Φ. Then, using equation (K.1), we can compute $\Sigma_{\mathbf{YY}}$, $\Sigma_{\mathbf{YE}}$, and $\Sigma_{\mathbf{YE}}$ as follows.

$$\Sigma_{\mathbf{YY}} = \Phi \cdot \Sigma_{\mathbf{EE}} \cdot \Phi' + \Sigma_{\mathbf{WW}}, \quad \Sigma_{\mathbf{YE}} = \Phi \cdot \Sigma_{\mathbf{EE}}, \quad \text{and} \quad \Sigma_{\mathbf{EY}} = \Sigma'_{\mathbf{YE}}. \tag{K.2}$$

Using equation (K.2), aggregate shocks are smoothed as follows.

$$\mathbf{E}^{sm} := E[\mathbf{E}|\mathbf{Y}] = \Sigma_{\mathbf{EY}} \cdot \Sigma_{\mathbf{YY}}^{-1} \cdot \mathbf{Y} = \Sigma_{\mathbf{EE}} \cdot \Phi' \cdot (\Phi \cdot \Sigma_{\mathbf{EE}} \cdot \Phi' + \Sigma_{\mathbf{WW}})^{-1} \cdot \mathbf{Y}. \tag{K.3}$$

Using the smoothed shocks, I simulate the observable variables in the model as follows.

$$\mathbf{Y}^{sm} := \Phi \mathbf{E}^{sm} = \Phi \Sigma_{\mathbf{EE}} \cdot \Phi' \cdot (\Phi \cdot \Sigma_{\mathbf{EE}} \cdot \Phi' + \Sigma_{\mathbf{WW}})^{-1} \cdot \mathbf{Y}. \tag{K.4}$$

In Figure K.1, I plot the simulated observable variables ($\mathbf{Y}^{sm}$) and their data counterpart ($\mathbf{Y}$), showing that they track each other very closely. $\mathbf{Y}$ and $\mathbf{Y}^{sm}$ are not exactly equal only because smoothed measurement errors $E[\mathbf{W}|\mathbf{Y}]$ are not included in the simulation. Specifically,

$$\mathbf{Y} = E[\mathbf{Y}|\mathbf{Y}] = \Phi \cdot E[\mathbf{E}|\mathbf{Y}] + E[\mathbf{W}|\mathbf{Y}] = \mathbf{Y}^{sm} + E[\mathbf{W}|\mathbf{Y}].$$

$$\therefore \mathbf{Y} - \mathbf{Y}^{sm} = E[\mathbf{W}|\mathbf{Y}].$$

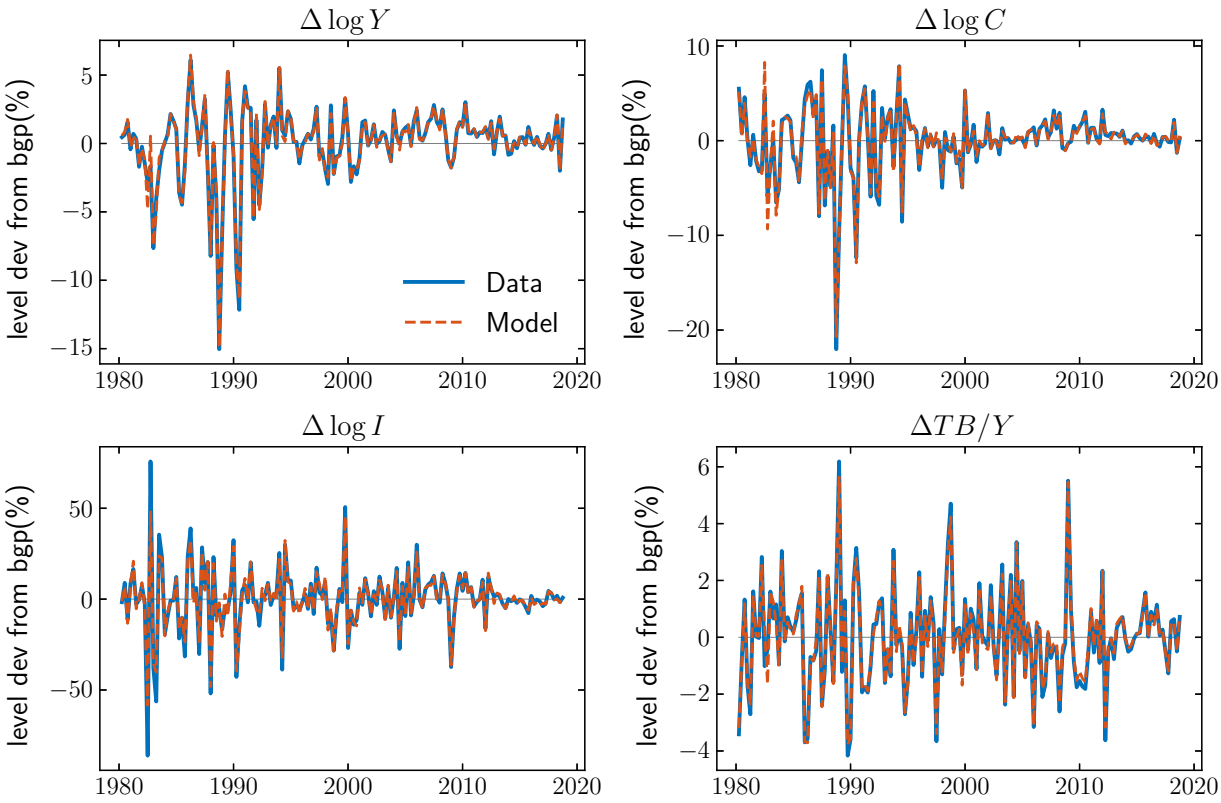

Figure K.1: Simulated Observable Variables using Smoothed Shocks

Notes: This figure plots simulated observable variables $[d\Delta \log Y_t, d\Delta \log C_t, d\Delta \log I_t, d\Delta(TB_t/Y_t)]$ using smoothed shocks (labeled 'Model') and their data counterpart (labeled 'Data').

As discussed in Online Appendix J, I simulate the consumption dynamics of workers within each earnings decile using smoothed shocks and decompose them into the dynamics generated by each shock. Figure J.4 plots the workers' consumption dynamics and their decomposition in the bottom and top deciles only. In Figure K.2 below, I plot them within each of all ten deciles. This figure shows that the graphs change gradually across deciles.

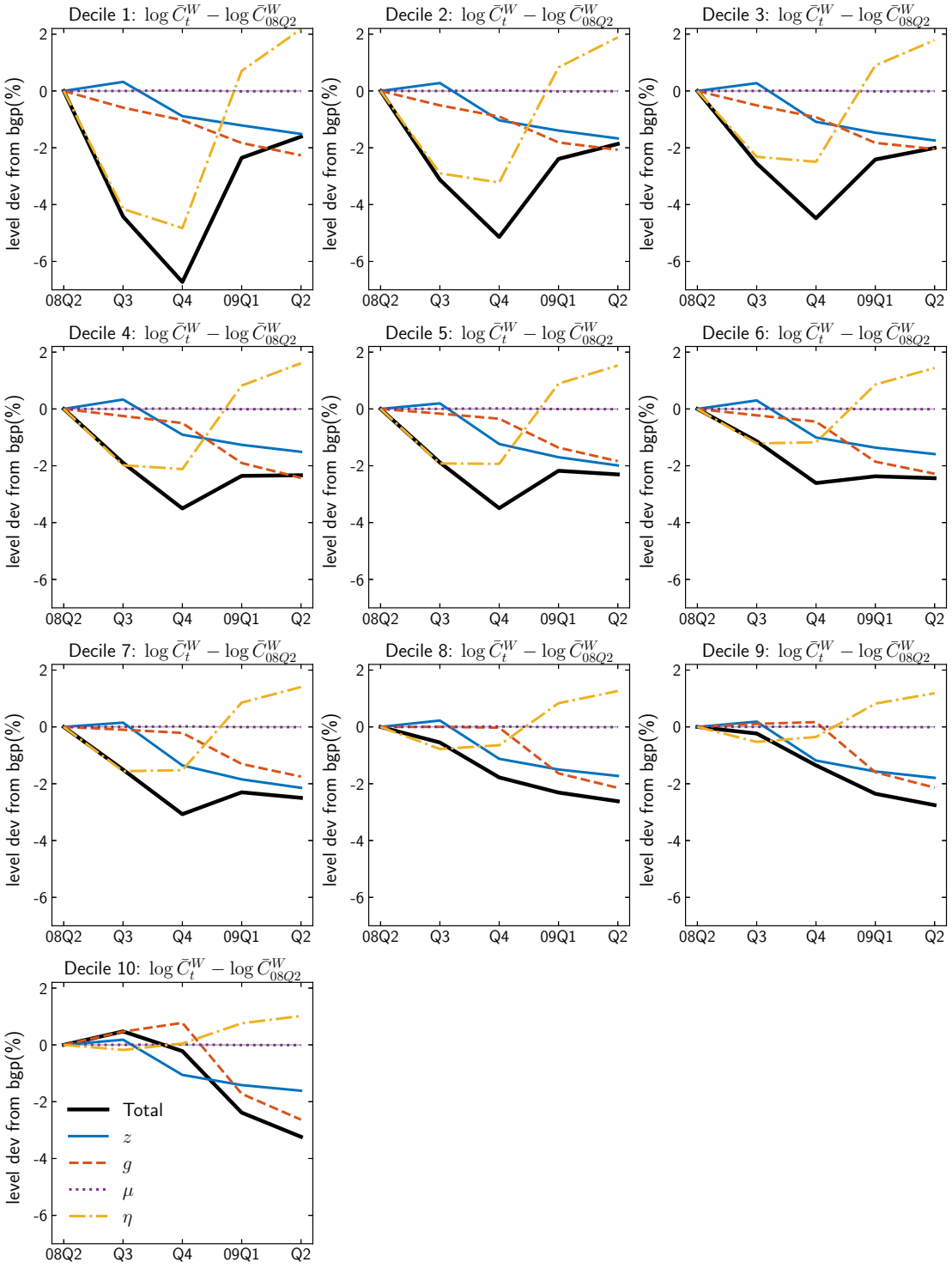

Figure K.2: Decomposition of Smoothed Workers' Consumption Fluctuations across Shocks within Each Earnings Decile

Notes: This figure plots the smoothed average workers' consumption fluctuations within each earnings decile and decomposes them into fluctuations driven by each shock.

L Additional Figures

In this section, I present additional figures that are omitted in the main text for brevity.

L.1 Impulse Responses of Main Drivers to a Stationary Productivity Shock (z)

In section 5, I compare the consumption response decomposition result between the benchmark and counterfactual economies. One of the main findings is that the consumption response to a z shock is far weaker in the counterfactual economy than in the benchmark economy because the consumption responses driven by $w_t\bar{l}_t$ and r_t^a are far weaker. In principle, there are two possible channels that can yield this result: i) the drivers ($w_t\bar{l}_t$ and r_t^a) themselves might respond less to a z shock in the counterfactual economy, or ii) households might face similar fluctuations of these drivers but translate them far less into consumption fluctuations in the counterfactual economy.

To distinguish these two possible channels, in Figure L.1, I compare the impulse responses of the drivers ($w_t\bar{l}_t$ and r_t^a) to a z shock between the benchmark and counterfactual economies. Figure L.1 shows that the impulse responses of the drivers to a z shock are very similar between the benchmark and counterfactual economies, showing that it is the second channel that drives the weaker consumption response to a z shock in the counterfactual economy.

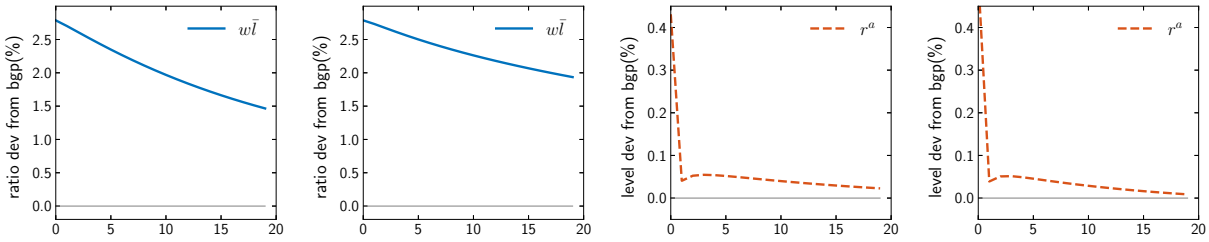

(a) $w_t\bar{l}_t$, Benchmark (b) $w_t\bar{l}_t$, Counterfactual (c) r_t^a, Benchmark (d) r_t^a, Counterfactual

Figure L.1: Impulse Responses of Main Drivers to a z Shock: Benchmark vs. Counterfactual

Notes: The impulse responses to a one-standard-deviation shock are computed at each posterior draw, and their means across the posterior distribution are plotted.

L.2 Impulse Responses of All Equilibrium Variables

In this subsection, I plot the impulse responses of all equilibrium variables to each aggregate shock in the RASOE (z, g, μ) model and the HASOE (z, g, μ, η) model.

L.2.1 RASOE (z, g, μ) Model, z Shock

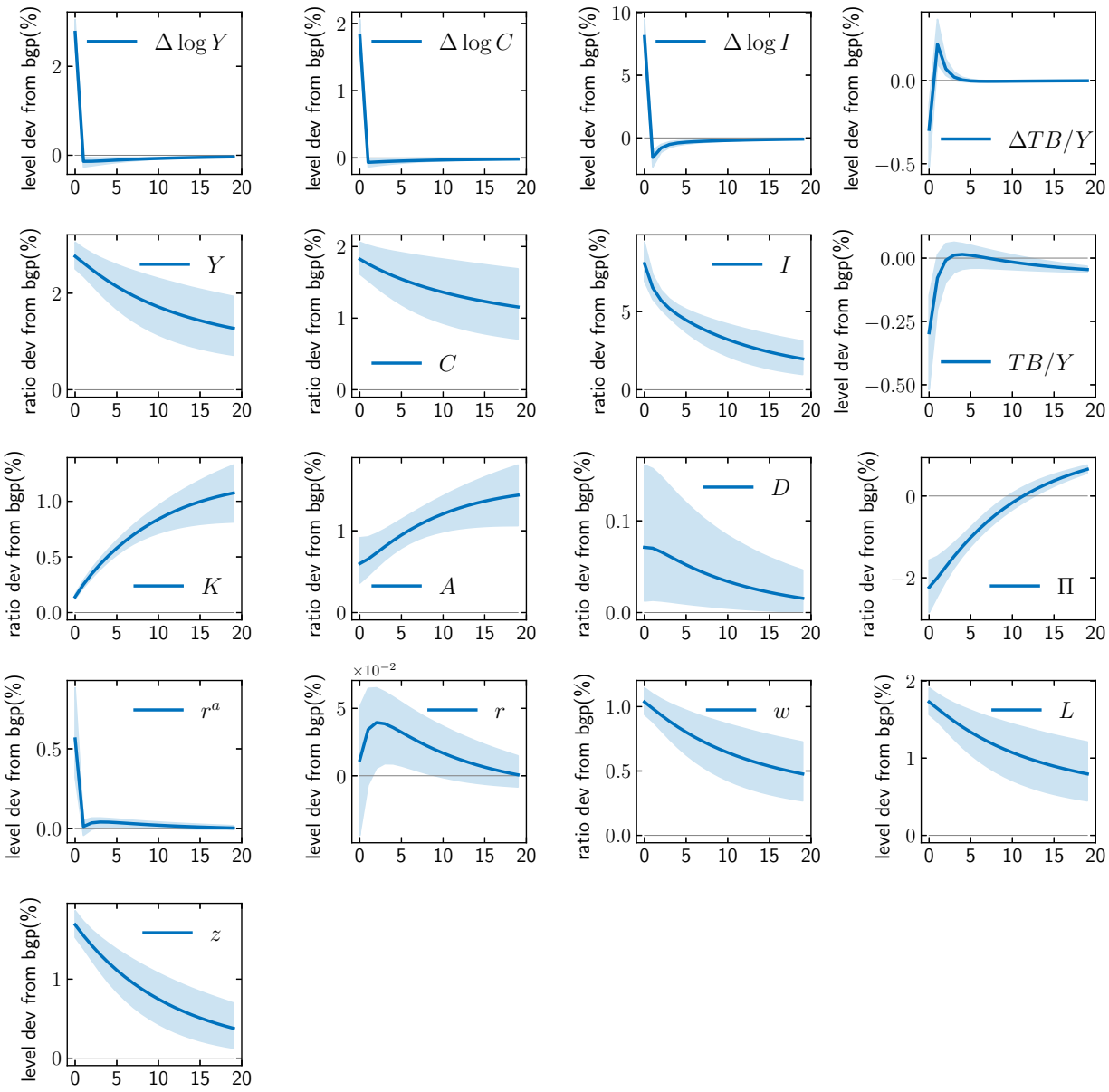

Figure L.2: Impulse Responses of All Equilibrium Variables: RASOE (z, g, μ) Model, z Shock

Notes: The impulse responses to a one-standard-deviation shock are computed at each posterior draw, and their means across the posterior distribution are plotted. Shaded areas represent 90% credible bands.

L.2.2 RASOE (z, g, μ) Model, g Shock

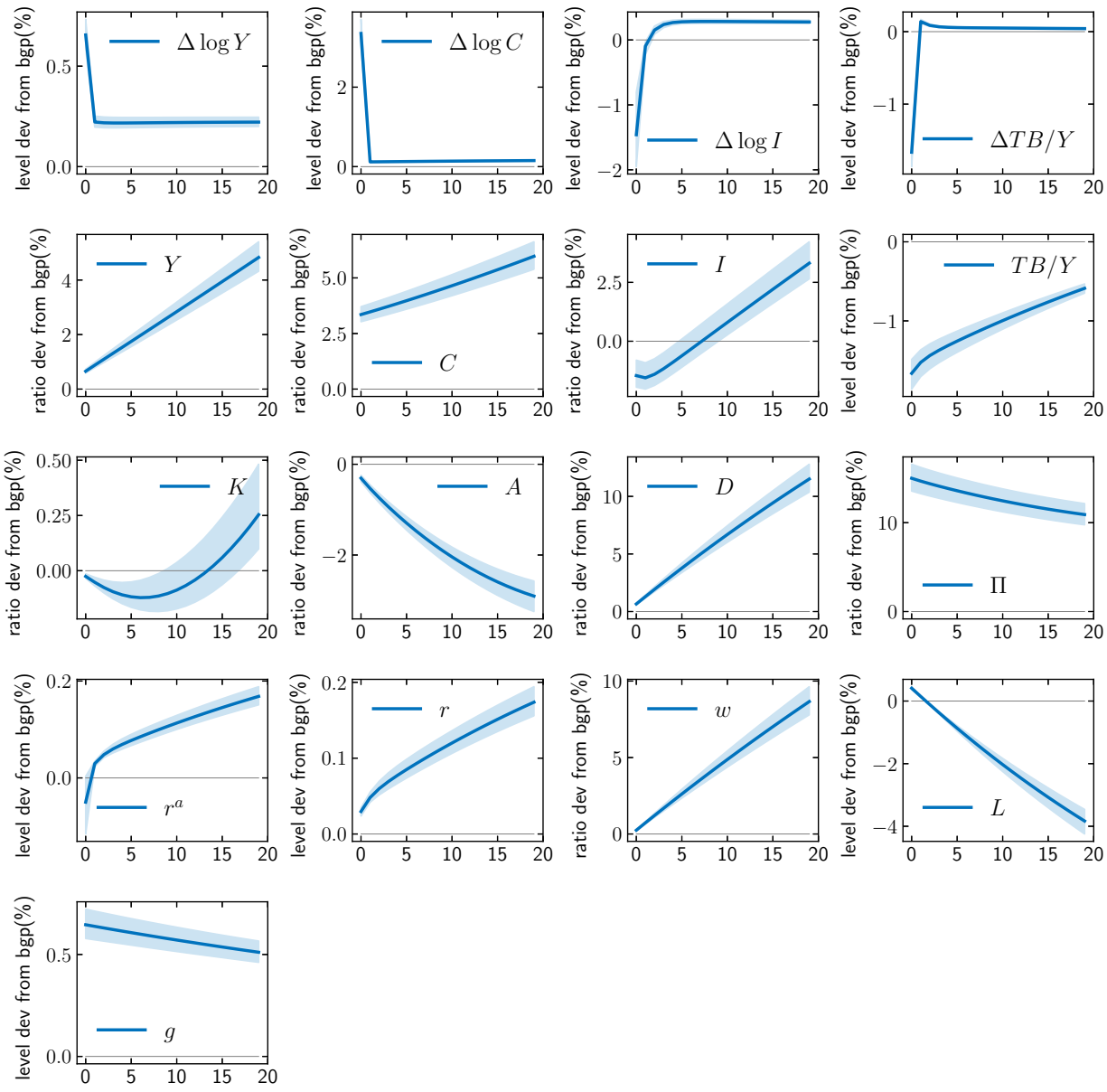

Figure L.3: Impulse Responses of All Equilibrium Variables: RASOE (z, g, μ) Model, g Shock

Notes: The impulse responses to a one-standard-deviation shock are computed at each posterior draw, and their means across the posterior distribution are plotted. Shaded areas represent 90% credible bands.

L.2.3 RASOE (z, g, μ) Model, μ Shock

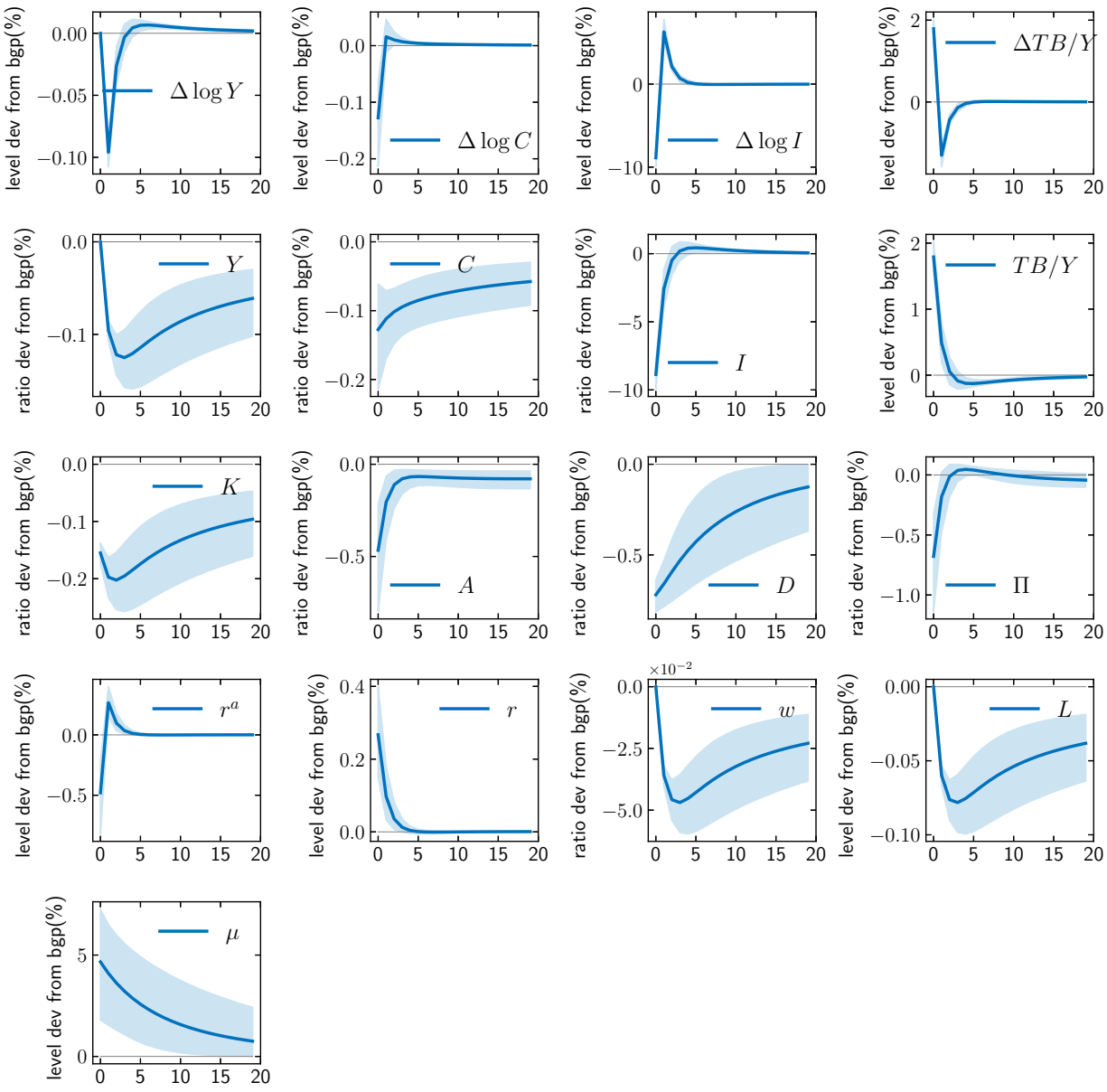

Figure L.4: Impulse Responses of All Equilibrium Variables: RASOE (z, g, μ) Model, μ Shock

Notes: The impulse responses to a one-standard-deviation shock are computed at each posterior draw, and their means across the posterior distribution are plotted. Shaded areas represent 90% credible bands.

L.2.4 HASOE (z, g, μ, η) Model, z Shock

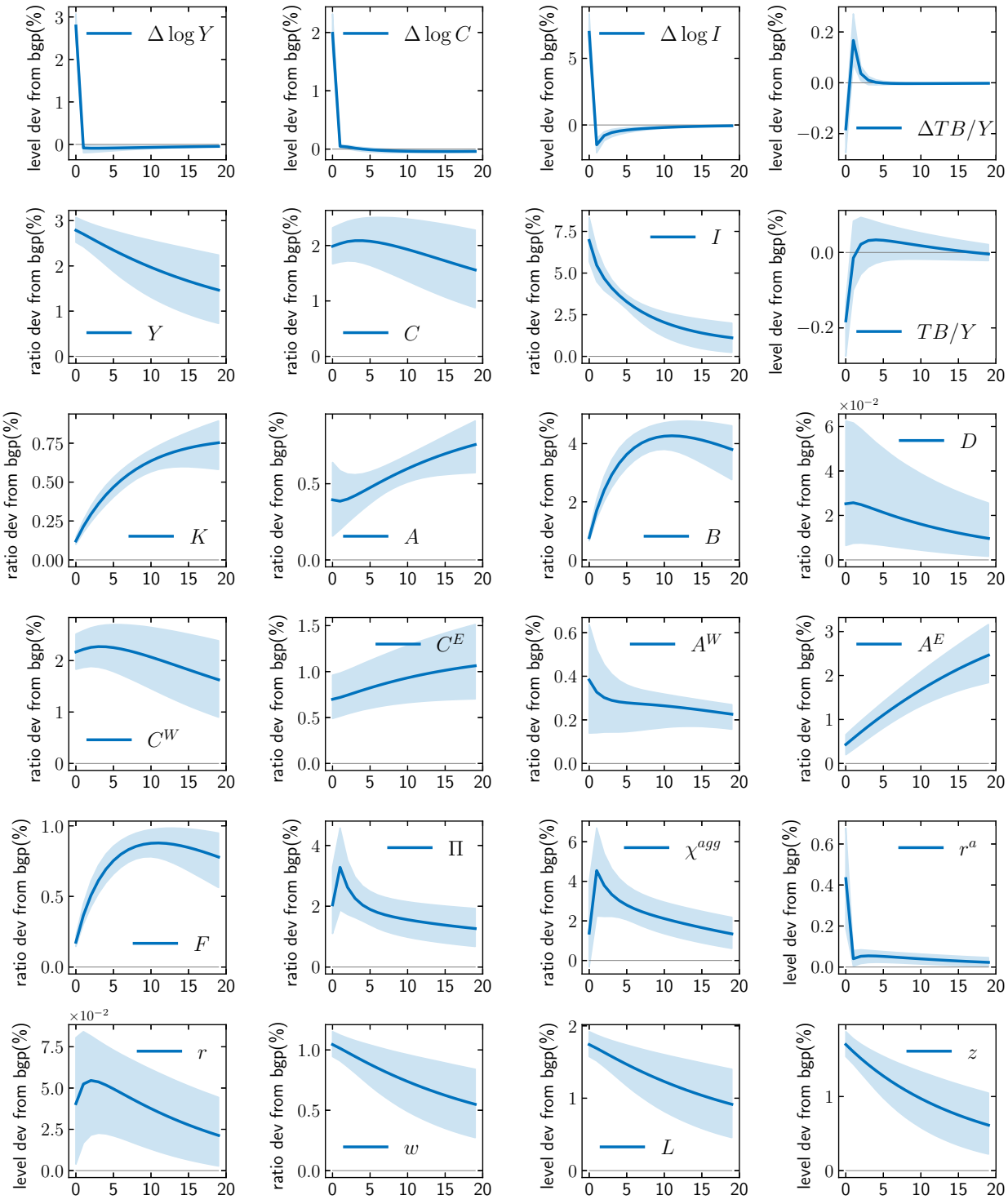

Figure L.5: Impulse Responses of All Equilibrium Variables: HASOE (z, g, μ, η) Model, z Shock

Notes: The impulse responses to a one-standard-deviation shock are computed at each posterior draw, and their means across the posterior distribution are plotted. Shaded areas represent 90% credible bands.

L.2.5 HASOE (z, g, μ, η) Model, g Shock

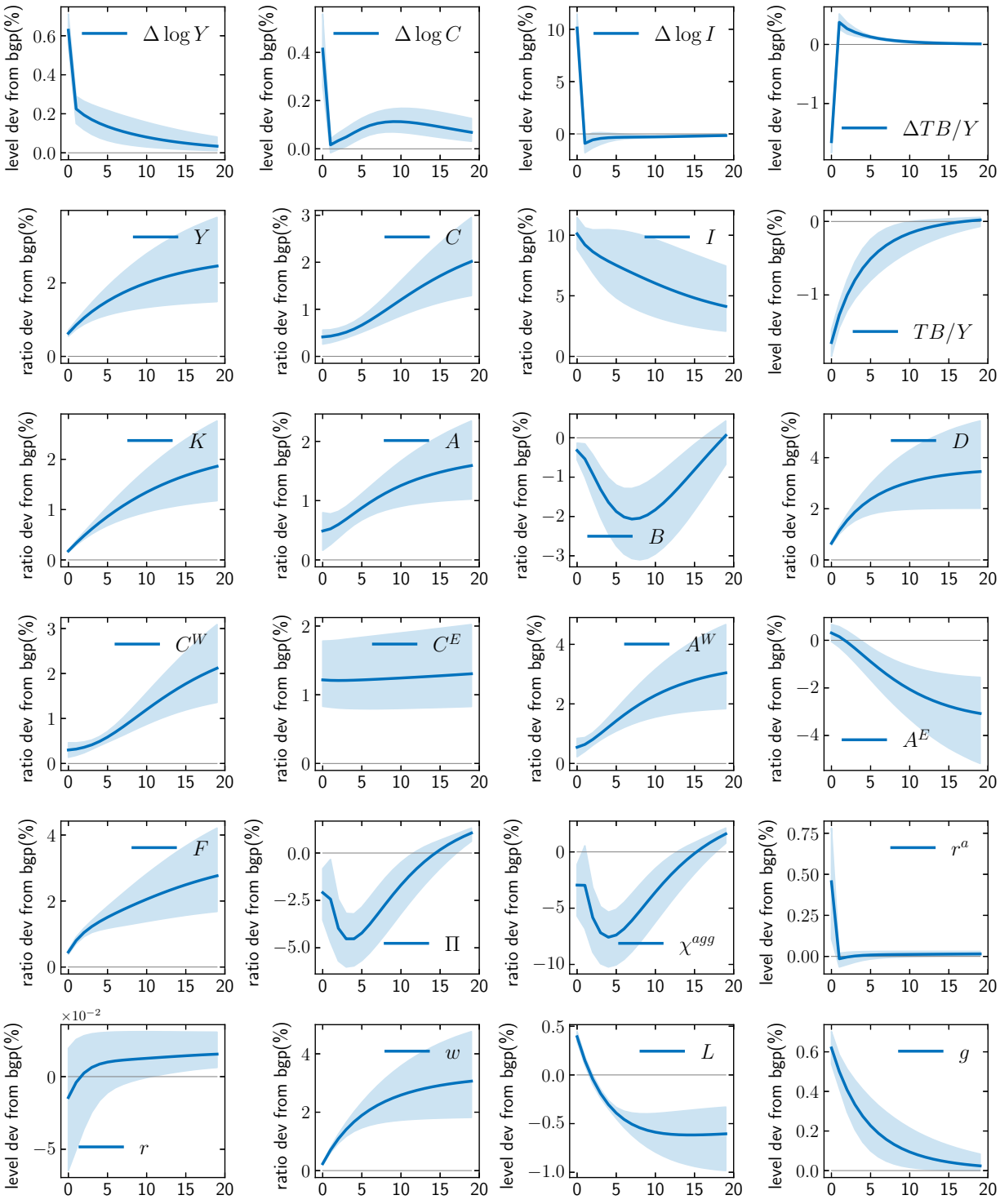

Figure L.6: Impulse Responses of All Equilibrium Variables: HASOE (z, g, μ, η) Model, g Shock

Notes: The impulse responses to a one-standard-deviation shock are computed at each posterior draw, and their means across the posterior distribution are plotted. Shaded areas represent 90% credible bands.

L.2.6 HASOE (z, g, μ, η) Model, μ Shock

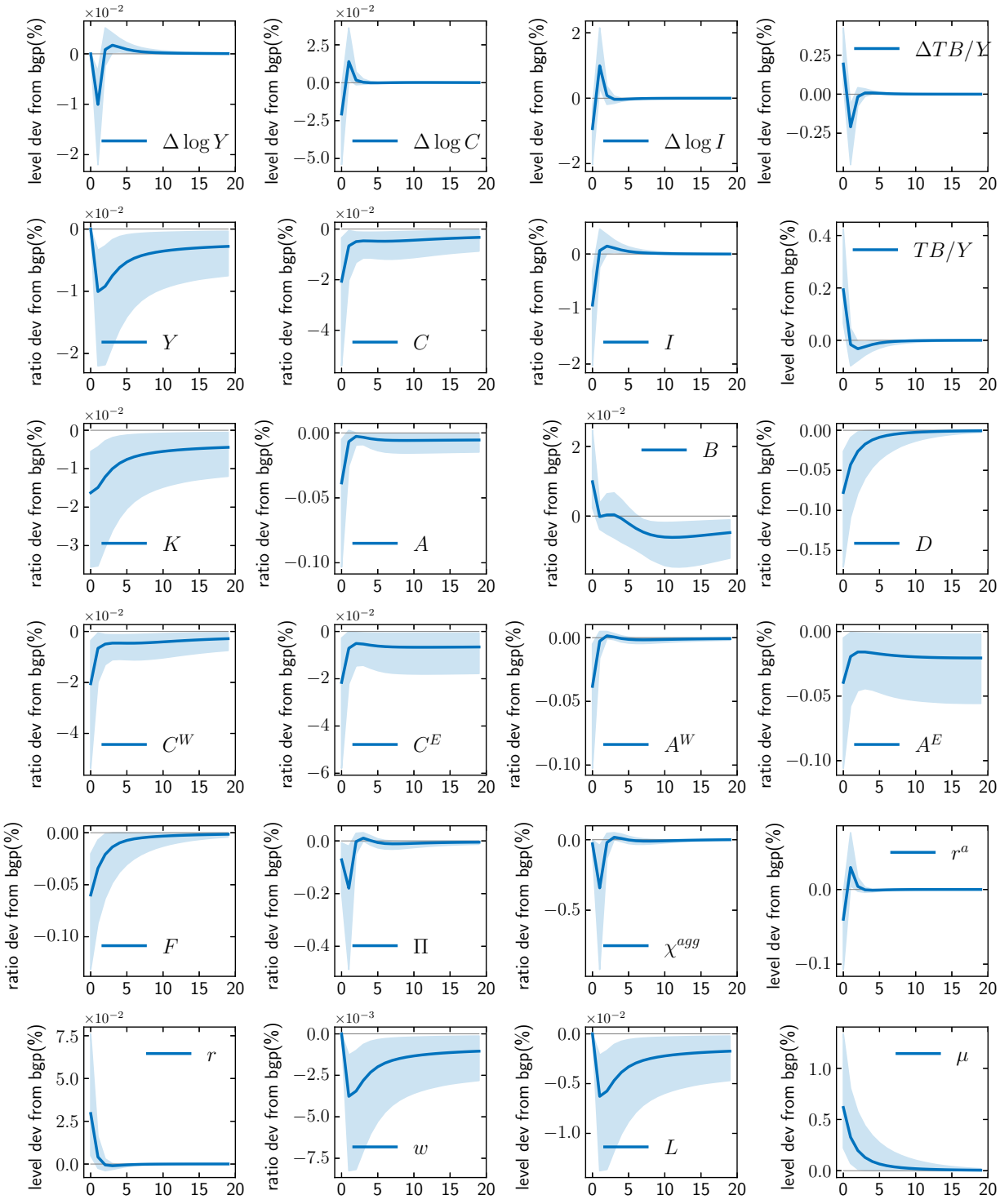

Figure L.7: Impulse Responses of All Equilibrium Variables: HASOE (z, g, μ, η) Model, μ Shock

Notes: The impulse responses to a one-standard-deviation shock are computed at each posterior draw, and their means across the posterior distribution are plotted. Shaded areas represent 90% credible bands.

L.2.7 HASOE (z, g, μ, η) Model, η Shock

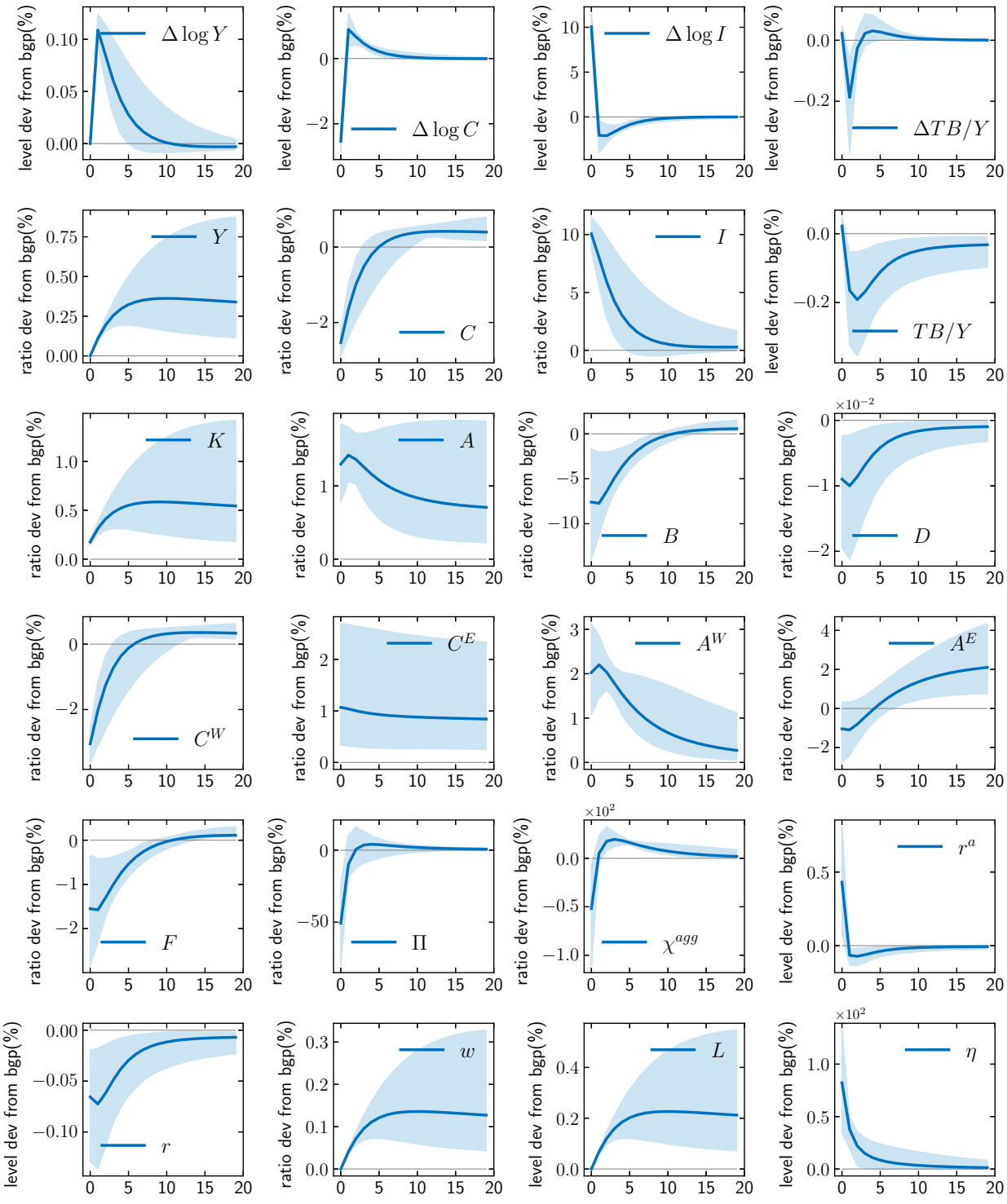

Figure L.8: Impulse Responses of All Equilibrium Variables: HASOE (z, g, μ, η) Model, η Shock

Notes: The impulse responses to a one-standard-deviation shock are computed at each posterior draw, and their means across the posterior distribution are plotted. Shaded areas represent 90% credible bands.

References

Aguiar, M. and G. Gopinath (2007). Emerging Market Business Cycles: The Cycle Is the Trend. *Journal of Political Economy 115*(1), 69–102.

Alvaredo, F., A. B. Atkinson, et al. (2021). Distributional National Accounts Guidelines: Methods and Concepts Used in the World Inequality Database. WID Working Paper No. 2016/2, revised June 2021.

Auclert, A., B. Bardóczy, M. Rognlie, and L. Straub (2021). Using the Sequence-Space Jacobian to Solve and Estimate Heterogeneous-Agent Models. *Econometrica 89*(5), 2375–2408.

Bianchi, J. (2011). Overborrowing and Systemic Externalities in the Business Cycle. *American Economic Review 101*(7), 3400–3426.

Blanchard, O. J. and C. M. Kahn (1980). The solution of linear difference models under rational expectations. *Econometrica: Journal of the Econometric Society*, 1305–1311.

Blundell, R., L. Pistaferri, and I. Preston (2008). Consumption Inequality and Partial Insurance. *American Economic Review 98*(5), 1887–1921.

Carroll, C. D. (2006). The Method of Endogenous Gridpoints for Solving Dynamic Stochastic Optimization Problems. *Economics Letters 91*(3), 312–320.

Chang, R. and A. Fernández (2013). On the Sources of Aggregate Fluctuations in Emerging Economies. *International Economic Review 54*(4), 1265–1293.

Crawley, E. (2020). In Search of Lost Time Aggregation. *Economics Letters 189*, 108998.

Diaz-Gimenez, J., V. Quadrini, and J.-V. Rios-Rull (1997). Dimensions of Inequality: Facts on the US Distribution of Earnings, Income and Wealth. *Federal Reserve Bank of Minneapolis Quarterly Review 21*(2), 3–21.

Economic Commission for Latin America and the Caribbean (2010). *Preliminary Overview of the Economies of Latin America and the Caribbean*.

Floden, M. and J. Lindé (2001). Idiosyncratic Risk in the United States and Sweden: Is There a Role for Government Insurance? *Review of Economic Dynamics 4*(2), 406–437.

Garcia-Cicco, J., R. Pancrazi, and M. Uribe (2010). Real Business Cycles in Emerging Countries? *American Economic Review 100*(5), 2510–31.

Gilchrist, S. and E. Zakrajšek (2012). Credit Spreads and Business Cycle Fluctuations. *American economic review 102*(4), 1692–1720.

Guntin, R., P. Ottonello, and D. Perez (2022). The Micro Anatomy of Macro Consumption Adjustments. *The American Economic Review*, Forthcoming.

Hong, S. (2022). MPCs in an Emerging Economy: Evidence from Peru. *Journal of International Economics*, Forthcoming.

Kaplan, G. and G. L. Violante (2010). How much consumption insurance beyond self-insurance?

American Economic Journal: Macroeconomics 2(4), 53–87.

Kaplan, G., G. L. Violante, and J. Weidner (2014). The Wealthy Hand-to-Mouth. *Brookings Papers On Economic Activity*, 77–138.

Krueger, D. and F. Perri (2006). Does Income Inequality Lead to Consumption Inequality? Evidence and Theory. *The Review of Economic Studies 73*(1), 163–193.

Mendoza, E. G. (2010). Sudden Stops, Financial Crises, and Leverage. *American Economic Review 100*(5), 1941–66.

Neumeyer, P. A. and F. Perri (2005). Business Cycles in Emerging Economies: the Role of Interest Rates. *Journal of Monetary Economics 52*(2), 345–380.